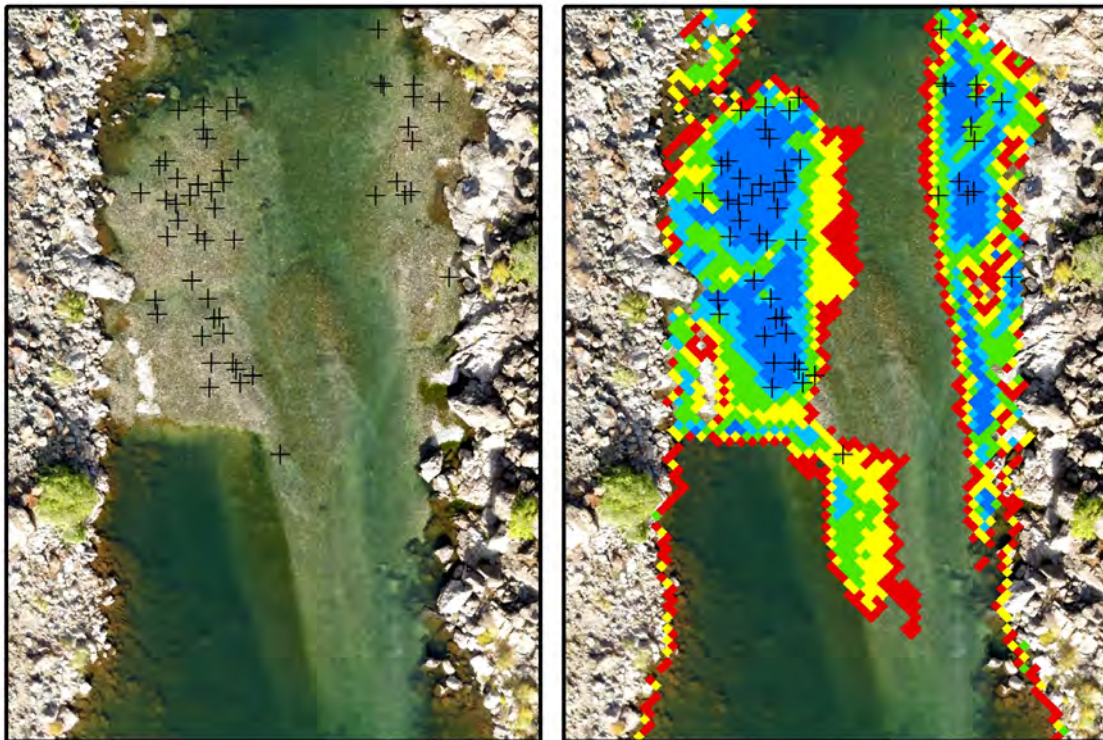


MONITORING AND ASSESSMENT OF GRAVEL/COBBLE AUGMENTATION IN THE ENGLEBRIGHT DAM REACH OF THE LOWER YUBA RIVER, CA: 11/01/2011 TO 12/1/2012



Aerial photo (left) and predicted physical habitat (right, blues) are preferred habitat with observed redds (+) for autumn 2012

Prepared for:
U.S. Army Corps of Engineers
Sacramento District
Englebright/Marlis Creek Lakes
PO Box 6
1296 Englebright Dam Road
Smartsville, CA 95977

Prepared by:
Rocko A. Brown, MS, EIT
Gregory B. Pasternack, PhD, AM. ASCE
University of California, Davis

September 1, 2013

Abstract

The Army Corps of Engineers injected ~5,000 short tons of gravel/cobble into the Yuba's Englebright Dam Reach just downstream of the Narrows 1 powerhouse July - August 2012. Previously they injected ~5,000 short tons at the same location November 2010 to January 2011. Before that they injected 453 short tons in the Narrows II pool in November 2007. This study evaluated the status of the effort with regard to making progress toward meeting the geomorphic and ecological goals of the Corps' Gravel Augmentation Implementation Plan. This is still a very early stage of the overall effort, with only ~16 % of the minimum gravel deficit being addressed. Gravel/cobble sluicing once again proved effective and safe; it is recommended for continued use. This time gravel/cobble was added in the summer just before Chinook spawning, so there was a riffle available when spawners arrived. Chinook were observed to heavily use the new habitat, but it was still a small area given the small amount added. 2D physical habitat modeling accurately predicted utilized and avoided areas, with 80% of spawners present on the small area of model-predicted high-quality physical habitat. In addition, two small alluvial landforms created downstream from previously injected sediment were used. Topographic change was mapped for October 2011 to October 2012 to see where sediment moved during winter 2012. Another analysis was done for 2007 to October 2012 to see cumulative changes. The overall sediment budget yielded a small overage, indicating that the method can account for the injected material. Spatial maps of sediment deposition show that injected material has spread throughout EDR, with only a very small amount exported to the Narrows. Overall, gravel/cobble injection by gravel sluicing is working in that coarse sediment is going into the channel, it can be used to create a temporary spawning riffle in the injection zone, sediment moves downstream to create landforms, and it is staying in the canyon for now (helping to reduce the sediment deficit). Further, hydraulics over deposits include high-quality spawning habitat and Chinook spawners are making use of that habitat. Annual gravel/cobble addition needs to continue until the sediment deficit is eradicated. At that point, the long-term plan in the GAIP should commence.

Keywords: gravel augmentation, gravel addition, river rehabilitation, spawning habitat enhancement, mountain river fluvial geomorphology, mountain river physical habitat analysis, topographic change detection, regulated rivers, human impacts on rivers.

Citation: Brown, R.A. and Pasternack, G.B. 2013. Monitoring and assessment of the 2012 gravel/cobble augmentation in the Englebright Dam Reach of the lower Yuba River, CA: 11/01/2011 to 12/1/2012. Prepared for the U.S. Army Corps of Engineers, Sacramento District. University of California at Davis, Davis, CA.

Study Questions and Answers

- Q: Did the USACE add gravel and cobble to the lower Yuba River in 2012?
 - Yes. They added ~5,000 short tons just downstream of the Narrows 1 powerhouse in the bedrock canyon of the lower Yuba River in July and August 2012.
- Q: What was the method of gravel/cobble addition?
 - Sediment was trucked to a road switchback overlooking the injection point where a frontloader scooped it up and poured it into a hopper that blended it with water pumped down from Englebright Lake and sluiced it down the hillside to the river below. At the river end, a crew controlled how and where the sediment entered the river.
- Q: Didn't adding all that dirty rock to the river cause a water quality problem?
 - Adding rocks to a river does create a small, manageable, temporary turbidity plume, and the slower it is added, the less impact there is. The river-rounded gravel and cobble was washed three times at the quarry before delivery and then it was washed down a sluice pipe at a moderately slow rate into a river with ~200-500 times that flow rate. In addition, because no heavy equipment was operated near the river, there was no turning up of the riverbed by any machinery and no chance for oil and gas spills or road-related impacts. Water quality was carefully monitored 300' downstream of the injection point by the USACE and results were reported to a regulatory agency.
- Do you recommend this method be used in the future at this location?
 - Yes. This is the second time the method has been used here and it worked even better this time than the first time, as systemic improvements were made to the technology. The method is slower than others, but it worked well for this remote location and it was safe and harmless to the environment compared with other methods.
- Are there limitations to meeting the GAIP in using this method?
 - The size distribution of injected sediment is somewhat limited by the size of pipe used, but larger sizes may be added with care. At present, particles > 5" (127 mm) are being screened out during each drop by the front loader

into the hopper and then large cobbles are individually being fed into the sluice pipe by hand between front loader drops.

- Do you recommend use of the sediment size distribution specified in the original Gravel Augmentation Injection Plan (GAIP)?
 - No. A new mix design was developed for this project on a collaborative basis among Yuba stakeholders and experts based on lower Yuba River research. It is recommended that this new mix design be used for all future injections. Last year's report explained the problems with the original mix design.
- The Gravel Augmentation Implementation Plan has three geomorphic goals, how did the project perform relative to those goals?
 - The first goal was to increase the cobble/gravel storage in the reach. That goal was met: ~16% of the minimum gravel deficit is now filled.
 - The second goal was to allow for downstream transport and deposition. Figures 39 and 40 show the spatial pattern of deposition throughout EDR. Remarkably, the injected sediment has spread throughout the reach and is beginning the long-term process of restoring a mixed alluvial-bedrock riverbed.
 - The third goal was to provide morphologic unit diversity. Thus far only ~10-16% of the reach's sediment deficit has been addressed and individual projects have been kept small to enable development of required science and technology. As a result, the alluvial landforms being built downstream are still small and highly localized. Nevertheless, there are new, self-formed, coherent alluvial landforms emerging in the river as a result of gravel/cobble injection. It will just take more material and time to get to the desired outcome.
- The Gravel Augmentation Implementation Plan has three ecological goals, how did the project perform relative to those goals?
 - The first goal was to increase the quantity of high-quality habitat for spawning adult spring-run Chinook salmon. That goal was met. As illustrated in the cover photo for this report, injecting sediment in the summer yielded a riffle with high-quality spawning habitat that was heavily used by Chinook spawners. Because the injected amount was small, the corresponding amount of habitat added was small. Also,

downstream deposits of sediment from the 2010-2011 injection were again used in autumn 2012. As those sites grow through time, they will be used more, but so far too little sediment has been added to serve the present Chinook population.

- The second goal was to provide adult and juvenile refugia in close proximity to spawning habitat . That goal was met. Analysis revealed an abundance of these habitat types within 10 m of the observed redds. Just downstream of the injection deposit was a deep, large pool for adults to hold. Meanwhile, suitable depths, velocities, and cover types are present along the flanks of the spawning riffle for use by rearing fry and juveniles.
- The third goal was to provide morphological diversity to support ecological diversity within the study reach. That goal was met, though the size and abundance of alluvial landforms remains small, commensurate with the small fraction of the total sediment deficit met by injections thus far.
- Let me ask the question a different way. American taxpayers are investing a lot of money into these projects. The expectation is that these projects serve a lot of spring-run Chinook salmon. Exactly how many salmon are being served?
 - When a house builder pours the concrete foundation to a new home under construction, no one asks if the homeowner is enjoying the stainless steel stove yet. Salmon do not spawn on shovel-fulls of gravel, they spawn on fluvial landforms, especially riffles, riffle transitions, and runs in the Yuba River. So far the real project presented in the GAIP is not yet built- only ~10-16% of construction has been done. Each annual “project” is not a complete project, but a single small step towards the larger purpose. Thus, it is simply premature to expect or demand a significant quantity of spawning relative to the population size of spring-run Chinook salmon on the LYR. Yes, spawners are using the injected gravel (see cover photo for proof), but it will take much more gravel to get what the taxpayers expect out of this project. The reason to take small steps in the early phases of the GAIP is to enable the required scientific and technological developments to make this work. Those gains are being made and the GAIP is working as planned.

- If the project isn't done yet, then why do you have any confidence that in the end the GAIP will serve a large number of spring-run Chinook salmon?
 - The two annual studies of EDR gravel injection have found that we can highly accurately predict where Chinook salmon will choose to spawn. This year, 80% of spawning took place where the model predicted it would occur- down to the nearest 3-ft cell. This is a remarkable success rate for prediction in extremely high detail. By comparison, any gambler who could predict casino outcomes with an 80% success rate would make a fortune, while casinos only need a success rate of 50.1% to make their living. This level of predictive success yields a near-certain confidence that expert-based final designs for gravel augmentation can be produced to serve the entire current population of Yuba River spring-run Chinook salmon in EDR.
- Based on the results so far, how much sediment do you recommend be injected annually?
 - In 2013 there will be 5,000 short tons added. Everything significant that needed to be learned at this annual injection rate is now learned. It is highly recommended that future annual injections beginning in 2014 involve at least 10,000 tons per year. The sooner the gravel/cobble deficit is eliminated, the better.

Acknowledgements

This project was sponsored by the United States Army Corps of Engineers under Cooperative Ecosystem Studies Unit Award # W912HZ-11-2-0038.

The authors thank James Jackson, Leah Kammel, Duane Massa, and Joshua Wyrick for assistance with river surveying; Lloyd Howry and Skip Stevenson with pebble counts; Sean W. Smith with construction and implementation support and lessons learned; Doug Grothe for contracting and coordination; and Duane Massa and Casey Campos from PSMFC for help with biological data collection and interpretation.

DRAFT

Preface

This report marks the 2nd year of monitoring the Englebright Dam Reach of the lower Yuba River to evaluate the status of cobble/gravel injection associated with the Army Corps' 2010 Gravel Augmentation Implementation Plan. A report dated December 15, 2012 presented the finding for the period of November 1, 2007 to November 1, 2011. During that time there was a small pilot cobble/gravel injection in late November 2007 and a substantial one in November 2010 to January 2011. Now this new report covers the period November 1, 2011 to December 1, 2012. During this latest interval there was a gravel/cobble injection during July to August 2012.

This report duplicates many of the methods and analyses from the previous report, so several sections have been carried over from the previous year's monitoring report. In some cases minor typographical errors and citation errors have been fixed. These sections are mostly background information and methods that apply to both years. These sections will have an asterisk (*) next to the section heading so that readers who are familiar with the prior year's results can skip these sections and focus on new results.

Table of Contents

Abstract.....	ii
Study Questions and Answers.....	iii
Acknowledgements	vii
Preface	viii
Table of Contents	ix
List of Tables.....	xii
List of Figures	xiv
1.0 Introduction.....	1
1.1. Environmental Problem*	1
1.2. USACE Program to Address Problem*	2
2.0 Goals and Objectives*	4
2.1. GAIP Hypothesis Testing*	5
2.1.1. GAIP Geomorphic Goals*	5
2.1.2. GAIP Ecological Goals	7
2.2. Iterative Learning and Improved Actions	9
3.0 2012 EDR Gravel Augmentation Project.....	9
3.1. Peak Flow Hydrology Before and after Injection.....	13
4.0 Post-Project Data Collection.....	15
4.1. Topography and Bathymetry.....	15
4.2. Water Depth & Surface Elevation Data	17
4.3. Water Velocity Vector Data*	18
4.4. Wolman Pebble Counts*	18
4.5. Blimp Aerial Imagery*	19
4.6. Topographic Map Construction	20
4.7. 2D Numerical Model.....	21
4.8. Fish Observations	22
5.0 Data Analysis Methods*	24
5.1. Areal Extent of Gravel/Cobble Deposits from Blimp Imagery*	24
5.2. 2D Model Validation*	24
5.2.1. Mass Conservation Standard*	25

5.2.2.	Types of Variables Assessed*	25
5.2.3.	Validation Tests and Performance Standards*	26
5.3.	Topographic Change Detection By DEM Differencing	28
5.3.1.	TCD Components	28
5.3.2.	TCD Production Workflow	29
5.3.3.	Volume and Weight Gravel/Cobble Budgeting*	31
5.4.	Evaluating Habitat Quality and Spawning Use	31
5.4.1.	Comparing Observed Redds with Deposition	32
5.4.2.	Spawning GHSI Modeling	32
5.4.3.	Bioverification of Chinook Spawning GHSI	33
5.4.4.	Proximity Analysis of Observed Redds to Refugia	35
6.0	Results	35
6.1.	Wolman Pebble Counts	35
6.2.	Blimp Image Analysis	37
6.3.	2D Model Validation	38
6.3.1.	Mass Conservation Checks	38
6.3.2.	WSE Validation	38
6.3.3.	Water Speed Validation for 966 cfs	42
6.3.4.	Velocity Direction Validation for 966 cfs	49
6.4.	Redd Observations	52
6.5.	Survey and Instrumentation Error (SIE) Functions	55
6.6.	TCD and Sediment Budget Analyses	61
6.6.1.	October 2011 to October 2012 TCD	61
6.6.2.	Narrows Reach Reconnaissance	67
6.6.3.	2007 to October 2012 TCD	68
6.6.4.	Gravel/Cobble Storage Mechanisms	74
6.7.	Habitat Suitability Modeling	75
6.7.1.	GHSI Bioverification	75
6.7.2.	Abundance of Preferred Habitat	76
6.7.3.	2D Model Chinook Spawning Habitat Predictions	78
6.7.4.	Observed Spawning use and Deposition	84
6.7.5.	Redd proximity analysis	85

7.0	GAIP Hypothesis Testing Evaluation.....	87
7.1.	Hypothesis 1 - Total Sediment Storage Should Be At Least Half of the Volume at the Wetted Baseflow	87
7.2.	Hypothesis 2.....	87
7.2.1.	Hypothesis 2a - SRCS Require Deep, Loose River Rounded Sediment for Spawning.....	87
7.2.2.	Hypothesis 2b - Spawning Habitat Should Be As Close To GHSI High Quality Habitat as Possible.....	88
7.3.	Hypothesis 3 – Structural refugia in close proximity to spawning habitat should provide resting zones for adult spawners and protection from predation and holding areas for juveniles.	88
7.4.	Hypothesis 4a - Designs Should Promote Habitat Heterogeneity and Provide Habitat for All Species and Life stages.....	88
7.5.	Hypothesis 5a - There are no mechanisms of riffle-pool maintenance in the EDR and it is not feasible in this section of the river.....	89
7.6.	Hypothesis 5b - Flows overtop Englebright Dam and erode placed sediments	89
8.0	Annual Volume and Placement Design	89
8.1.	Gravel Placement Design Development.....	89
8.2.	Annual Injection Volume Assessment.....	90
9.0	Lessons Learned	91
9.1.	Gravel Sluicing Operations	91
9.2.	Enhanced Yuba-specific Gravel Mix.....	91
9.3.	Gravel/Cobble Sourcing*	92
10.0	Conclusions	93
11.0	References	95

List of Tables

Table 1. GAIP Study Hypotheses and Tests.....	4
Table 2. Scale dependent sediment storage mechanisms in the EDR.	7
Table 3. Original gravel/cobble mix design in the GAIP.....	10
Table 4. Observed 2010-2011 LYR redd substrate composition.	11
Table 5. Planned 2012 gravel/cobble mix design.....	11
Table 6. YRS gage discharges during survey dates in 2012.	16
Table 7. Discharge during 2012-2013 EDR Spawning Observations.....	23
Table 8. Nonexceedence probabilities for 966 cfs WSE deviations (unsigned) meeting different thresholds of performance.	40
Table 9. Comparison of Water Surface Elevation Model Validation for the 2012 and 2013 Monitoring Report.....	41
Table 10. Percent of 2D model velocity predictions meeting different thresholds of performance for all data (unsigned) as well as above and below the 2 ft/s threshold.	42
Table 11. Comparison of Velocity Magnitude Model Validation for the 2012 and 2013 Monitoring Report.....	48
Table 12. Percent rank of 966 cfs absolute velocity direction deviations meeting different thresholds of performance for the main flow (e.g. no eddies).	50
Table 13. Comparison of Velocity Direction Model Validation for the 2012 and 2013 Monitoring Report.....	52
Table 14. Ranges of applicability and SIE functions with R ² values for the downstream area of the 2007 data.....	59
Table 15. Ranges of applicability and SIE functions with R ² values for the upstream area of the 2007 data.	59
Table 16. Ranges of applicability and SIE functions with R ² values for the downstream area of the October 2012 data.....	59
Table 17. Ranges of applicability for SIE functions with R ² values for the downstream area of the October 2011 data.....	60
Table 18. Ranges of applicability for SIE functions with R ² values for the upstream area	

of the October 2011 data	60
Table 19. Ranges of applicability for SIE functions with R ² values for the upstream area of the October 2012 data	60
Table 20. Upstream injection area volumes of erosion and deposition for the October 2011 to October 2012 epoch.....	62
Table 21. Downstream area volumes of erosion and deposition.....	62
Table 22. Volumes of erosion and deposition for upstream area for the 2007 – October, 2012 epoch.....	70
Table 23. Volumes of erosion and deposition for upstream area for the 2007 – October, 2012 epoch.....	70
Table 24. Planned 2012 gravel/cobble mix design.....	92

DRAFT

List of Figures

Figure 1. Like in any phased construction scheme, an individual “project” will not yield the benefits anticipated for the complete structure. No one asks how many humans are living in a home after the foundation is poured. Similarly, the GAIP will not yield the desired and expected benefits to salmonid populations until the sediment deficit in EDR is erased. Interim monitoring and assessment provides insights about geomorphic mechanism and small-scale ecological functionality. 8

Figure 2. The relocated hopper at the switchback on the dam access road. 12

Figure 3. The sluice pipe outlet in the river without barges and only a limited cableway (top) showing that the pipe is pushed downstream by the flow and there is less control on cobble/gravel placement. When barges and cableway are used (bottom) there is excellent control on pipe length and positioning..... 12

Figure 4. Discharge recorded at the Smartsville gage (<http://cdec.water.ca.gov>; YRS) during the period between September 2011 and January 2013. Note that these are mean daily values so hourly data would reveal more insight into actual peak flows, but this plot does show the overall trend in discharge..... 14

Figure 5. Discharge recorded at the Smartsville gage (<http://cdec.water.ca.gov>; YRS) during the period between August 2012 and January 2013..... 14

Figure 6. Survey limits and collected points in July 2012. 16

Figure 7. Survey limits and collected points in October 2012. 17

Figure 8. Final mosaic for the 2012 blimp imagery. 20

Figure 9. Extent of EDR 2D model computational mesh for in-channel low flows. 22

Figure 10. Cumulative particle-size distribution of injected sediment during the 2012 injection. 36

Figure 11. Cumulative distributions of four in river locations relative to that from the plan and the average from the gravel injection material stockpiled at the hopper. . 36

Figure 12. Photograph illustrating the effect of armoring on injected gravel deposits. When this area was first filled with gravel all areas had very similar grain size distributions but as flow poured through area B this zone coarsened relative to the other areas limiting any further incision..... 37

Figure 13. Red polygons outline areas of gravel deposition that were discernible using blimp imagery and visual inspection in ArcGIS. Other significant deposits occurred

where it was too deep to see visually, but are revealed by TCD.....	38
Figure 14. Histograms evaluating 2D model WSE performance at 996 cfs. Numbers shown go with the right edge of the bin. Negative numbers mean the 2D model underpredicted WSE.	40
Figure 15. Longitudinal profile of observed and predicted WSEs at 966 cfs.	41
Figure 16. Histogram of percent velocity error (signed) for all observations.	43
Figure 17. Scatter plot of 2D model modeled water speed versus observations showing linear regression equation and coefficient of variation. The blue line is $X=Y$ (i.e., perfect prediction ideal) and the black line is the regression of modeled versus observed measurements. The grey triangles are observations made below the first rapid downstream of the USGS gaging station. The regression in grey excludes those observations.	45
Figure 18. Spatial plot of observed (with DAVC adjustment) minus modeled velocity deviations. Darker red values are where the model under predicted velocity and darker blue is where it has over predicted. Note that legend is not equally centered.	46
Figure 19. Scatter plot of 2D model predicted water speed versus observations showing linear regression equation and coefficient of variation when the data is segregated at 2 ft/s. Red colors pertain to values greater than or equal to 2 ft/s and black colors for values less than 2 ft/s.....	47
Figure 20. Histogram evaluating 2D model velocity direction performance at 966cfs, with deviations centered on -45 to 45.	50
Figure 21. Scatterplot evaluating 2D model velocity direction performance at 966 cfs for the main flow (e.g. no eddies).....	51
Figure 22. Blimp image, flow direction observations, and 2D model predicted flow directions for a two-cell eddy on river left near the beginning of Sinoro Bar ~700 feet upstream of Narrows Gateway. Red arrows show observed directions and black arrows show model-predicted directions.	51
Figure 23. Observed redds and polygon boundaries of visually identified gravel deposits.	53
Figure 24. Zoomed in views of the three spawning clusters observed showing that they occurred on deposits from the gravel injection, though fill depth was variable.	54
Figure 25. Plots of elevation error and local surface elevation variation (σZ ; LEFT) and standard deviation of elevation error ($\sigma\Delta Z$) versus local surface elevation variation	

(σZ ; RIGHT) for the downstream area of the 2007 data.....	56
Figure 26. Plots of elevation error and local surface elevation variation (σZ ; LEFT) and standard deviation of elevation error ($\sigma\Delta Z$) versus local surface elevation variation (σZ ; RIGHT) for the upstream area of the 2007 data.	56
Figure 27. Plots of elevation error and local surface elevation variation (σZ ; LEFT) and standard deviation of elevation error ($\sigma\Delta Z$) versus local surface elevation variation (σZ ; RIGHT) for the downstream area of the October 2012 data.	57
Figure 28. Plots of elevation error and local surface elevation variation (σZ ; LEFT) and standard deviation of elevation error ($\sigma\Delta Z$) versus local surface elevation variation (σZ ; RIGHT) for the downstream area of the October 2011 data.	57
Figure 29. Plots of elevation error and local surface elevation variation (σZ ; LEFT) and standard deviation of elevation error ($\sigma\Delta Z$) versus local surface elevation variation (σZ ; RIGHT) for the upstream area of the October 2011 data.	58
Figure 30. Plots of the elevation error and local surface elevation variation (σZ ; LEFT) and standard deviation of elevation error ($\sigma\Delta Z$) versus the local surface elevation variation (σZ ; RIGHT) for for the upstream area of the October 2012 data.	58
Figure 31. Upstream injection area patterns of erosion and deposition for the October 2011 to October 2012 epoch.	63
Figure 32. Elevation change histogram for the upstream area for the October 2011 to October 2012 epoch.	64
Figure 33. Spatial patterns of deposition and erosion for the downstream area for the October 2011 to October 2012 epoch.	65
Figure 34. Close up of TCD in the vicinity of the large boulder just downstream of the main rapid. The legend is the same as in Figure 31.	66
Figure 35. Elevation change histograms for the downstream area for the October 2011 to October 2012 epoch.	67
Figure 36. Evidence of injected gravel in the Narrows Reach from a reconnaissance on August 2, 2012 at two locations (A,B).	68
Figure 37. Elevation change histogram for the upstream area for the 2007 to October 2012 epoch.	71
Figure 38. Elevation change histogram for the downstream area for the 2007 to October 2012 epoch.	71
Figure 39. Spatial patterns of deposition and erosion for the upstream area for the 2007	

to October 2012 epoch.....	72
Figure 40. Spatial patterns of deposition and erosion for the downstream area for the 2007 to October 2012 epoch.....	73
Figure 41. Electivity index (EI) for each GHSI bin. Bars above thick black line were preferred by spawners and those below the dark grey line were avoided. For the category of 0-0.2, that is excluding values of exactly 0. Therefore, the available area used in calculating EI excluded the vast area with an EI=0, because that would skew the results in exactly the way that makes the forage ratio invalid (i.e. yield such small areas for the non-zero GHSI bins that all GHSI bins would have a high EI)..	76
Figure 42. Model predicted fractional area for each GHSI bin at 996 cfs, including 0 values for the entire wetted area of the EDR. At this time most of the river lacks an alluvial, gravel/cobble bed.	77
Figure 43. Model predicted fractional area at 996 cfs for each GHSI bin, excluding areas where GHSI=0 (i.e., non-habitat).....	78
Figure 44. DHSI, VHSI, HHSI, and GHSI predicted by the 2D model for 966 cfs.....	80
Figure 45. Close views of the GHSI raster for 966 cfs with observed redds shown as magenta colored crosses for the a) lower, b) middle, and c) upper clusters. The color legend is the same as in Figure 44.....	81
Figure 46. Close views of the a)DHSI, b)VHSI, and c)GHSI raster for 966 cfs with observed redds shown as magenta colored crosses for the constructed spawning riffle. The color legend is the same as in Figure 44.....	83
Figure 47. Observed redds and boundaries for upstream and downstream TCD analysis. Note that the upper cluster is located in the constructed riffle and the middle cluster was outside of the TCD boundary.....	84
Figure 48. Histogram of TCD predicted deposition and redds showing the thickness of deposits for redds. Black represents redds that were not associated with any TCD predicted deposition, blue represents redds associated with TCD deposition outside of the constructed spawning riffle, and green are redds built on the constructed spawning riffle.	85
Figure 49. 10-m buffers around the redds in the three clusters. Redds are indicated with a black "X" and buffers are shown in transparent green. Also shown in light blue are pool morphologic units <i>as they existed in 2007</i> from Wyrick and Pasternack (2012).....	86

1.0 Introduction

1.1. Environmental Problem*

Englebright Dam on the Yuba River blocks anadromous fish migration into the upper watershed, which has impacted the potential size of the spring-run Chinook salmon meta-population in the Sacramento River watershed, of which the Yuba is a major contributing subbasin. A substantial amount of the annual spring-run Chinook salmon individuals immigrating into the Yuba River each year attempt to spawn in September in the uppermost reach below the dam, which is also the most impacted and presently unsuitable for Chinook salmon reproduction. This reach, called the Englebright Dam Reach (EDR), was decimated by cumulative effects associated with (1) local mechanized channel disturbance by gold miners, (2) overabundance of large angular rock from dam construction and landsliding, and (3) a lack of river-rounded gravel/cobble supply (Pasternack et al., 2010). The last of those is a result of the sediment supply from upstream being ruined by hydraulic gold mining, which necessitated that Englebright Dam be built to hold back the excessive waste that is well mixed with the small beneficial fraction of gravel/cobble. In 2011, non-governmental organization plaintiffs suing the National Marine Fisheries Service et al. gave expert testimony in which they stated that spring-run Chinook salmon in the Yuba River face “irreparable injury” if measures are not taken right away to address problems in the EDR. Further, in the NMFS 2012 Biological Opinion, NMFS wrote that the “lack of spawning substrate limits spawning habitat and fish production.” Note the use of the word “limits”- not that the lack of substrates is one of many stressors, but is the *limit* on habitat and fish production. NMFS went on to say that, “Lack of adequate spawning substrate presents a high risk to salmonids.” As a result, there is a consensus among diverse stakeholders and experts that the most important need for sustaining and potentially recovering spring-run Chinook salmon abundance below the dam involves addressing the geomorphic deficiencies in the EDR reach.

The scientific foundations for understanding the hydrogeomorphology of the lower Yuba River have been laid out as well as any river in the region thus far in numerous scientific technical reports and journal articles (Gilbert, 1917; Pasternack, 2008a; James et al., 2009; Pasternack et al.; 2010; Sawyer et al., 2010; Escobar and Pasternack, 2010; White et al., 2010), culminating in a YCWA relicensing existing-information report on the (Pasternack, 2010b) and a review in the GAIP (Pasternack, 2010a). Meanwhile, the Yuba Accord River Management Team has nearly completed comprehensive suite of geomorphic studies for the entire LYR as part of its Monitoring and Evaluation Plan (YARMT, 2009), including associated reports addressing 2D hydrodynamic modeling (Barker, 2011; Abu-Aly, 2012), analysis of fluvial landforms (Wyrick and Pasternack,

2011, 2012), and analysis of geomorphic change (Carley et al., submitted). Therefore, this study has a highly focused purpose to use and build on existing knowledge to facilitate science-based, transparent river rehabilitation in the EDR, which is where the dam's blockage of the gravel/cobble supply impacts the river (Pasternack, 2008a).

1.2. USACE Program to Address Problem*

The United States Army Corps of Engineers (USACE) has been injecting a mixture of coarse sediment in the gravel (2-64 mm) and cobble (64-256 mm) size range into the lower Yuba River (LYR) below Englebright Dam, with an emphasis on gravel. The first effort occurred in November 2007 and consisted of ~500 short tons of gravel/cobble sediment being injected into the Narrows II powerhouse pool. The second effort occurred November 2010 through January 2011 and consisted of ~5000 short tons of gravel/cobble sediment being injected into the chute just downstream of the Narrows I powerhouse. Future gravel injections are anticipated as part of the Corps' Gravel Augmentation Implementation Plan, which guides a long-term gravel augmentation program to provide salmon spawning habitat in the bedrock canyon downstream of Englebright Dam on the lower Yuba River.

The Gravel/Cobble Augmentation Implementation Plan for the Englebright Dam Reach (EDR) of the Lower Yuba River, CA (GAIP) describes present and proposed future efforts based on the data and information available at the time (Pasternack, 2010a). In brief, the long-term plan calls for continuing gravel/cobble injection into the EDR until the estimated coarse sediment storage deficit for the reach is eradicated, and then it calls for subsequent injections as needed to maintain the EDR sediment storage volume in the event that floods export material downstream of the reach. Monitoring is required to keep track of the sediment budget for the reach to know injections are needed and how much to add. Monitoring will also assess ecological outcomes.

Although the GAIP promotes a necessarily long-term effort to recover and sustain alluvial landforms and ecological functionality in the EDR, it does call for each year's gravel injection to try to yield a temporary riffle of value for spring-run Chinook spawning and embryo incubation in the subsequent autumn and winter. Figure 5.3 in the GAIP illustrates simple riffle design concepts for the temporary riffle to be built during gravel injection. In the upper section of EDR where the gravel is injected, the canyon is narrow and scour risk during floods is high. Pasternack (2008) reported that in the most constricted location upstream of the 2010-2011 injection point, a state of "partial transport" in which overrepresented finer gravels are scoured disproportionately begins at ~10,000cfs and full mobility of the riverbed begins at ~25,000 cfs (see figure 108 of Pasternack, 2008). Therefore, when the flows in the period

between gravel injection and Chinook spawning remain below ~10,000 cfs alluvial landforms built during injection will remain intact and usable for spawning. Take note that these estimates and conclusions were based on an assumed coarser mixture than what the USACE subsequently injected. *Having such intact features at the injection site is not a primary goal of the GAIP*, as the sustainable alluvial deposition sites are further downstream in EDR where the river widens substantially (see Figure 122 of Pasternack, 2008). The GAIP makes this clear when it says:

“If the gravel introduced in the first year washes downstream consistent with design objective #5, then that is fine, as the eroded material would still be serving the primary plan goal (design objective 1). Future injections would use the next amount of material purchased to rebuild as much of Area A, then Area B, and then Area C as possible. It is possible that frequent floods could preclude the complete design concept from ever being achieved, and that is an acceptable outcome consistent with the overall goals of the plan and the specific design objectives.”

As a result, there is extra value possible when the river’s hydrologic regime enables temporary riffle stability, but it is not an expectation or requirement.

To assess the outcome of each year’s project and the cumulative progress toward the long-term goals, the GAIP includes a formal experimental design with design objectives, hypotheses, methods, and tests (Table 1). Following through on this experiment requires science-based monitoring and evaluation of the fate of previous injections. Notably, the initial injections are the first building blocks for ecological recovery in the reach, and the response to sequential injections is not expected to be linear (e.g., Elkins et al., 2007). The outcome of hypothesis testing at incremental stages throughout the recovery of a normal volume of sediment storage will foster a better understanding of the linked physical-biological functionality of the reach, thereby enabling further improvement of the GAIP, including identification and development of potentially more detailed rehabilitation activities related to Englebright Dam impacts and the impacts of mechanized gold mining in the same reach.

Table 1. GAIP Study Hypotheses and Tests

Design objective	Design hypothesis	Approach	Test
1. Restore gravel/cobble storage	1A. Total sediment storage should be at least half of the volume of the wetted channel at a typical base flow under a heavily degraded state (Pasternack, 2008b).	Inject gravel into the river to fill up recommended volume of sediment storage space.	Use DEM differencing of bed topography over time to track changes in storage
2. Provide higher quantity of preferred-quality Chinook spawning habitat	2A. SRCS require deep, loose, river-rounded gravel/cobble for spawning (Kondolf, 2000).	Add river-rounded gravel/cobble.	Perform Wolman pebble counts of the delivered sediment stockpile and in the river after each gravel injection to insure that the mixture's distribution is in the required range.
	2B. Spawning habitat should be provided that is as close to GHSI-defined high-quality habitat as possible (Wheaton et al., 2004b)	Place and contour gravel to yield depths and velocities consistent with salmon spawning microhabitat suitability curves.	Measure and/or simulate the spatial pattern of GHSI after project construction to determine quantity of preferred-quality (GHSI>0.4) habitat present.
3. Provide adult and juvenile refugia in close proximity to spawning habitat.	3A. Structural refugia in close proximity to spawning habitat should provide resting zones for adult spawners and protection from predation and holding areas for juveniles.	Create spawning habitat in close (<10 m) proximity to pools, overhanging cover, bedrock outcrops, boulder complexes, and/or streamwood.	Measure distance from medium and high GHSI quality habitats to structural refugia and check to see that most spawning habitat is within reasonable proximity.
4. Provide morphological diversity to support ecological diversity, including behavioral choice by individuals.	4A. Designs should promote habitat heterogeneity to provide a mix of habitat patches that serve multiple species and lifestages.	Avoid GHSI optimization of excessively large contiguous areas of habitat; design for functional mosaic of geomorphic forms and habitat.	Large (>2 channel widths) patches of homogenized flow conditions in hydrodynamic model and homogenized habitat quality in GHSI model results should not be present at spawning flows.
5. Allow gravel/cobble to wash downstream	5A. Suitable mechanisms of riffle-pool maintenance are not present or realistically achievable in the upper section of the EDR	no specific action required	Conduct annual recon of EDR to track where injected gravel/cobble goes.
	5B. Flows that overtop Englebright Dam erode sediment off the placement area	no specific action required	Measure and/or simulate the spatial pattern of Shields stress and identify areas with values >0.06

2.0 Goals and Objectives*

The overall goal of this report is to evaluate the status of the EDR and the efficacy of past gravel injections into the EDR with regard to making progress toward meeting the geomorphic and ecological goals stated in the GAIP. The GAIP says that the geomorphic goal of gravel/cobble augmentation is to reinstate interdecadal, sustainable sediment transport downstream of a dam during floods, which is necessary to support and maintain diverse morphological units, such as riffles, pools, point bars, and backwaters. It says that the ecological goal of gravel/cobble augmentation that yields self-sustainable morphological units is to have the associated assemblages of physical

attributes that are preferred for each of the freshwater life stages of salmonids. To achieve these goals, it lays out a long-term plan of gravel/cobble re-introduction and monitoring to track outcomes.

2.1. GAIP Hypothesis Testing*

The GAIP includes five specific design objectives to facilitate achieving these goals), and for each one there is a specific, transparent test that can answer whether (or to what degree) the injection projects are achieving the design objectives (Table 1). Therefore, the specific objectives of this monitoring and evaluation project involve performing the tests stated in the GAIP and writing a report explaining the outcome.

2.1.1. GAIP Geomorphic Goals*

Geomorphic goals for the GAIP include 1) increasing the cobble/gravel storage, 2) allowing for downstream transport and deposition, and 3) providing morphologic unit diversity. Depending on the size of any individual gravel injection and its timing in the progression of GAIP implementation, the third objective may not be suitable for interim evaluation. It is hypothesized that gravel/cobble storage will occur as both nested depositional features and through lateral and vertical bar growth when the supplied sediment is in excess of the spatially explicit transport capacity of specific locations in the river (Table 2). Even as sediment storage increases in the reach, it is natural and expected that over time added gravel/cobble will eventually migrate downstream out of the reach. The greater the storage, the greater likelihood that sediment will export and in higher quantity. This is an outcome of the general scientific principle of flux driven by concentration gradients (e.g analogous to Fick's, Fourier's, Darcy's, and Ohm's laws): the more of something there is in one area relative to another, the more of it will be in transport for any given flow condition.)

Compared to the original conceptualization in Pasternack (2008), observations of the fate of the 2007 gravel injection expanded the scope of sediment storage processes evident in EDR. It is hypothesized that zones of sediment accumulation will fall into five categories (Table 2) tied to channel scale (Brown and Pasternack, 2012). First, at the smallest scale of bedrock fractures, small bedrock outcrops, individual boulders and large cobbles, it is hypothesized that selective deposition will occur as bedload in motion will get trapped by existing bed material larger than that in transport (Pasternack, 2009). This may account for a surprising amount of material, but it is impossible to quantify with modern technology. Second, at the hydraulic unit scale (10^{-1} - 10^0 channel widths) large bedrock outcrops and boulder clusters protrude into the flow creating obstructions that interrupt flow streamlines. Some amount of gravel and

cobble cannot manage the deflection and end up trapped in the stagnation zone upstream of the obstruction. Third, these same features also create convective acceleration and flow convergence zones around them that focus and route sediment until it reaches an abrupt expansion eddy immediately downstream of the outcrop. Some of the gravel and cobble will get pushed and pulled into the eddy and deposit there. Fourth, morphologic unit scale (10^0 - 10^1 channel widths) channel curvature can create positive feedbacks between topographic steering of the flow field, secondary flow circulation, and inward (i.e. towards the origin of curvature) deposition due to variations in cross-channel sediment competence and inward transport at the bed. Finally, as gravel accumulates locally and from curvature effects it is expected that valley scale ($>10^1$ channel widths) expansion zones will promote depositional features that may increase bed relief that can provide positive feedbacks with the prior scale dependent sediment deposition mechanisms mentioned earlier. These five mechanisms driven by different causes of topographic variation are the basis for the scientific expectation that gravel/cobble injected into the EDR will move downstream from the constricted injection zone and deposit within the reach.

Table 2. Scale dependent sediment storage mechanisms in the EDR.

Scale (Channel Widths)	Sediment Deposition Hypothesis	Dominant Topographic Elements	Detectable by TCD*?	Represented in 2D Model?
$<10^{-1}$	At the smallest scale of bedrock fractures, small bedrock outcrops, individual boulders and large cobbles, selective deposition will occur as bedload in motion will get trapped by existing bed material larger than that in transport.	Cobbles, small bedrock outcrops (<25 feet), boulders	No	No
$10^{-1}-10^0$	Large bedrock outcrops and boulder clusters protrude into the flow creating obstructions that create upstream backwater zones of preferential deposition.	Large bedrock outcrops (>25 feet), multiple boulders	Yes	Yes
$10^{-1}-10^0$	These same features also create convective acceleration and flow convergence zones around them that focus and route sediment until it reaches an abrupt expansion eddy immediately downstream of the outcrop where some of the gravel and cobble will get pushed and pulled into the eddy and deposit there.	Large bedrock outcrops (>25 feet), multiple boulders	Yes	Yes
10^0-10^1	Channel curvature can create positive feedbacks between the topographic steering of the flow field, secondary flow circulation, and inward (i.e. towards the origin of curvature) deposition due to variations in cross channel sediment competence and inward transport at the bed.	Gravel/Cobble Bars	Yes	Yes
$>10^1$	Finally, as gravel accumulates locally and from curvature effects it is expected that valley scale expansion zones will promote depositional features.	Valley scale curvature of reach	Yes	Yes

*TCD is topographic change detection.

2.1.2. GAIP Ecological Goals

Ecological goals for the GAIP are to 1) increase the quantity of high-quality habitat for spawning adult spring-run Chinook salmon, 2) provide adult and juvenile refugia in close proximity to spawning habitat, and 3) provide morphological diversity to support ecological diversity within the study reach. *It is essential to understand that at this early stage of GAIP implementation, the sediment deficit in EDR is so large that each annual augmentation is but a fractional down payment on the overall real project to erase the deficit, which is ~13-20 times the size of current annual injections (Fig. 1).* On the basis of the explanation provided in section 1.2 above and depending on several factors (i.e. the size of any individual gravel injection, its timing relative to the timing of floods and that of the freshwater life stages of salmonids, and finally, its timing in the progression of

GAIP implementation), these objectives may not be suitable for interim evaluation. To increase the quantity of high quality habitat for Chinook salmon, it is hypothesized that the augmented gravel riffle in the injection zone will be available as an ephemeral feature so long as flows are < 10,000 cfs and the median size of the injected material is ~60 mm. It is hypothesized that transported gravel/cobble will form spawning habitat downstream once there is sufficient deposition to yield suitable fluvial landforms. Similarly, it is hypothesized that self-formed spawning habitat will occur in close proximity to (e.g. < 10 m) structural refugia, such as deep pools, bedrock outcroppings, boulders, and large cobbles. These are common features of river canyons that the 2012 NMFS Biological Opinion also identifies as components of rearing habitat. To provide morphologic unit diversity it is hypothesized that floods will induce redistribution of injected gravel/cobble that will yield alluvial landforms at the scale of ~1-10 channel widths. These features in turn topographically steer in-channel flows to yield a diversity of micro- and meso-habitat conditions



Figure 1. Like in any phased construction scheme, an individual “project” will not yield the benefits anticipated for the complete structure. No one asks how many humans are living in a home after the foundation is poured. Similarly, the GAIP will not yield the desired and expected benefits to salmonid populations until the sediment deficit in EDR is erased. Interim monitoring and assessment provides insights about geomorphic mechanism and small-scale ecological functionality.

2.2. Iterative Learning and Improved Actions

The GAIP included an initial, simple gravel placement design that consistent of three sections to provide flexibility depending on how much cobble/gravel would be added each year, ranging from ~5,000 to ~13,000 short tons. The 2010-2011 project ended up injecting ~5,000 short tons during the wet season when flows were higher to get the long-term effort underway. However, there was high uncertainty about how gravel sluicing would perform in this setting and what its opportunities and limitations would be. Based on the experience in the 2010-2011 injection and the subsequent analyses, most questions about gravel transport and downstream habitat creation under conditions of minimal cobble/gravel availability were answered (see Brown and Pasternack, 2012). Lessons from all that work were used to improve the process and outcome for the 2012 project. The timing, environmental conditions and outcome of the 2012 project were totally different from those of previous ones, so this is an important opportunity to add new understanding that shores up the overall conceptualization of how the system works and what the opportunities and constraints are on the GAIP. With each subsequent project to meet the long-term goals of the GAIP, further lessons will arise and help guide future efforts.

3.0 2012 EDR Gravel Augmentation Project

The gravel/cobble injection began with gravel entering the river on July 18, 2012 and ended with the last gravel going in the last week of August 2012. It took a few days prior to that for the initial set up of the sluicing system according to the layout in the GAIP. During the first two weeks of injection additional safety measures and *ad hoc* system improvements were incrementally implemented to add layers of protection to avoid potential problems.

Pursuant to the prior year's monitoring report (Brown and Pasternack, 2012) several modifications were made to the sluicing operation. First, the hopper was relocated at the switchback on the dam access road (Fig. 2). Second, a more sophisticated system of barges, pulleys, and cableways was implemented that increased control over the outlet of the sluice pipe in the river (Fig. 3). The pulley and cableway system was instrumental in first placing gravel on river left and then gradually shifting the pipe outlet to river right as the channel filled. Barges allowed the pipe system to extend further across and downstream than previously configured, so cobble/gravel could be placed in a more controlled way further downstream, rather than just washing down there. An additional key learning outcome was that using instream boulders as structural elements upon which to directly injected gravels increased structural stability, especially in the center of the channel. Overall, the project proceeded at a much quicker rate than the prior year.

As discussed in section 9.2 of Brown and Pasternack (2012), a consensus emerged in early 2012 among project participants and LYR stakeholders that the 2006 sediment mix specified by the LYR Technical Working Group on the basis of USFWS observations on the Stanislaus River (Table 3) was not suitable for LYR spawning habitat, especially in the EDR. As summarized by Brown and Pasternack (2012) several scientific studies of riverbed sediment on the LYR in recent years now provide an accurate portrayal of salmonid spawning substrates. Whereas the Stanislaus mix design had >42.5 % of material < 32 mm, LYR spawning substrates have only 19 % of material < 32 mm (Table 4). On the basis of actual LYR conditions and sediment-slucing considerations, a new cobble/gravel mix design was developed (Table 5). Project participants, governmental regulators, and other stakeholders all approved the new mix.

During gravel injection there was regular communication between the construction contractor, USACE staff, and the authors of this report (who helped oversee the project and troubleshoot issues as they arose). USACE staff monitored turbidity downstream of the injection site and performed pebble counts on the delivered material. The authors of this report assisted with injection activities at the sluice outlet and provided guidance on how much gravel to put in different sections of the injection zone. A few times, the staff of the UC Sierra Foothills Research and Extension Center helped out with machine shop tinkering of parts and receiving deliveries. The construction contractor did an excellent job of keeping everyone involved informed of the project's status. Periodic visits by observers were facilitated by the participants upon request.

Table 3. Original gravel/cobble mix design in the GAIP.

Size class (mm)	Size class (in)	% retained	Fractional %
102-127	4 to 5	0 - 5	2.5
51-102	2 to 4	15 - 30	20
25-51	1 to 2	50 - 60	35
19-25	¾ to 1	60 - 75	15
13-19	½ to ¾	85 - 90	15
6-13	¼ to ½	95 - 100	10
<6	< ¼	100	2.5

*Based on Stanislaus River information

Table 4. Observed 2010-2011 LYR redd substrate composition.

Size class (mm)	Size class (in)	% retained	Fractional %
>256	>10	0.87	0.87
128-256	5 to 10	11.15	10.28
90-128	3.5 to 5	41.34	30.19
32-90	1.25 to 3.5	81.31	39.97
2-32	0.08 to 1.25	99.47	18.16
<2	<0.08	100	0.53

Table 5. Planned 2012 gravel/cobble mix design.

Size class (mm)	Size class (in)	% retained	Fractional %
90-128	3.5 to 5	30	30
32-90	1.25 to 3.5	80	50
19-32	$\frac{3}{4}$ to 1.25	88	8
13-19	$\frac{1}{2}$ to $\frac{3}{4}$	96	8
6-13	$\frac{1}{4}$ to $\frac{1}{2}$	100	4



Figure 2. The relocated hopper at the switchback on the dam access road.



Figure 3. The sluice pipe outlet in the river without barges and only a limited cableway (top) showing that the pipe is pushed downstream by the flow and there is less control on cobble/gravel placement. When barges and cableway are used (bottom) there is excellent control on pipe length and positioning.

3.1. Peak Flow Hydrology Before and after Injection

The last report covered the period of November 1, 2007 to November 1, 2011. This report picks up at that point and goes through December 1, 2012. During this period, the hydrograph for the Smartsville gage below Englebright Dam showed two floods where the bankfull discharge of 5,000 cfs was approached or exceeded (Fig. 5). The December through February period of 2012 that exhibits the highest monthly precipitation on average over the long term turned out to not produce any notable flows. Then the first flood came during mid-March, peaking at just over 12,300 cfs. The second peak of ~10,000 cfs came later in the spring at the end of April. Both of these events happened at a time when there was already very little cobble/gravel in the injection zone due to flows in December and January 2011 (Brown and Pasternack, 2012), so the primary effect was to continue to redistribute the sediment from the 2010-2011 injection throughout the reach. Based on the results of previous studies, these flows are known to be sufficient to cause topographic change and sediment transport in the EDR. Right at the end of this study period an atmospheric river came across the Pacific Ocean and dumped a large intensity of rain in early December. That event and its effects are not covered in this report, but will be addressed in the next report. This report aims to document and analyze the geomorphic and ecological response to the cumulative effects of the 2010-2011 and 2012 cobble/gravel injections as observed in autumn 2012 right up to the December flood. Looking at the hydrograph within a more restricted window for autumn salmon spawning conditions, flows were quite constant, especially during 10/1 to 11/4 (Fig. 5). Flows fluctuated a little more in November.

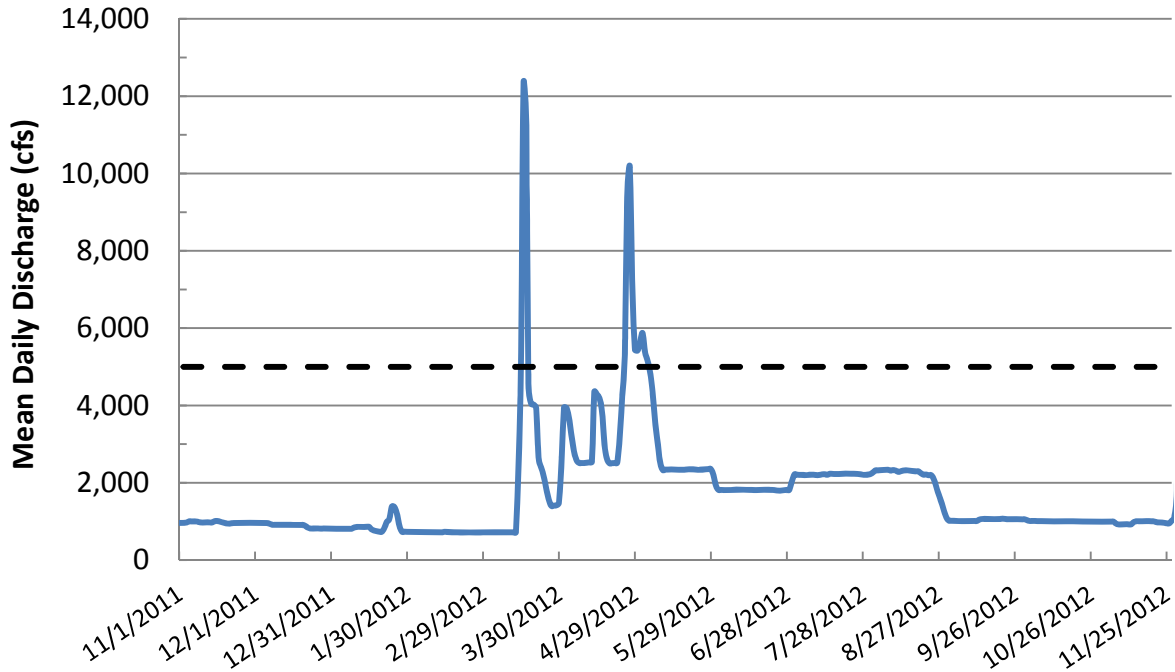


Figure 4. Discharge recorded at the Smartsville gage (<http://cdec.water.ca.gov>; YRS) during the period between September 2011 and January 2013. Note that these are mean daily values so hourly data would reveal more insight into actual peak flows, but this plot does show the overall trend in discharge.

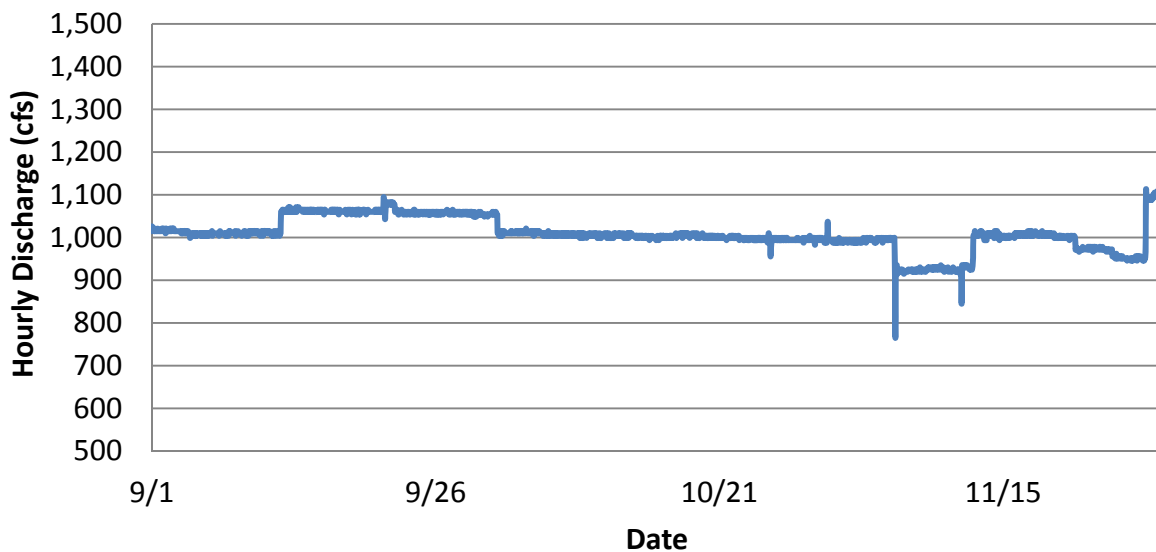


Figure 5. Discharge recorded at the Smartsville gage (<http://cdec.water.ca.gov>; YRS) during the period between August 2012 and January 2013.

4.0 Post-Project Data Collection

Data collection and project monitoring took place in two phases- first in the summer before the 2012 cobble/ ravel injection was begun and second in the fall after it was completed. All of the feasible topographic data was collected, enabling evaluation of GAIP design hypotheses building on the work of the previous report. In addition, an independent weekly redd survey was undertaken and reported on by the Pacific States Marine Fisheries Commission with assistance from the Yuba Accord RMT. The data from that effort was used in this report to address GAIP design hypotheses as well.

4.1. Topography and Bathymetry

The baseline EDR topographic map for analysis of channel change and sediment-budget computation dates to a period from 2005-2007 when EDR was mapped (Pasternack, 2008). New topographic and bathymetric surveys took place a few weeks before and after the injection a week span during July and October of 2012. Existing topographic ground control for the EDR was used that is tied into the State Plane California Zone 2 coordinate system in units of feet with NAD 1983 and NAVD88 horizontal and vertical datums, respectively. Terrestrial (and some wadable aquatic) surveying was done using a Leica TPS1200 total station and a Trimble R7 RTK GPS to map emergent and shallow gravel. Bathymetric mapping where depth > 1.0' was performed using the same methodology as last year where a kayak was outfitted with an echosounder and RTK GPS. The approach used involved a Sonarmite echosounder (Seafloor Systems, Inc., Folsom, CA) coupled with a Trimble R7 RTK GPS for geographic positioning mounted onto a kayak.

To collect data for the pre-injection condition a modest survey campaign occurred on July 10th that leveraged an existing study by the RMT to model juvenile rearing habitat. As part of this effort, kayak based bathymetric mapping in the channel and ground based Total Station mapping on river left occurred. The total number of points collected was 5,776 over an area of 50,900 ft², yielding an overall point density of 0.11 points per square foot (Fig. 6).

Post-injection terrestrial and bathymetric data were collected ds in October 2012. All areas within the study reach were surveyed with the exception of the area immediately upstream and the center of the rapid downstream of the USGS gaging station due to safety reasons and problems with air bubbles confounding the echosounder. For the October 2012 survey the total number of points collected was 29,683 of which 27,855 were used in the analyses over an area of 304,603 ft², yielding a point density of 0.09 points per square foot, which is ~1 point per square meter (Fig. 7).

During the summer survey on July 10th the Smartsville gage was ~2,198 cfs and for the October survey flows were ~996 cfs (Table 6). These flow values are important because they are used in 2D models for sections 6.3 and 6.7 for model validation and subsequent Chinook adult spawning habitat predictions. Table 6 shows that for each survey period there was a standard deviation of 6-8 cfs (~1% of total discharge) as the river discharge fluctuated over these days. This is a small fraction, but it does cause some small uncertainty in comparing predictions against observations, because the predictions are for fixed discharge values and the observations are for ones with small fluctuations.

Table 6. YRS gage discharges during survey dates in 2012.

Dates	Average Discharge	Standard Deviation
July 10th	2,198	5
October 25,26	995	8
October 29,30	996	7

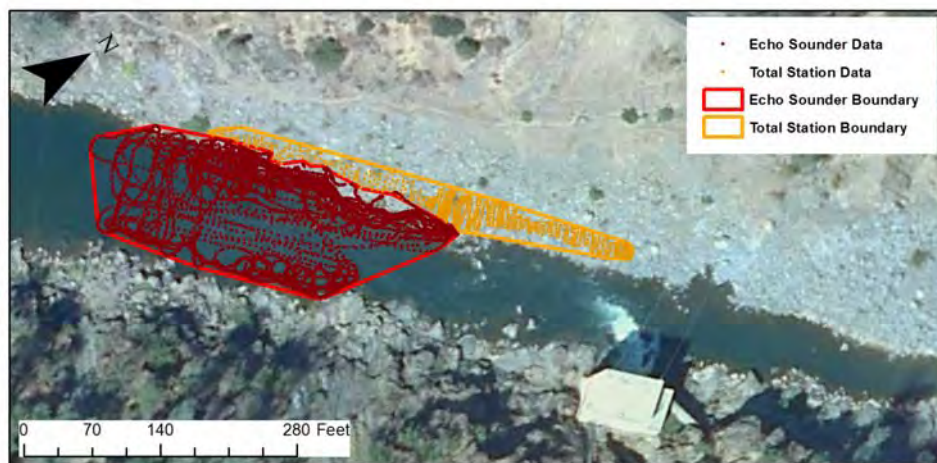


Figure 6. Survey limits and collected points in July 2012.

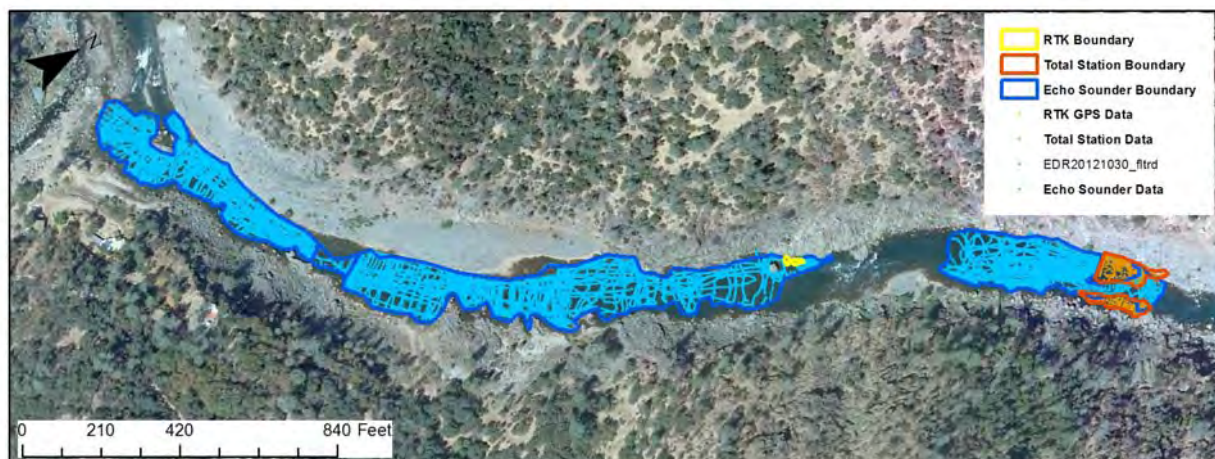


Figure 7. Survey limits and collected points in October 2012.

4.2. Water Depth & Surface Elevation Data

A benefit of using the kayak-based approach to bathymetric surveying is that each depth sounding may be combined with local bed elevation and sensor depth to obtain observed water surface elevation (WSE). Because the kayak bobs up and down in the water, the observed WSE value can deviate from the correct value (whereas this does not affect bed elevation mapping), suggesting that some averaging be used to smooth that out. A 2D model may be validated against either depth or WSE, since they contain the same information, but WSE is more useful for understanding model performance relative to topographic controls, so that was the approach in this study. Depth observations were collected at 0.2-1.0 Hz continuously, so the data was filtered to yield areal averages suitable for assessing the longitudinal pattern of WSE, which is a primary indicator of model performance, especially in terms of the suitability of the bed roughness parameter.

To obtain WSE areal averages from observations, the data was averaged within 20'-spaced rectangles aligned down the river. First, the river was stationed with cross-sections in 10' intervals. Next, the cross-sections were buffered upstream and downstream by 10' to obtain rectangular polygons. Then the WSE point observations at each discharge within each polygon were averaged and the average value assigned to a field within the polygon attribute table. Similarly, the 2D-model-predicted WSEs at each discharge were averaged within each polygon and the average value assigned to a field within the polygon attribute table. In section 6.3.2 these values are compared against those predicted by the 2D model as a test of model performance.

4.3. Water Velocity Vector Data*

As part of Yuba Accord RMT scientific investigations, Barker (2011) developed, tested, and applied a new kayak-based tracer method for validating 2D model performance in velocity prediction that not only tests water speed, but also tests flow direction. The ability to predict flow direction is what distinguishes 2D modeling, but prior to the development of this new method, measurement of flow direction was too time consuming and broadly ignored in 2D model studies. There are five key elements to this new method. First, a kayak is used as a tracer to move with the current along a selected streamline and an RTK GPS on the kayak records accurate positions on a fixed time interval (depending on velocity- high velocity gets high sampling frequency and low velocity gets low sampling frequency). Second, the kayaker is responsible for selecting diverse streamlines to sample the full range of velocities as equally as possible and the kayaker must keep the kayak moving at the same speed and direction as the ambient flow, as indicated by air bubbles, sticks, and other ambient debris that helps visualize the ambient velocity field. Third, the distance between two adjacent boat positions on a streamline is divided by the time between observations to obtain the surface speed and this value is assigned to the midpoint between the two boat positions. Also, the direction of velocity at each midpoint is computed based on the orientation of the line segment drawn between the two boat positions. Fourth, surface speed is correlated against 2D model prediction of depth-averaged speed and surface speed is adjusted to a depth-averaged value using a depth-average velocity constant (DAVC). By making detailed observations of the vertical velocity profile on the lower Mokelumne River, Pasternack et al. (2006) found a DAVC value of 0.71 by least squares regression. Note that the correlation coefficient (R) is insensitive to the DAVC, because multiplying all surface velocities by the DAVC results in a uniform shift that does not change the relative structure of the data for correlation analysis. Finally, because the method is capable of yielding an order of magnitude more observations spanning a wider range of ambient velocities than traditional methods (when done for an equal amount of time), statistical tests of 2D model performance end up having far higher confidence and adherence to statistical assumptions. By using the Barker (2011) method to evaluate 2D model performance, this study applied the broadest and strictest standards for determining if the model was valid or not.

4.4. Wolman Pebble Counts*

Wolman pebble counting is a method for measuring and characterizing the grain size distribution of the surface of a river bed (Wolman, 1954). Studies have shown that for a homogenous mixture, a Wolman pebble count yields the same results as a weight-based sieving procedure (Kellerhals and Bray, 1971). Such counts were performed regularly

on the gravel/cobble injection supply at the holding pile adjacent to the hopper used in the 2012 project, so there is a good characterization of the mixture as it was just before going into the river. Because the material was slowly sluiced into the river, it likely fractionated by size through the mechanism of hydraulic sorting in the sluice pipe, again as it trickled into the high-velocity flow of the river.

Towards the end of the gravel/cobble injection project on August 16th four wadable instream locations on river right were identified and assayed for particle size distribution. At each location, 100 particles were sampled using a standard gravel template (i.e., measuring b-axis dimensions of clasts) over a ~3x3-m² section of the bed. Less than 1% of particles within the ~3x3-m² area were removed from the bed during sampling; thus, there was negligible alteration to substrate texture as a result of sampling (Moir and Pasternack, 2010). From these data, the sediment sizes of which 50 and 90% of the samples are finer (i.e., D₅₀, D₉₀) were computed, among other metrics.

4.5. Blimp Aerial Imagery*

Ultra-high-resolution (<5x5-cm² pixels) aerial imagery of the EDR was desired to facilitate gravel/cobble injection planning and to track gravels at transparent depths. The approach used in this study involved lofting a ~3'x6' (oblong ellipsoid) tethered helium kite-blimp with a 14.7 megapixel digital camera (Canon Powershot SD990 IS). Numbered plywood tiles were laid out on the river banks on both sides of the channel for the full reach at a spacing of approximately 50 feet for georeferencing.

Over five separate periods in October and November 2012 the kite-blimp was lofted above the riverbed and moved up and down the reach to gather aerial images. Photos were later examined to pick the best ones for use in creating a series with ~30% overlap between sequential images.

The program Agisoft Photoscan was used to automatically mosaic blimp images. Each set of images was reduced into 2-4 mosaics to keep file sizes manageable, while retaining full resolution in the source images. The basic workflow is to add photos, match photos using scale invariant keypoint matching (Lowe, 2004), and mosaic. After a mosaic was constructed, the final image was georectified in ArcGIS using known targets on the prior year's mosaic (Fig. 8).



Figure 8. Final mosaic for the 2012 blimp imagery.

4.6. Topographic Map Construction

Because this study evaluated time-dependent changes in topography, it was necessary to create topographic maps for the three times considered. The times considered here are October 2011 (baseline reference map from the end of the previous study period), July 2012 (upstream pre-project condition before the 2012 injection), and October 2012 (post-project condition for the entire EDR in the fall after the injection was done and salmon spawning was underway). The data available from each time were used to map the surveyed areas, not to produce a complete map of the whole EDR for each time. The baseline map for October 2011 was previously produced and reported by Brown and Pasternack (2012); it is a complete map of EDR including hillsides. The mapped areas for July and October 2012 are shown in Figure 6 and Figure 7. The partial maps from these recent times were the ones relevant for answering questions about channel change and gravel/cobble erosion and deposition.

In addition to these partial maps, a new comprehensive map for the whole EDR was made blending the most recent observations available at each location; some locations, especially the hillsides, continue to use older data from 1999 and 2005-2007, because they are out of the channel and not a priority to re-map. Because it remains infeasible to map the center of the rapid below the USGS gaging station (just as it was previous efforts), it was necessary to use breaklines and artificial contours to create the best representation as possible for that small but important location that acts as a hydraulic control on channel upstream of it. This new complete EDR map was used to make a new 2D model of the reach to assess physical processes and fish habitat representing the autumn 2012 state of the river.

Topographic maps and associated digital elevation models (DEMs) were made in ArcGIS 10 using 3D Analyst. For each survey, boundary polygons were drawn around the new data collected at that time. Then a triangulated irregular network (TIN) was created using the points in the boundary polygons and the boundary itself as a hard clip. Finally, the TIN was converted to a 3'x3' raster for that point in time. IN all, the rasters for all times were the data used for evaluating topographic changes through time, which are indicative of gravel/cobble erosion and deposition as well as pre-existing channel change 2011-2012. A similar procedure was used to create a TIN and 3'x3' raster of the new complete EDR map. The final 3'x3' EDR raster map was converted to a uniform point grid and these point data were used in the procedure to make the new 2D model.

4.7. 2D Numerical Model

A major tool used in this study to evaluate the design hypotheses was a 2D (depth-averaged) hydrodynamic model. 2D models can simulate the spatial pattern of depth and velocity at points in a river. They are rapidly increasing in their use in private and academic settings as the necessary tool needed to assess geomorphic and ecological outcomes associated with river management and engineering (Pasternack et al., 2004; Brown and Pasternack, 2009; Pasternack, 2011). A 2D model solves the two dimensional equations for the conservation of water mass and momentum within a specified spatial domain. A downstream boundary of measured WSE is used along with an upstream boundary water inflow rate. Two model parameters (channel roughness and a turbulence closure parameter) must be specified as well.

The software used to perform 2D modeling was SRH-2D (with the aid of SMS 10.1 for computational mesh generation). SRH-2D was developed by the U.S. Bureau of Reclamation and is freely available to the public. This modeling software was used by the RMT to simulate 2D hydraulics for the entire LYR using the 2008-2009 topographic map for flows ranging from 300 to 110,400 cfs. It was also used for the 2D model simulations in the GAIP. The model uses a finite volume numerical scheme that can handle subcritical and supercritical flow. The algorithm is extremely efficient and stable for handling wetting and drying as well as steady or unsteady flows. Model outputs include water surface elevation, water depth, depth-averaged velocity components, depth-averaged water speed, Froude number, and shear stress. For more information, see <http://www.usbr.gov/pmts/sediment/model/srh2d/index.html>.

Based on lessons learned from previous modeling efforts and advances in the science of 2D modeling, a new computational mesh was created in 2011 for EDR to go with the current and future topographic maps. The mesh has 134,702 computational elements

with ~3' inter-nodal spacing. The mesh extends up the canyon walls to enable it to be useful for future efforts to simulate a range of flows (Fig. 9). Compared to the pre-GAIP models constructed in 2007-2010, the location and alignment for the current model's exit flow boundary was shifted to be upstream of the crest of the Narrows Gateway rapid and to cross the channel where there is a more uniform cross-channel WSE. This remains an uncertainty, because the Narrows Gateway rapid appears to be eroding unevenly, making the WSE change somewhat through time. The new alignment is still consistent with the observational WSE data used to create the stage-discharge rating curve for this reach, but that curve is likely changing over time. Topographic points from the new complete EDR map on a 3'x3' grid were imported into SMS and used to interpolate the elevations of the new computational mesh nodes in the new 2D model.

SRH-2D requires the user to select a turbulence closure scheme. Traditionally, 2D models of the lower Yuba River were made using parabolic (Zero-Equation) closure with an eddy viscosity coefficient value of 0.6 (Moir and Pasternack, 2008; Sawyer et al., 2010; Barker, 2011). New research by co-author Pasternack suggests that 0.1 performs better by decreasing overpredicting of low velocities, so the RMT's flood models for flows $\geq 10,000$ cfs use that value. In this study, both of those values as well as a completely different turbulence close scheme ($k-\epsilon$ model) were tested using the observational data for WSE and velocity vectors. This study eventually settled on the $k-\epsilon$ model due to its balanced performance across all indicators during the autumnal spawning flows that were evaluated, as explained later.



Figure 9. Extent of EDR 2D model computational mesh for in-channel low flows.

4.8. Fish Observations

Among other things, this study sought to bioverify 2D physical habitat suitability modeling, so that the approach can be used to evaluate the GAIP's habitat-related design hypotheses. Redd surveys were done by Campos and Massa (2013) from September 19, 2012 to January 30, 2013, but observations in December 2012 were hampered by two floods. Campos and Massa (2013) evaluated four aspects of physical

habitat for Chinook salmon in the EDR including the number of redds, the spatial and temporal distribution of redds, the level of redd superimposition, and physical characterization of redds. Substrate was visually characterized at each redd according to a protocol established by the RMT (Campos and Massa, 2012). This study only makes use of the data up to and including 11/26/12, because the goal is to assess habitat utilization when conditions were suitable for spawning, not in the midst of large floods. Also the effects of the December 2012 floods will be addressed in a subsequent report. Within this truncated period, average weekly flows ranged from 947 to 1063 , while the instantaneous discharge during this period ranged from 765 to 1,094 cfs (Table 7).

Table 7. Discharge during 2012-2013 EDR Spawning Observations.

Weekly Spawning Survey End Date	Flow Previous Week (cfs)		Number of Redds
	Average	Standard Deviation	
9/19/2012	1059	13.2	3
9/24/2012	1063	7.3	7
10/1/2012	1057	3.5	4
10/11/2012	1007	4.0	2
10/17/2012	1003	3.6	16
10/22/2012	1002	3.5	6
10/31/2012	995	5.6	6
11/7/2012	967	37.8	4
11/13/2012	947	36.3	1
11/19/2012	1006	4.3	4
11/26/2012	971	17.2	5
1/9/2013*	2028	132.8	2
1/24/2013*	1961	71.6	1
1/30/2013*	1692	95.1	3

*These data after floods were not used in this study.

5.0 Data Analysis Methods*

5.1. Areal Extent of Gravel/Cobble Deposits from Blimp Imagery*

A first step in assessing the spatial position of the gravel/cobble deposits was to determine areas of deposition of augmented gravels from the blimp imagery. To do this, the bright-light mosaic was processed in ArcGIS 10 using the image analysis toolbar to help visualize the deposits better. Adjustment of image brightness and contrast provided the best way to isolate patches of new gravel. Once areas were identified their spatial extents were mapped by creating a polygon shapefile. The final mosaic images had raster resolutions of 0.19 feet (5.8 cm).

5.2. 2D Model Validation*

A necessary step in using any model is validating predicted outputs to real world observations. Two-dimensional models have inherent strengths and weaknesses, thus uncertainty in modeled results needs to be understood and accepted (Van Asselt and Rotmans, 2002). There are no agreed upon scientific standards for deciding whether a 2D model is accurate or not, so it is necessary to set transparent performance indicators and validation thresholds. Some examples of studies that have done 2D model validation include Lane (1998), Lane (1999), Gard (2003), Stewart (2000), Pasternack et al. (2004, 2006), Brown and Pasternack (2008), Moir and Pasternack (2008), and Pasternack and Senter (2011). In this study, more and stricter criteria for model performance were used to insure a rigorous analysis and characterization of model uncertainty.

Previous studies using 2D hydrodynamic models for gravel-bed rivers comparable to the lower Yuba River have validated the model for this application and provide valuable information regarding model utility and uncertainty (Pasternack et al., 2004, 2006; Wheaton et al., 2004a; MacWilliams et al., 2006; Elkins et al., 2007; Brown and Pasternack, 2008). However, in this study the canyon setting is far more topographically complex, so it was important to evaluate model performance. As part of model development, the model was first tested with a few different Manning's n channel roughness values and turbulence closure parameter values to evaluate the effects on deviation between the observed and predicted longitudinal profiles of water surface elevation. Then predicted and observed water speeds and velocity directions at independent locations were compared to provide an assessment of model accuracy and uncertainty.

In addition, past studies evaluating 2D model performance over a wide range of discharges (i.e. one to three orders of magnitude) found no systematic differences in model performance for velocity prediction associated with discharge (Pasternack and

Senter, 2011; Barker, 2011). Discharges to be simulated in this study were all in a narrow range of baseflow conditions, so validation was done on a single day at a single flow.

Almost all published studies that included validation used some test of accuracy for depth or WSE (since they include the same information) as well as for water speed in the direction of flow. Velocity in a 2D model is a vector, not a scalar, so it has both magnitude and direction or two velocity components. Very few studies report mass conservation performance. Similarly, very few studies evaluate flow direction or the velocity components independently, despite this being the unique identifying aspect of a 2D model. Some exceptions are Lane (1999), Barker (2011), and now this study.

5.2.1. Mass Conservation Standard*

Surprisingly few studies evaluate mass conservation performance, especially for long, complex model reaches where mass loss can be significant. By comparison, discharge gaging at USGS gaging stations is normally within ~5-10% of the actual value, so having substantially higher accuracy than that hardly matters. A mass loss > ~2-3% of the flow input for a long segment is a sign of poor model performance (Pasternack and Senter, 2011). For a short reach such as EDR, mass loss should be < ~0.1-0.5 % based on simple reasoning. For example, for an input of 1000 cfs, a mass loss of 0.1-0.5 % would correspond with ~1-5 cfs.

5.2.2. Types of Variables Assessed*

Due to relatively steady discharge during fall 2012 (Fig. 5; Table 7) it was only necessary to make a 2D model for one flow. To validate the model three variables were assessed including water surface elevation (WSE), velocity magnitude, and velocity direction. For each variable, some tests are done on the raw values, some on the raw (i.e. signed) deviations between observed and predicted, some on the absolute value (i.e. unsigned) deviations, and some on the signed or unsigned percent errors. WSE has to be analyzed in terms of deviations, not percent error. The reason is that WSE values are generally high numbers when a river is far from the ocean, so a small water surface deviation is a minuscule fraction of WSE. For example, a WSE deviation of 2 ft would yield a percent error of 0.1 % if the WSE happens to be 2000 ft high on a mountain for the datum and coordinate system used in a given study. That creates the false impression that the error is small (0.1%), but in fact a WSE deviation of 2 ft is usually considered unacceptably high. In contrast, for depth and speed validation, percent error is a meaningful number, because the deviations are a substantial fraction of the observed values. Percent error is a variable that is easily recognized and interpreted by most

readers. Sometimes percent error is not evaluated for low values of depth or velocity, because the difference between a depth of 0.01' and 0.1' is usually not meaningful, but it does yield an enormous numerical error. That is why some studies report deviations instead of percent errors.

5.2.3. Validation Tests and Performance Standards*

For each of the variables, there are different tests to assess model performance. One approach is to make a cross-sectional or longitudinal plot of observed and predicted conditions, which allow for visual inspection of the lateral pattern of accuracy, which can reveal the cause of inaccuracy (e.g. Pasternack, et al., 2004, 2006). However, statistical tests provide a more robust and objective basis for evaluation, so sectional plots should only be used as a secondary basis for evaluation. In hydrological modeling (i.e. rainfall to runoff), it is very rare for modelers to show head-to-head scatter plots, and in hydraulic modeling it is only sometimes done. One argument against analysis of a scatter plot is that it does not convey an understanding as to why individual points are deviating from a one-to-one line. Instead, cross-sectional comparisons show the role of eddy viscosity limitations and patterns of topographic variability. On the other hand, a scatter plot provides the most rigorous quantitative evaluation of the entire data set as opposed to specific locations. For larger study areas this is a preferred approach because it looks at systemic, rather than local, deviations in performance.

Statistics for signed and unsigned variables are useful performance metrics because they can be generated and compared against reference data and past studies. For all signed variables, statistics and plots should show that the data are centered on zero, which means there is no bias in the model predictions. There is no standard as to how much bias is permitted before a model is invalid, but the closer to zero, the better. In hydrodynamic modeling the statistical distributions of depth and WSE deviations should be compared to that from topographic deviations obtained from testing of different survey methods to make sure that model prediction deviations are no noisier than topographic uncertainty. For example, if topographic error is biased, then it could prove difficult for 2D model predictions to avoid bias as well. Also, if the underlying map is accurate to within 0.5 ft, then it cannot be expected that 2D model depth predictions should be accurate to much better than that, because topographic error is the predominant factor explaining 2D model error in depth prediction (Pasternack et al., 2006). There is no standard for how accurate depth prediction has to be relative to topographic uncertainty before the model is invalid, but as a starting point one could use the standard that the metrics for topographic deviations should not be exceeded by those for depth or WSE deviations.

Correlation and regression analyses are highly useful for evaluating 2D model performance. Some studies report R-values, but that can be misleading and it is fairer to report R^2 values. R^2 is always higher for depth (~0.7-0.8) and lower for water speed, as the latter is highly sensitive to the nonlinear terms of the momentum equation. Based on a review of the literature, people have deemed their models valid even with R^2 values as low as ~0.4 for water speed. Many 2D models yield R^2 values of ~0.6 for water speed, with the best performing models for natural rivers being in the ~0.7-0.85 range. Barker (2011) found that for RMT's 2D model of the alluvial LYR, the R^2 value for velocity was 0.79. Note that 2D models of flumes with bed undulations and porous beds have R^2 -values of 0.9-1.0, indicating that topographic accuracy and channel complexity are key factors explaining why 2D models of natural rivers are not as good as 2D models are capable of predicting.

A major drawback of relying only on R^2 as a model test is that it only indicates the degree to which one variable is predictive of another, but that is not the same as testing accuracy. Given the linear regression equation between predicted vs. observed velocity, the slope of the equation indicates whether the model is biased or not. Several studies have reported a bias toward over predicting low velocities and under predicting high velocities. This has been attributed to excessive lateral mixing caused by the parabolic turbulence close scheme using an eddy viscosity coefficient value of ~0.5-0.8 (MacWilliams et al., 2006; Pasternack et al., 2006). Meanwhile, the y-intercept of the regression equation indicates whether the model has an overall shift of over- or under-prediction, which might be due to an inappropriate Manning's n value. There are no standards for these metrics, but as a starting point we propose that the slope be >0.8 and the intercept be <10% of V_{\max} . Once there are more studies using these metrics, these thresholds can be revisited.

Another important set of measures of model accuracy comes from statistical analysis of unsigned percent error of depth and velocity. Commonly 2D models yield a mean error of ~10-15% for depth and ~20-30% for velocity. Median error is usually lower than mean error, due to the influence of a few outliers on the mean value. There are no set standards, but if the mean velocity error >40%, then that would be unusually poor performance compared to past studies. Another test that is sometimes done is to break up velocity tests for low and high values, recognizing that a small deviation in velocity at low velocity can yield an unusually high percent error. There is no specified cut-off, but some studies have used 2 or 3 ft/s to differentiate the performance at lower and higher velocities.

Finally, there are no proposed metrics for accuracy in prediction of velocity direction. Only two previous studies have ever tested the 2D flow pattern at velocity observations (Lane, 1999; Barker, 2011). Lane (1999) analyzed 3D velocity components and used

similar metrics as commonly used for water speed in the direction of flow. Barker (2011) tested flow direction based on particle tracking with RTK GPS. For observations generally made in the mean flow direction, that study reported an unsigned direction angle deviation of -0.11° , a mean signed deviation of 5.5° , an R^2 between observed and predicted direction angle of 0.80, and a linear regression slope for that comparison of 0.90. For unsigned deviation, an average of 10° is proposed as the cutoff above which a model is not validated. In addition, Barker (2011) illustrated locations of poor model performance at some large eddies and explained why those problems occurred.

5.3. Topographic Change Detection By DEM Differencing

Per the GAIP, the test for design hypothesis one is an evaluation of topographic change from difference of DEMs (Wheaton et al, 2010a,b; Carley et al., 2012). In simplest terms, a DEM difference is just the subtraction of one topographic map (i.e. a raster map) from another with the resulting difference indicating the locations and magnitudes of landform change. The map of topographic change itself may be represented by a DEM, so it is termed the DEM of Difference (DoD). However, topographic maps have uncertainties in them that people normally do not think much about. When a DoD is produced, it not only has the errors from each source map, but also the errors of propagation through the mathematics. As a result, it is crucial to characterize DoD uncertainty instead of relying on analysis of a raw DoD. Topographic change detection (TCD) by DoD analysis including uncertainty is a rapidly progressing technique for monitoring and understanding rivers (Wheaton et al., 2010a,b; Carley et al., 2012). For this study, three sets of topographic data were used in four topographic change scenarios to evaluate changes in topography using the method developed by the RMT for use on the lower Yuba River (Carley et al., 2012).

5.3.1. TCD Components

Because of the significant role of the rapid downstream of the USGS gaging station in serving as a topographic control on channel hydraulics, EDR was divided into two sections for TCD by DOD analysis at this location, segregated by a red line in the results figures. The upstream area (injection zone to crest of rapid) was isolated to assess sequential fill and scour periods that occurred between the October 2011 and October 2012 surveys. The downstream area (rapid crest to Narrows Gateway entrance) was isolated to analyze the overall net change in the river between the October 2011 and October 2012 surveys. Further, both areas were also assessed between the 2007 and October, 2012 survey as well to evaluate the status of gravel injections in the study reach.

5.3.2. TCD Production Workflow

The Carley et al. (2012) method of accounting for uncertainty with geomorphic change detection was once again utilized to perform topographic change detection and analysis with an additional improvement related to generating a survey and instrumentation error (SIE) function. This method is based on the idea that locations where there is a lot of topographic variation in the raw point data for a topographic map are the ones that are most uncertain (Heritage et al., 2009). Consequently, the more variation a location has, the higher the bar has to be to consider raw DoD values as real as opposed to an artifact of map errors. Topographic variation stems from measurement error as well as natural sharp features (e.g. steep banks, boulder clusters, and sedimentary bars). By focusing on the existence of topographic variation regardless of its cause, the method is less sensitive to expert-based decisions as to potential native sources of topographic error.

A departure from the analysis of Brown and Pasternack (2012) was the development and use of data driven survey and instrumentation error (SIE) functions. The methodology developed by Milan et al. (2011) was used to achieve this. This method develops data specific SIE functions for each survey period and extent based on the raw surveyed point elevations, Z_S , the raster interpolated elevations, Z_R , the local surface elevation variation, σ_Z , and the standard deviation of elevation variation, $\sigma_{\Delta Z}$. The analysis involved the following steps in ArcGIS 10 adapted from Milan et al. (2011):

- a.
 1. Convert final topographic TIN for each time point to 1-ft raster and clip to TCD extents
 2. Convert each raster to points, creating the raster elevation Z_R dataset.
 3. Create a standard deviation raster with a 3-ft grid, producing the σ_Z data set.
 4. Merge all raw surveyed point data sets so that they have the same field for surveyed elevation values, Z_S .
 5. Spatial join Z_S with Z_R
 6. Calculate $\Delta Z = Z_R - Z_S$
 7. Sample the σ_Z data set to the point file with Z_S with Z_R .
 8. Make scatterplot of ΔZ vs. σ_Z
 9. Aggregate ΔZ values within 0.25' intervals of σ_Z and compute $\sigma_{\Delta Z}$ for each bin.
 10. Plot $\sigma_{\Delta Z}$ vs σ_Z and fit the best trendline to that possible. The trendline is the SIE function needed.

•
With an SIE function for each survey epoch and TCD extent, implementation of the Carley et al. (2012) method used in this study involved the following steps in ArcGIS 10:

1. Create a uniform {x,y} point grid with 1' point spacing.
2. Elevate the 1' point grid using the topographic data for each map to create oversampled topographic point datasets for {x,y,z}_{time1} and {x,y,z}_{time2} that capture all available topographic information in the source DEMs.
3. For each 1' {x,y,z} topographic dataset, create a raster of standard deviation (SD) of point elevation with a 3'x3' cell size (yielding nine points per cell in the statistical computation).
4. Apply the appropriate survey and instrument error (SIE) empirical equation to the SD rasters to obtain the SIE raster for each topographic map.
5. Produce a Level of Detection (LoD) grid that combines the two SIE rasters into a single error raster using the t-value for 95 % confidence (1.96) and the statistical equation for error propagation given by:

$$6. LoD = t\sqrt{(SIE_{time1})^2 + (SIE_{time2})^2}$$

7. Create the raw DoD raster with a 3'x3' cell size.
8. Create separate deposition and erosion rasters using the "Con" function in the ArcGIS raster calculator.
9. Remove the LoD from each raster by subtracting it from the deposition-only raw DoD and adding it to the erosion-only raw DoD.
10. Create spatial coherence polygons to clip deposition and erosion rasters.
 - a. Con statements were used to turn deposition and erosion rasters into presence/absence polygons.
 - b. The area of each erosion and deposition polygon was calculated.
 - c. A minimum threshold of 100 ft² (~9 raster cells) was used to distinguish coherent change.
 - d. The original deposition and erosion rasters were clipped to exclude the areas of change below the size threshold.
11. Clip to lowest extent of data set survey limits.

An additional modification to the TCD procedure and final result in this report compared to the previous one was that the exclusion of a uniform threshold for all surveys was not utilized because the SIE functions capture this aspect of the data

intrinsically. The uniform exclusion had been +/- 0.16 ft, but it is not necessary with the new procedure.

5.3.3. Volume and Weight Gravel/Cobble Budgeting*

Once a final DoD raster with a 95% confidence was developed it was necessary to quantify erosion and deposition volumetrically and by weight. To do this, the volume of topographic change for each raster cell was determined by multiplying each cell's change value by the cell's area (3'x3'). This was performed separately for erosion and deposition.

Converting volume to mass required an estimate of gravel/cobble bulk density as present in the river. For this study, we used a value of 110 lbs/ft³ that came from five experimental bucket tests on gravel density performed at a quarry as material was stockpiled for a gravel augmentation on the Mokelumne River (Merz et al., 2006). Sawyer et al. (2009) analyzed full-scale bulk density at gravel placement sites on the Mokelumne River and found that the actual values varied around this one depending on how much front loaders had driven over the material. Given that the EDR sediment was not driven over and was recently redistributed and deposited by flow, it has been found to be loosely packed. When a person walks on one of these deposits, one feels the material slides down and away from each footfall. Therefore, its bulk density is probably similar to that from the bucket tests. Given this bulk density value, the conversion from ft³ to short tons involved multiplying the volume by the bulk density and dividing by the conversion factor of 2,000 lbs per short ton.

5.4. Evaluating Habitat Quality and Spawning Use

The GAIP states that a design objective (Design Objective 2) for gravel augmentation is to provide a higher quantity of preferred-quality Chinook salmon spawning habitat in the injection zone until the sediment moves downstream. Unlike the outcome of the 2010-2011 project that yielded little deposition in the injection zone, the 2012 project did yield a sizable gravel/cobble riffle directly utilized by spawning salmon in the autumn shortly after the injection (see cover photo). As a result, it was possible to strictly apply the GAIP's habitat tests. In addition, some of the gravel from the 2010-2011 project did wash downstream and form alluvial features, even though the injected volume was only a small percent of the total deficit for the reach. Therefore, this study chose to apply the tests to the both the created riffle in the injection zone and naturally self-formed downstream deposits where spawning has been occurring.

Hypothesis 2A posits that SRCS require deep, loose, river rounded gravel/cobble for

spawning. The test for this involves performing Wolman pebble counts and checking to see if the deposits match the size specifications for spawning presented in the GAIP. This test was performed using the results from grain size data described in section 4.4. Hypothesis 2B posits that spawning habitat should be provided that is as close to GHSI defined high-quality habitat as possible. The test for this requires performing 2D modeling of the reach and applying LYR Chinook salmon spawning habitat suitability curves to obtain the GHSI pattern for representative flows at which spawning occurred in fall 2012. The GHSI patterns were then checked to quantify the amount of preferred habitat available on the new downstream deposits.

In addition, the RMT conducted weekly redd surveys through the spawning season (section 4.8), so that made it possible to do testing beyond the explicit GAIP hypotheses. First, the redd data were analyzed to see how many were present on the deposited sediment. This was only applied to the downstream section where natural features were created because the constructed riffle in the injection location had fill depths \gg 18 inches. Second, post injection surveys and subsequent change detection analyses were used to infer whether or not redds corresponded with newly injected gravel and at what sediment thickness. Finally, a bioverification procedure was used to find out if the fish were showing a higher utilization of model-predicted preferred spawning habitat than would be expected from the availability of the habitat (e.g. Elkins et al., 2007; Brown and Pasternack, 2012). This was done for the entire EDR, spanning both constructed and naturally formed alluvial features.

5.4.1. Comparing Observed Redds with Deposition

The GPS redd data were compared against the final adjusted DoD from TCD analysis for the 2011-2012 time epoch for the downstream section. This was performed in ArcGIS 10 by joining the final adjusted DoD grid values of the deposition raster to the redd data shapefile. This was not performed for the upstream TCD area, because the spawning occurred on the constructed riffle, which is obviously not a naturally formed depositional landform. In addition, this was not performed for erosion, because there were no redds located in those areas for this case.

5.4.2. Spawning GHSI Modeling

Simulated patterns of Chinook salmon spawning physical habitat were needed to assess design hypotheses 2, 3 and 4. In the emerging discipline of ecohydraulics, physical habitat quality predictions are often made by extrapolating depth and velocity observations or predictions through independent habitat suitability curves (HSC) for depth and velocity that are developed locally or regionally to obtain a univariate habitat

suitability index (HSI) for each flow variable (Leclerc, 1995; Pasternack 2011). These are then geometrically averaged (sometimes often along with HSI for cover and substrate) to obtain a global (aka combined) habitat suitability index (GHSI). Some studies refer to GHSI as hydraulic habitat suitability index (HHSI), because it only considers depth and velocity. To account for uncertainty when hydraulics are obtained from 2D model predictions, Pasternack (2008) lumped GHSI values into broad classes, with GHSI = 0 as non habitat, $0 < \text{GHSI} < 0.2$ as very poor habitat, $0.2 < \text{GHSI} < 0.4$ as low quality, $0.4 < \text{GHSI} < 0.6$ as medium quality, and $0.6 < \text{GHSI} < 1.0$ as high quality habitat. In this study GHSI bins for 0.6-0.8 and 0.8-1.0 were broken out to show more detail, but both are still termed high quality habitat in this study.

Recognizing that the channel in the EDR is unsuitable for spawning in the absence of injected gravel/cobble, the channel was first segregated into potential and non-potential spawning habitat on the basis of substrate alone. The area of potential spawning habitat was defined as a polygon containing the areas determined by the DoD analysis to be fill (within the thresholded DoD for the 2011-2012 time period) (section 5.3.2) plus the areas identified from the blimp imagery as containing new gravel deposits (section 5.1). All areas not included in this polygon were by default given an HSI value of 0, meaning they are “non-habitat”.

LYR hydraulic habitat suitability curves (HSCs) for SRCS developed by Beak Consultants, Inc. (1989) on behalf of CDFG were based on utilization data using the method of non-parametric tolerance limits. As in Brown and Pasternack (2012), these HSCs were bioverified in this study and then applied to address the design hypotheses. Depth and velocity 3'x3' rasters were produced using the 2D model for the representative discharges for fall 2011. Combining Beak HSCs and hydraulic rasters, 3'x3' HSI rasters were computed for depth and velocity (DHSI and VHSI, respectively). As already explained, substrate was modeled as a presence-absence phenomenon where a value of 1 was assigned to suitable substrate and a value of 0 was assigned to non-suitable substrate. The final global habitat suitability index applied to the areas where gravel/cobble was present was calculated as $\text{GHSI} = (\text{DHSI} * \text{VHSI})^{0.5}$.

5.4.3. Bioverification of Chinook Spawning GHSI

The first step in habitat suitability analysis is to determine if the HSC's utilized in the study capture the actual observed selection of “good” habitat over “poor”. Following the work of Ivlev (1961) and Elkins et al. (2007), an electivity index (EI) based on the classic forage ratio was utilized to evaluate the HSC's ability to capture observed habitat preferences. The forage ratio in this context is the ratio of the proportion of redds observed in a region to the proportion of channel area within that region. The

regions used in bioverification testing can be anything, but in this case they are the areas within the specified ranges of GHSI values associated with different levels of habitat quality (e.g. $0.4 < \text{GHSI} < 0.6$ as medium quality habitat). Based upon new research performed by the RMT in 2012 making use of statistical bootstrapping methods (Pasternack et al., 2013), it has been determined with a high degree of confidence that a “preferred” region is one with $\text{EI} > 1.07$ (i.e. occurrence is significantly greater than random), a “tolerated” region is one with $0.93 < \text{EI} < 1.07$ (i.e. occurrence is similar as random), and an “avoided” region is one with $0 < \text{EI} < 0.93$. (i.e. occurrence is significantly less than random). The forage ratio has been heavily scrutinized over the decades (e.g. Lechowicz, 1982), but no consensus has ever emerged that a different metric works better for the type of assessment undertaken in this study. Although EI values based on the forage ratio could theoretically go to infinity, in practice they are typically < 10 in this usage. The primary concern in applying the forage ratio is when there is such a small number of observations or such a low area of a test region that the EI becomes spuriously high simply due to inadequate numbers. Care was used to avoid that problem in this study.

To achieve bioverification, two criteria have to be met using the EI. First, predictions must include areas that are “preferred” and “avoided”. A trivial prediction is one that says the whole channel is preferred, and then utilization is observed somewhere in the river, so presumably the prediction is correct. However, a prediction must have specificity. The higher the EI value of preferred regions, the riskier and more specific the predictions are. Second, the EI metric must result in higher EI values for higher GHSI regions and lower EI values for lower GHSI regions. In other words, if the prediction shows that there is disproportionately high utilization in a region, but the region was thought to be poor quality habitat, then the understanding of what constitutes high quality habitat is wrong and needs to be re-conceived. Utilization should be highest where the habitat quality is highest. If not, then the predictions are not bioverified.

The procedure for this analysis involved the following steps. First, GHSI rasters were made for all modeled flows representing fall 2012 spawning conditions. Second, the rasters were reclassified according to the habitat quality bins defined earlier and the reclassified raster was converted into polygons. Third, the area of each GHSI bin was determined and divided by the calculated total wetted area for that discharge to arrive at the % available habitat for each bin. Fourth, the GHSI at each redd location was determined from the GHSI raster. Fifth, the number of redds in each GHSI bin was computed and divided by the total number of redds to arrive at the % utilization for each bin. Finally, EI was computed as the ratio of % utilization to % available habitat.

5.4.4. Proximity Analysis of Observed Redds to Refugia

Hypothesis 3b of the GAIP states that structural refugia in close proximity (assumed to be < 10 m) to spawning habitat should provide resting zones and refugia from predators. To test this hypothesis each redd cluster was buffered by 10 m in ArcGIS creating a bounding polygon that encloses all observations. Next, visual inferences were made as to whether this area had structural elements such as proximity to deep pools, bedrock outcrops, boulders, large cobble, and large streamwood.

6.0 Results

6.1. Wolman Pebble Counts

During the 2012 injection 45 Wolman pebble counts were done to evaluate the particle-size distribution in the gravel supply pile. Most counts had a D_{50} between 20-55 mm and a D_{90} between 40-90 mm (Fig. 9). In addition, data was collected at four locations in river to compare the grain size distribution actually in river after being sluiced. Most of these counts collected had a D_{50} between 25-50 mm with a D_{90} between 65-75 mm (Fig. 10). Of note is that all counts show the majority of the injected sediments are finer than the plan specification. This shows that on average bed surface sediments do coarsen relative to stockpile counts taken at the staging area once in river due to “hydraulic sorting” (i.e. decrease in size in the downstream direction as depth increases and near-bed velocity decreases) and armoring (i.e. winnowing of finer particles off the bed surface leaving behind coarser particles). However, it would be preferable if more of the mix was as coarse as specified to help prevent material from redistributing downstream as easily as it is.

Hydraulic sorting and armoring are illustrated in a photograph taken on September 6, 2012 on river right (Fig. 12). The three areas in orange (e.g. A, B, and C) visually show how sorting can occur in the river. When this patch of gravel was first placed all of the areas had the same approximate grain size distribution. However, as flows began to funnel over this deposit a notch was created when the water flow became more concentrated through area B. This area “armored” itself with 3-5” gravels and this limited any further incision. The other two areas show the original grain sizes where armoring did not take place and visibly much finer than area B. Overall, this is a key reason why larger particles in the gravel mix are so important because they can stabilize river bed elevations through armoring leading to a greater temporal resilience of gravel features.

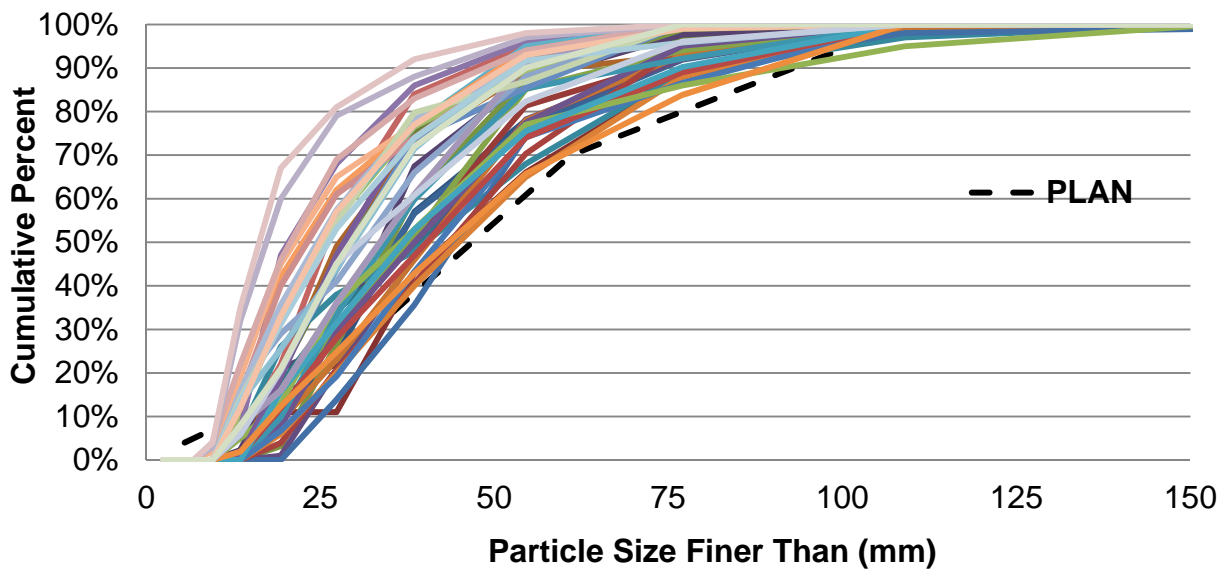


Figure 10. Cumulative particle-size distribution of injected sediment during the 2012 injection.

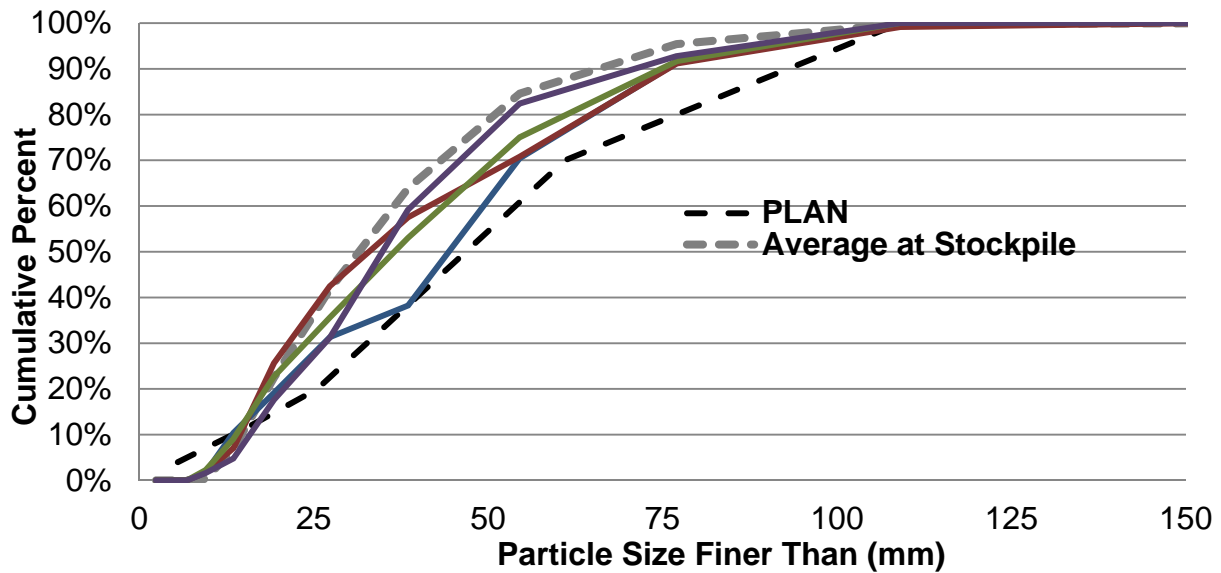


Figure 11. Cumulative distributions of four in river locations relative to that from the plan and the average from the gravel injection material stockpiled at the hopper.



Figure 12. Photograph illustrating the effect of armoring on injected gravel deposits. When this area was first filled with gravel all areas had very similar grain size distributions but as flow poured through area B this zone coarsened relative to the other areas limiting any further incision.

6.2. Blimp Image Analysis

A very low-resolution version of the final bright-light mosaic is shown in Figure 13 with areas of visually discernible gravel deposits enclosed in red. A larger digital map is available upon request. The areas shown were what could be visually identified as gravel deposits from this year's injection, as well as last year's, that matched the composition of injected gravels. The total area of the polygons is 42,259 square feet, which is 9% of the wetted area at 855 cfs from Narrows 1 to the confluence of Deer Creek at the study limit.



Figure 13. Red polygons outline areas of gravel deposition that were discernible using blimp imagery and visual inspection in ArcGIS. Other significant deposits occurred where it was too deep to see visually, but are revealed by TCD.

6.3. 2D Model Validation

6.3.1. Mass Conservation Checks

In a river with a highly complex terrain, there is a risk of poor model performance with mass conservation, especially at low flows. The mass conservation error was computed between the specified inflow and the model-predicted outflow. For the discharge modeled in this report, 996 cfs, the modeled outflow was 995.3 cfs, which has an error of 0.01%. This is right on par with the previous year's monitoring report which also had outflow errors of 0.01%.

6.3.2. WSE Validation

The ability of the 2D model to match measured WSE collected during the field campaign is an important test that reveals how good the model is at simulating flow depths and water surface slopes, both of which are key to estimating point scale velocities. In this test, we utilized data collected via kayak with an echo sounder for 996 cfs. For reference, the accuracy of bathymetric mapping with the method used in this study is usually in the 0.2-0.5 ft range, but the high variability of the bed roughness in the boulder-bedrock channel can yield larger uncertainties. Further, any change in boat buoyancy (e.g. bobbing up and down on waves, boils, and whirlpools as well as changes in boat weight as a result of taking on water into the boat, changing between people doing the mapping, changing boats, or changing the supplies carried in the boat) easily cause unaccounted for observational offsets and variability of approximately 0.05 to 0.5 ft. Therefore, WSE deviations should fall within the range of topographic

uncertainty and boat “draft” uncertainty and not exceed that.

For 966 cfs, the histogram of WSE deviations shows a small tendency toward overprediction (e.g. modeled –measured > 0), but not enough to warrant adjusting the Manning’s n value (Figure 14). The mean signed deviation between observed and 2D-model predicted WSE was 0.02 ft (slight average overprediction by the model), with the mean of the absolute value of deviations 0.13 ft. Under-predictions were mostly within the -0.1 to -0.2 range, while over-predictions had a peak within the 0 to 0.05 range. The maximum deviation was 0.42 feet.

To understand why there are underpredictions and where they are occurring, the longitudinal profiles of observed and predicted WSEs at 966 cfs were evaluated (Fig. 15). Dividing the river into three sections separated by the hydraulic controls at approximately stations 600 and 2,000 feet the mean signed deviations are 0.02, -0.07, and 0.2 and this is captured visually in the long profile as well. Beginning at the end of the model, WSE predicted extremely well (0.02 ft) until a major hydraulic control is reached where the channel constricts between Sinoro Bar and a bedrock outcrop forming a small bed step with a high-velocity chute. Upstream of that, the model underpredicts by -0.07 ft, which means water is getting through that chute more efficiently in the model than in reality or the draft. Unfortunately, it is very difficult to map that chute in detail and the TCD analyses by Brown and Pasternack (2012) revealed that this chute has been scouring over the years. The next hydraulic control upstream is the major rapid downstream of the USGS gaging station. Upstream of this control the model overpredicts WSE by 0.2 ft. Again, given that the field conditions make the depth of the echosounder difficult to know and maintain exactly the same through time, these deviations of within 0.2’ are unavoidable in this remote canyon setting with hydraulic jumps, standing waves, chutes, and other complex hydraulic features.

Overall, model-predicted WSE deviations for the EDR 2D model turned out to be significantly smaller than observed bed topographic variability, indicating that the model is validated across a suite of WSE performance indicators. The error in WSE longitudinal profiles at 966 cfs are most likely associated with the presentation of the two dominant hydraulic controls in the river at approximately stations 600 and 2000. Regardless, the measurements are on par with the level of topographic variation in the river so values were not adjusted. Compared to last year’s study (Brown and Pasternack, 2012), there were 100 times more observations collected, but only for one discharge. Overall, the performance metrics between the two years relate very well, with somewhat better mean signed deviation and slightly worse unsigned mean deviation this time (Table 9).

Table 8. Nonexceedence probabilities for 966 cfs WSE deviations (unsigned) meeting different thresholds of performance.

WSE deviation (ft)	Nonexceedence Probability
0.025	19%
0.05	30%
0.1	50%
0.14	63%
0.25	91%
0.41	100%

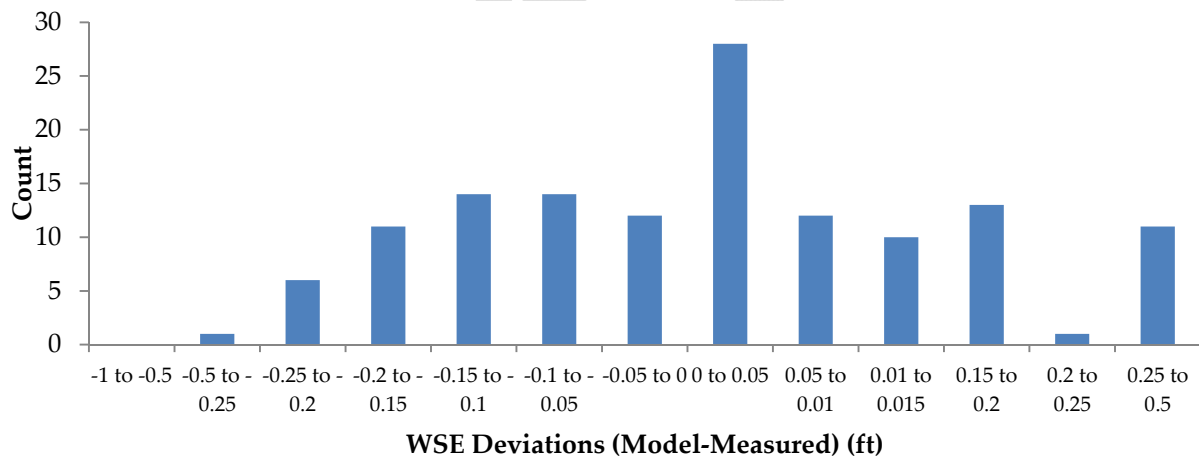


Figure 14. Histograms evaluating 2D model WSE performance at 996 cfs. Numbers shown go with the right edge of the bin. Negative numbers mean the 2D model underpredicted WSE.

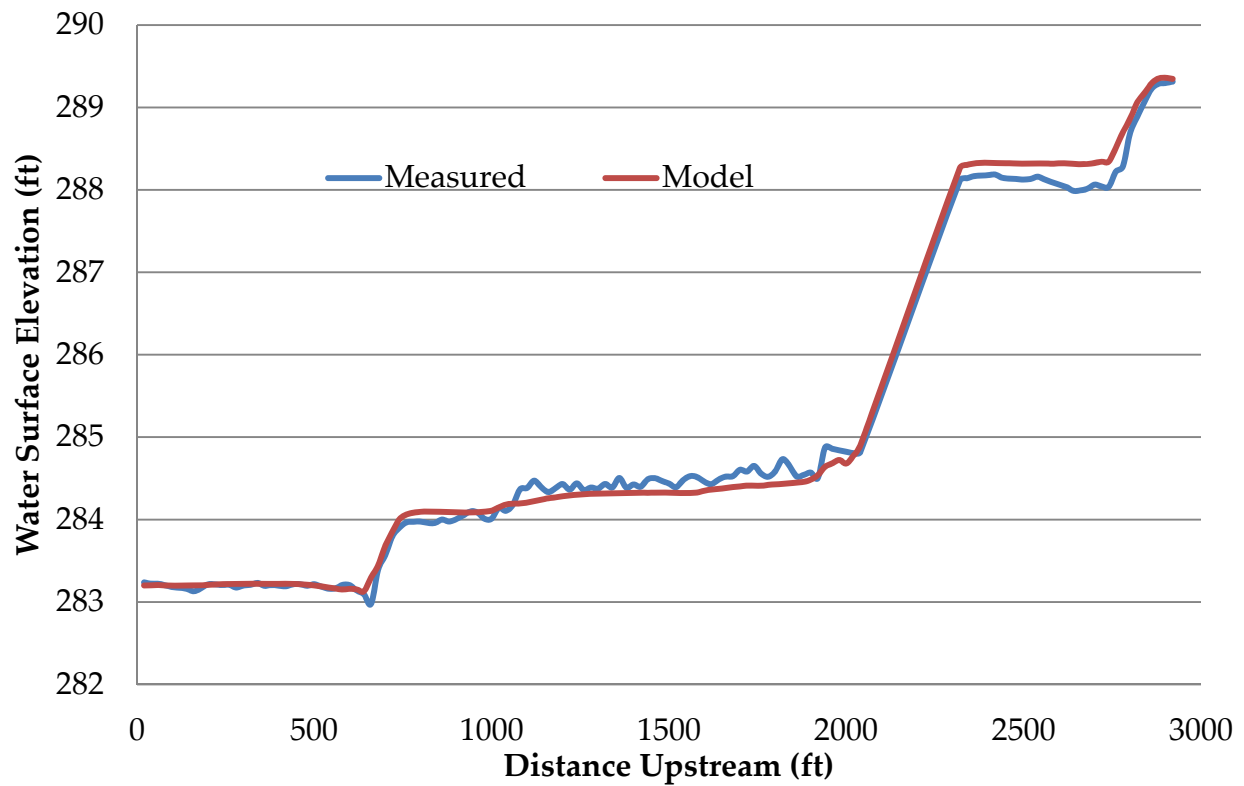


Figure 15. Longitudinal profile of observed and predicted WSEs at 966 cfs.

Table 9. Comparison of Water Surface Elevation Model Validation for the 2012 and 2013 Monitoring Report

	2012 Monitoring Report		2013 Monitoring Report
	870 cfs	951 cfs	996 cfs
Number of Observations	136	147	14,852
Range of Signed Deviations	-0.25 to 0.16	-0.15 to 0.65	-0.30 to 0.42
Mean Signed Deviation	-0.07	0.04	0.02
Mean Unsigned Deviation	0.1	0.07	0.11

6.3.3. Water Speed Validation for 966 cfs

After WSE validation at 966 cfs, the next step was to evaluate 2D model performance with predicting velocity magnitude in the direction of flow (i.e. water speed). For this suite of tests, statistical analyses were done comparing observed point velocities using the kayak-based positional tracking method and the 2D-model predicted velocities at the same locations for 966 cfs, which was the flow at which validation data was collected. This flow is representative of spring-run spawning conditions in September in EDR. Comparisons between observed and predicted values were done on signed and unsigned percent error, as explained in section 5.2.

Beginning with the analogous tests presented for WSE, velocity was checked for the balance of the statistical distribution of signed percent error around zero (Figure 16). For all velocity observations, the 2D model had a tendency to over predict velocities more than under predicting (Fig. 16). For the unsigned percent velocity error, the means for all data, below 2 ft/s, and above 2 ft/s were 37%, 47% and 18%, respectively. Recall that the standard performance reported in most studies is ~20-30% error on average, so these values are better with that. The model accuracy was better for higher velocities and poorer for lower values. For example, the mean unsigned error for velocities less than 0.5 ft/s is 69% but this decreases to 58% for values between 0.5 and 1 ft/s and to 20% for values greater than 1 ft/s. . Considering all observations, 44 % were within 20% error and 76% were within 50% error (Table 10).

Table 10. Percent of 2D model velocity predictions meeting different thresholds of performance for all data (unsigned) as well as above and below the 2 ft/s threshold.

% Error	% Non Exceedance		
	All Data	<2 ft/s	> 2 ft/s
5%	12%	8%	19%
10%	24%	17%	36%
20%	44%	32%	67%
25%	52%	39%	76%
50%	76%	64%	97%
100%	94%	90%	

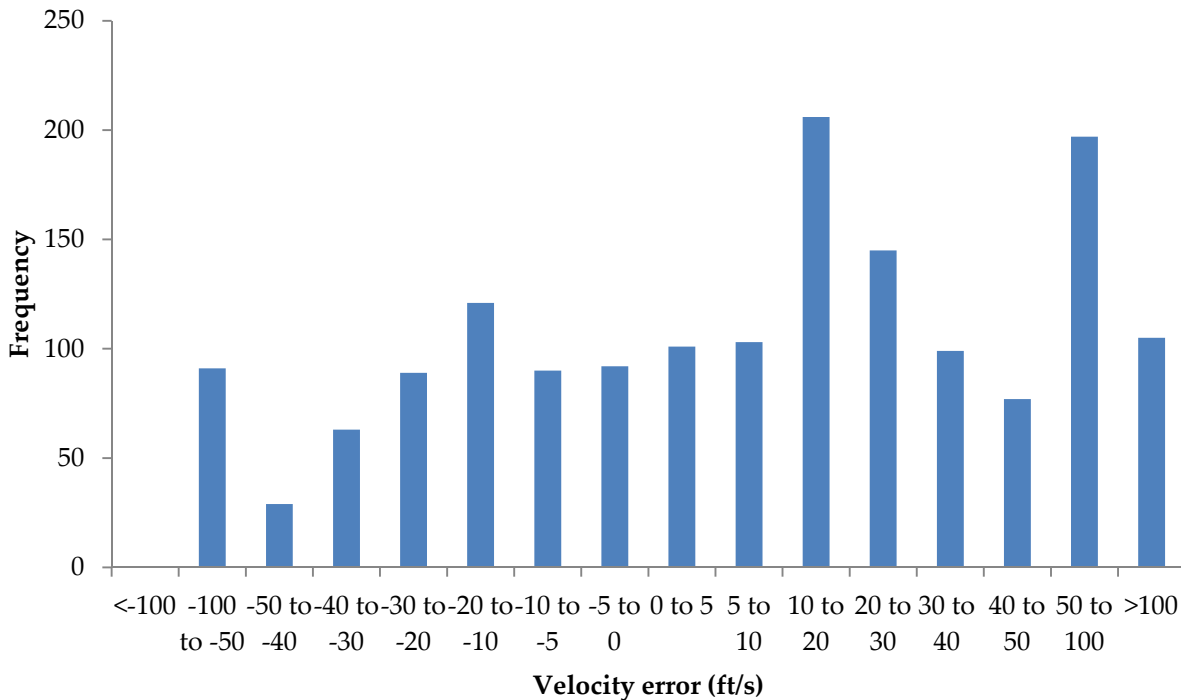


Figure 16. Histogram of percent velocity error (signed) for all observations.

In terms of correlation analysis, the R^2 value for the scatter plot was 0.8 for all observations and this increased to 0.85 (Fig. 17) when several points associated with the rapid below the USGS gaging station were removed (Fig. 18). These points were underpredicted by the model, because the exact location of any eddy fence in that area was not captured by the 2D model, so a slight lateral shift was the only cause of the model's mistake. This had the effect of making the eddy recirculation zone much larger than it is in reality, so some of the validation points were compared against eddying flow rather than the downstream oriented jet through the rapid.

The next step in model validation was to determine if specific ranges of velocities were predicted better or worse than others. When segregating the data on either side of 2 ft/s the R^2 was 0.81 for < 2ft/s and 0.47 for > 2 ft/s (Fig. 19). All of these coefficients of determination values are statistically significant above the 95% confidence level. These values are within the acceptable validation ranges suggested in section 5.2. Still, the slopes and y-intercepts all indicate a bias of overpredicting low velocities and underpredicting high velocities. This is a common problem with 2D models for several reasons, which can include challenges with representing (a) turbulent transfer of

momentum, (b) bank roughness, (c) porous riverbed that carry hyporheic flow, and (d) backwater effects and flow accelerations at major hydraulic controls.

Overall, this year's hydrodynamic model validation of water speed performed generally worse than last year's, but still performed on par compared with 2D model studies as a whole (Table 11). This year there were > 3 times more data points collected compared to the prior year. The mean signed and unsigned error was higher for all data and data stratified above or below 2 ft/s. The mean unsigned error above 2 ft/s was unusually high. On the other hand, the coefficient of determination between predicted and observed was higher for all data and data stratified above or below 2 ft/s.

This year a more thorough analysis of the geographic locations of good and mediocre model performances helped explained what was going on. The model performed very well downstream of the major rapid (Fig. 18). The reason that this year's model performed worse than last year's model for speeds > 2 ft/s is easily identifiable as being caused by two issues, both related to the major rapid. First and most importantly, velocities in the backwater zone upstream of the injected gravel riffle and the major rapid were too low and the WSE was too high (Fig. 18). That means that there is systematically too much backwater effect in the model at these two locations, causing an overestimation of WSE and underestimation of velocity. Second, velocities along the river-right eddy fence were actually in the eddy in the model, but not in the observed data. This slight lateral shift in eddy position caused a notably model error.

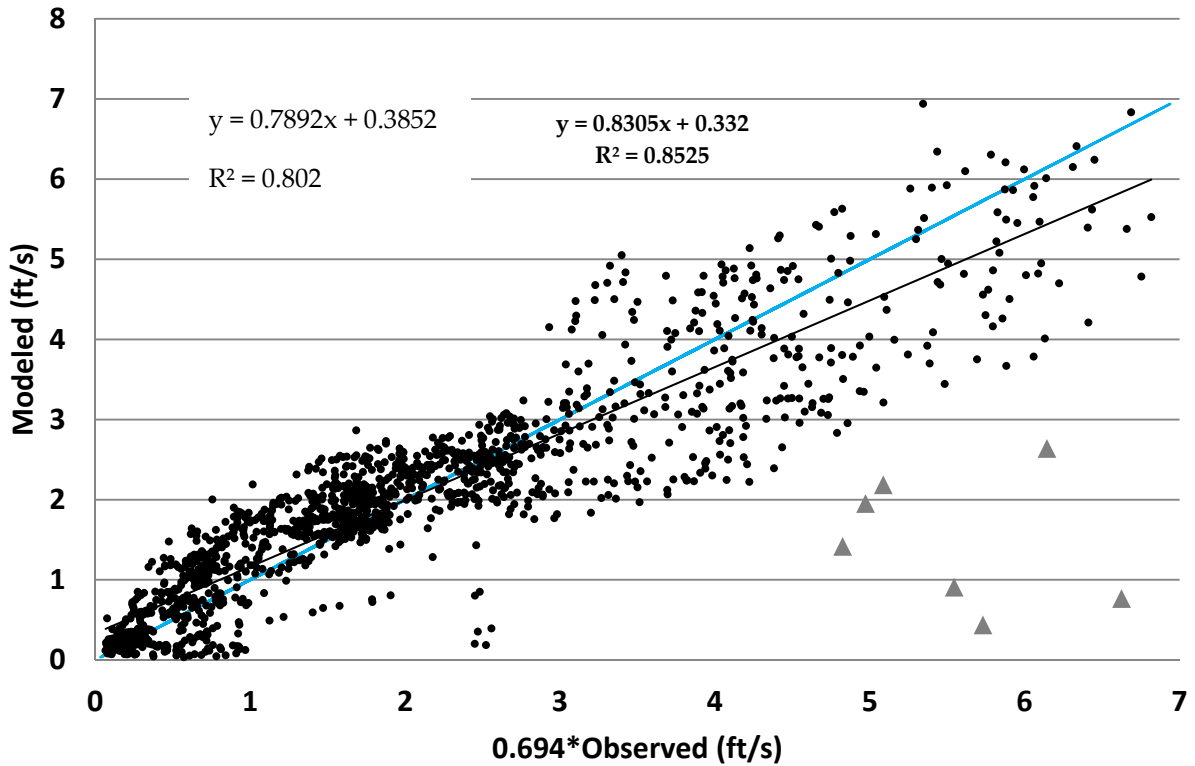


Figure 17. Scatter plot of 2D model modeled water speed versus observations showing linear regression equation and coefficient of variation. The blue line is $X=Y$ (i.e., perfect prediction ideal) and the black line is the regression of modeled versus observed measurements. The grey triangles are observations made below the first rapid downstream of the USGS gaging station. The regression in grey excludes those observations.

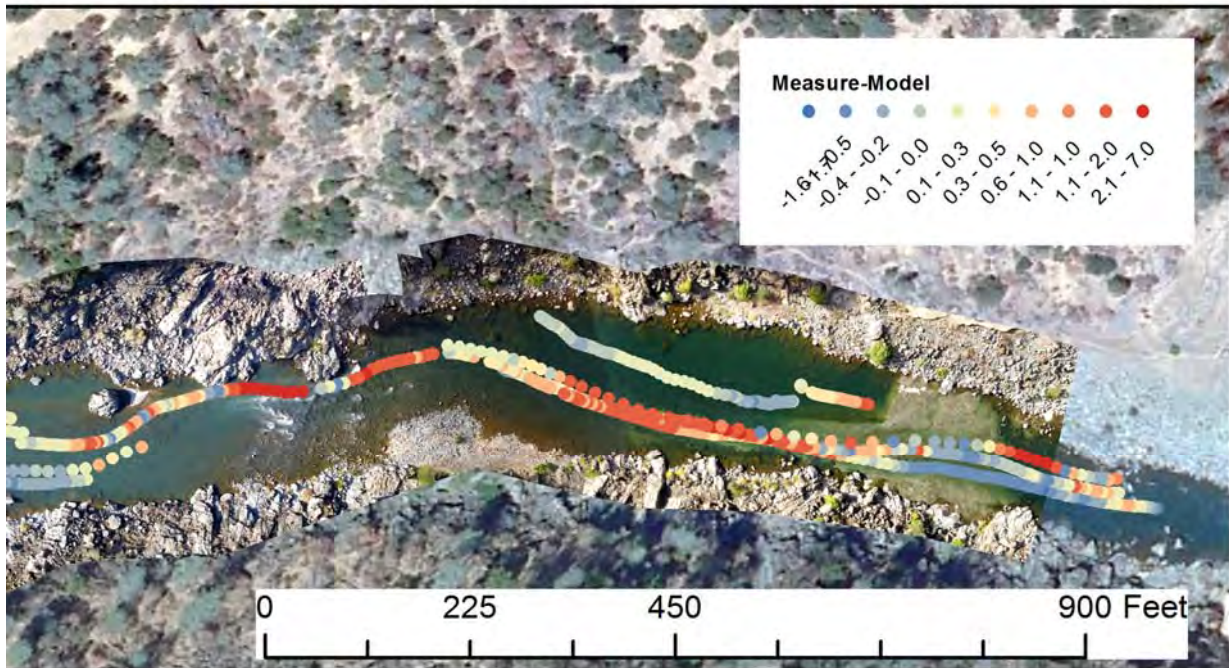


Figure 18. Spatial plot of observed (with DAVC adjustment) minus modeled velocity deviations. Darker red values are where the model under predicted velocity and darker blue is where it has over predicted. Note that legend is not equally centered.

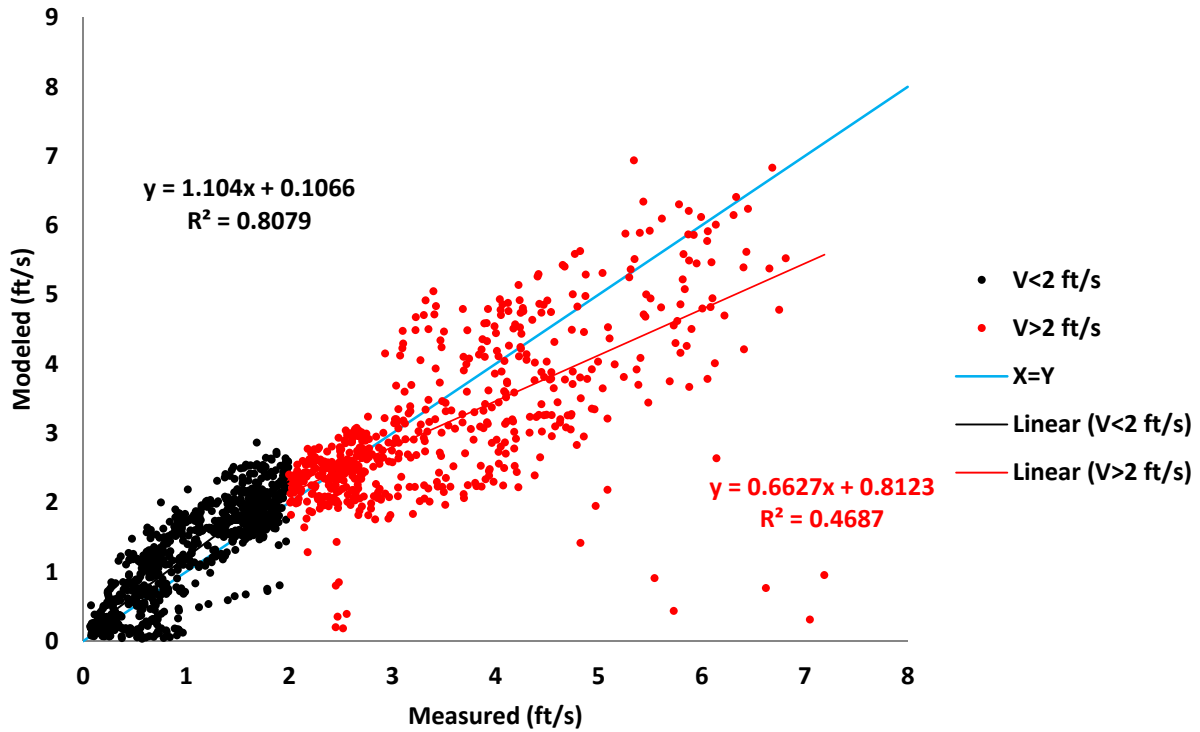


Figure 19. Scatter plot of 2D model predicted water speed versus observations showing linear regression equation and coefficient of variation when the data is segregated at 2 ft/s. Red colors pertain to values greater than or equal to 2 ft/s and black colors for values less than 2 ft/s.

Table 11. Comparison of Velocity Magnitude Model Validation for the 2012 and 2013 Monitoring Report

		2012 Report	Monitoring Report	2013 Report	Monitoring Report
		862 cfs		996 cfs	
Number of Observations		532		1609	
All Observations	Mean Signed Error	13%		18%	
	Mean Unsigned Error	26%		37%	
	R ²	0.7628		0.7892	
	Slope	0.8491		0.802	
< 2 ft/s	Mean Signed Error	21%		33%	
	Mean Unsigned Error	32%		47%	
	R ²	0.614		0.8079	
	Slope	0.9187		1.104	
> 2 ft/s	Mean Signed Error	-1%		-8%	
	Mean Unsigned Error	14%		18%	
	R ²	0.602		0.6627	
	Slope	0.8284		0.4687	

6.3.4. Velocity Direction Validation for 966 cfs

An additional test to validate the 2D model was to compare observed and predicted velocity direction. The mean and median signed angle deviations were 1.8° and -0.1° , respectively, while the same values for unsigned deviations were 8.1 and 4.3 degrees, respectively. Eighty-four percent of angle deviations were within the 10° threshold desired for good model performance (Table 12). The histogram of unsigned angle deviations shows that the model tends to over-predict velocity direction (e.g. model – observed >0), with the errors appearing to be approximately normally distributed around the mean (Fig. 20). The signed mean is higher than reported in Barker (2011), but still very low, and the unsigned deviation is close to the same. In terms of correlation and regression analyses, the EDR 2D model performed worse than that reported by Barker (2011). The R^2 was 0.3 and the regression slope was 0.69 (Fig. 21).

To understand 2D modeling performance in predicting flow direction a special analysis was done to see if the model could capture one of the large eddies in the reach as well the ambient flow direction in the thalweg adjacent to it. Observations were made in fall 2012 and compared to the flow pattern for the 2011 2D model (as reported in Brown and Pasternack, 2012) and the new 2012 2D model. Figure 22 shows observed flow directions as red arrows and model-predicted flow directions as black arrows. Visually, there is a remarkably good matching of observed and predicted flow directions. Both observations and predictions show a double vortex eddy.

Overall, observations and predictions of flow direction are visually similar in the free-stream flow field as well as in eddies (Fig. 22), but there are mathematical deviations in directions just as there are in velocity magnitude. Error of angle deviations show consistent good performance in terms of ~56% and ~80% of predictions within 5° and 10° , respectively. However, when considering the scatter plot of unsigned deviations there does appear to be a systematic bias in flow direction in the model where low directions are overpredicted and high directions are underpredicted. There is no significant difference in angle deviation between points with water speeds above versus below 2 ft/s. The error of angle deviations performs almost identically in the 2011 and 2012 2D models, whereas regression performance in the 2012 2D model is worse than in the 2011 2D model for no obvious reason. The cause of this is unknown and this is only the third study to evaluate flow direction quantitatively, so more studies may be needed before an understanding of the controls on direction error are understood.

For this study there are three times as many main flow direction observations and 10 times as many eddy flow observations than the prior year (Table 13). Compared to last year's study model validation for velocity direction for the main flow have approximately the same mean unsigned error, percent of unsigned deviations and slope, but the R^2 is poorer (Table 13).

Table 12. Percent rank of 966 cfs absolute velocity direction deviations meeting different thresholds of performance for the main flow (e.g. no eddies).

Angle deviation (deg)	Non-exceedance
1	14%
5	56%
10	84%
15	93%
20	95%
30	97%
45	98%

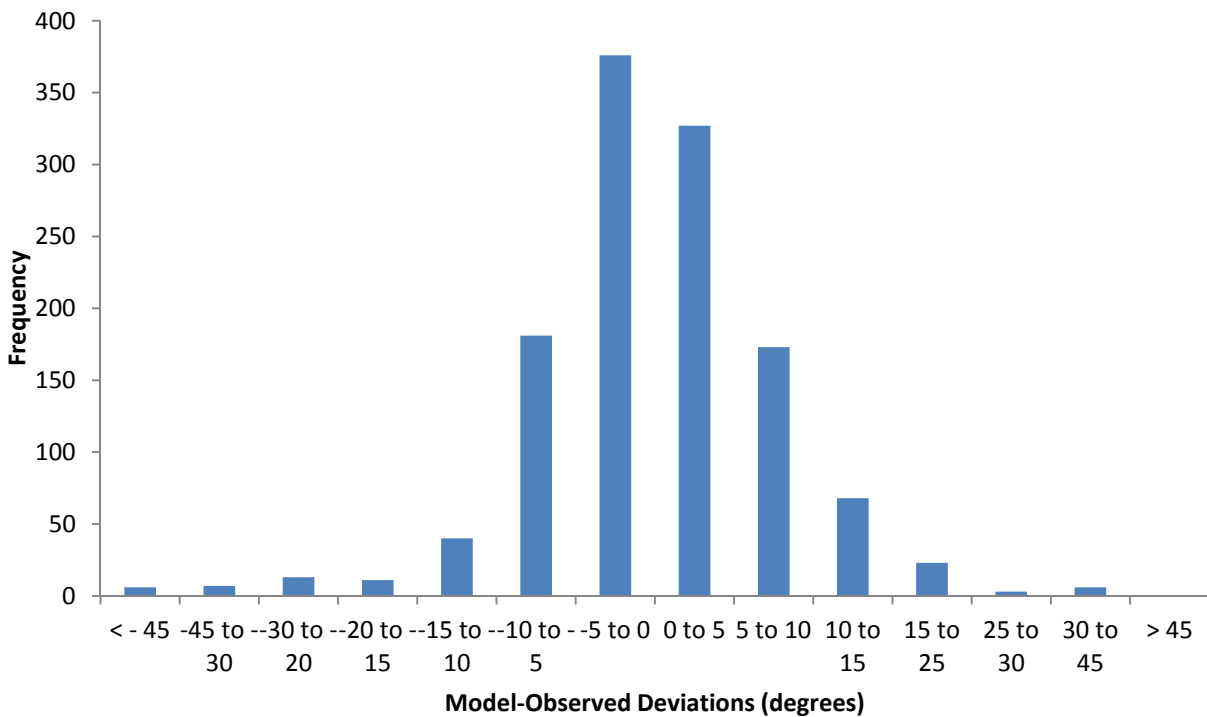


Figure 20. Histogram evaluating 2D model velocity direction performance at 966cfs, with deviations centered on -45 to 45.

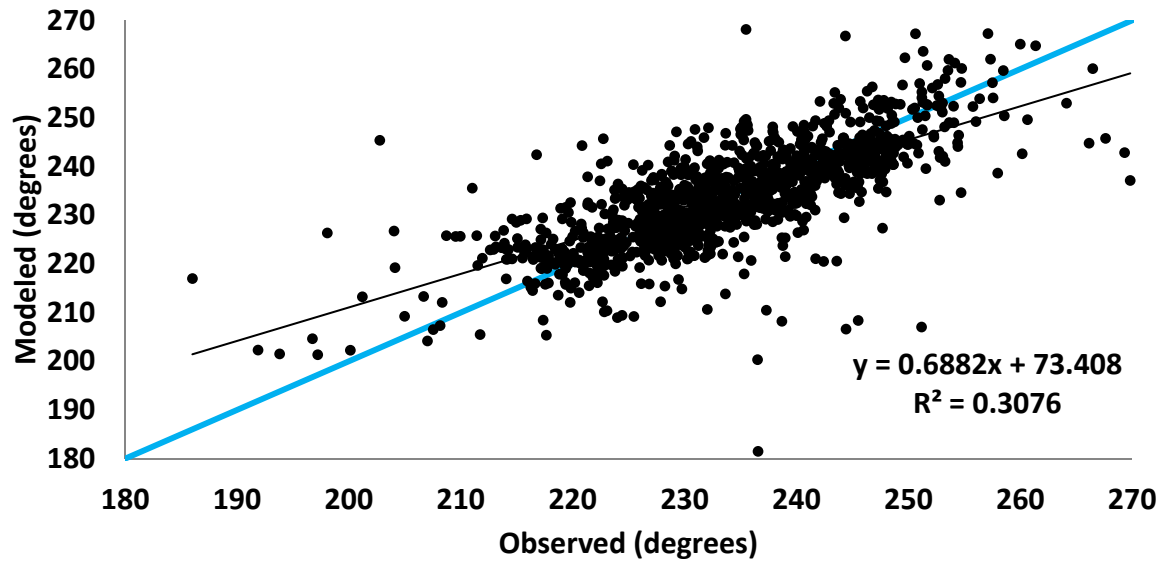


Figure 21. Scatterplot evaluating 2D model velocity direction performance at 966 cfs for the main flow (e.g. no eddies).

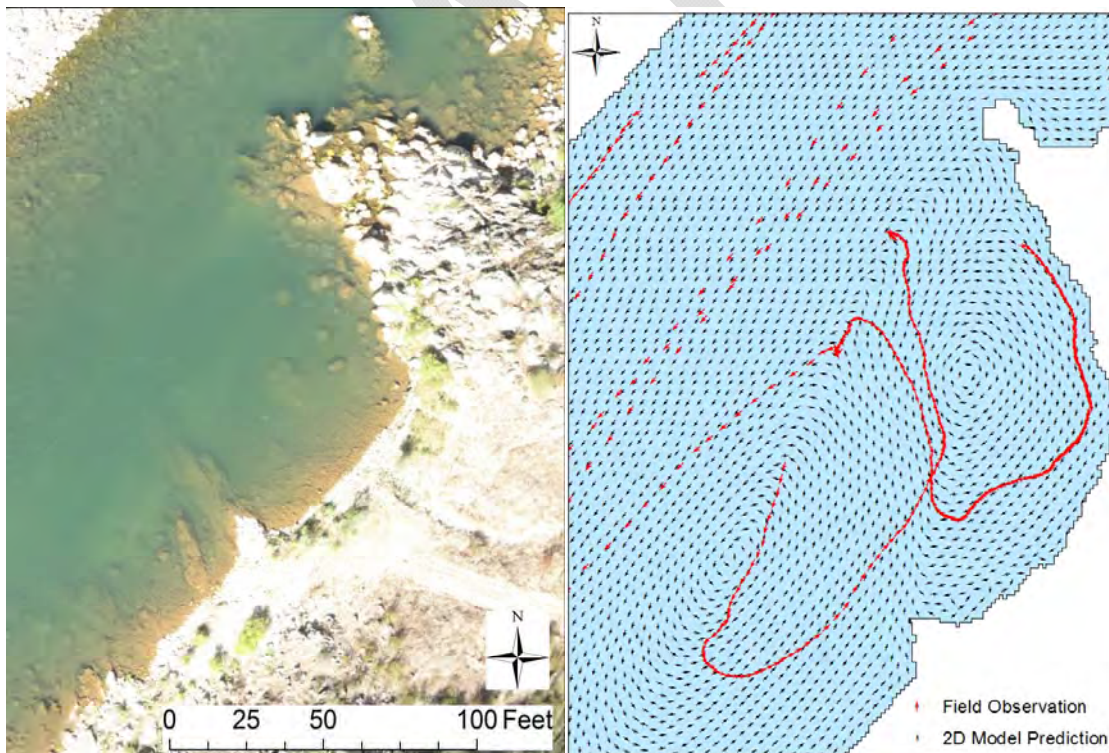


Figure 22. Blimp image, flow direction observations, and 2D model predicted flow directions for a two-cell eddy on river left near the beginning of Sinoro Bar ~700 feet upstream of Narrows Gateway. Red arrows show observed directions and black arrows show model-predicted directions.

Table 13. Comparison of Velocity Direction Model Validation for the 2012 and 2013 Monitoring Report

		2012 Monitoring Report	2013 Monitoring Report
		862 cfs	996 cfs
Main Flow	Number of Observations	492	1251
	Percent of Deviations < 10 Degrees	83%	84%
	Mean Unsigned Error	5.9	8.1
	R ²	0.6489	0.3076
	Slope	0.6001	0.6882

6.4. Redd Observations

The first step in assessing redd use was overlaying the observed data with the visually identified sediment deposits. All observed redds were located in very close proximity to areas of injected gravel deposits (both in the injection zone as well as where that sediment washed downstream and deposited), as identified from blimp- image analysis (Fig. 23). Spawning was focused in three distinct clusters (Fig. 24) and not necessarily where there was the most deposition, but anecdotally where deposits occurred in suitable hydraulics for spawning. The upper cluster was on the constructed riffle in the injection zone, with ~52 redds. The middle cluster (9 redds) was on the upstream submerged slope of the cobble bar adjacent to the large rapid. This site was also used in autumn 2011. The lower cluster (3 redds) was upstream of a bedrock outcrop that constricts the channel and acts as a barrier to gravel/cobble bedload transport, causing deposition. Both of these depositional sites have similar shallow depths and moderate velocities consistent with those suggested by the Beak, Inc. HSCs to be ideal for Chinook adult spawning. This was tested formally in section 6.7.



Figure 23. Observed redds and polygon boundaries of visually identified gravel deposits.

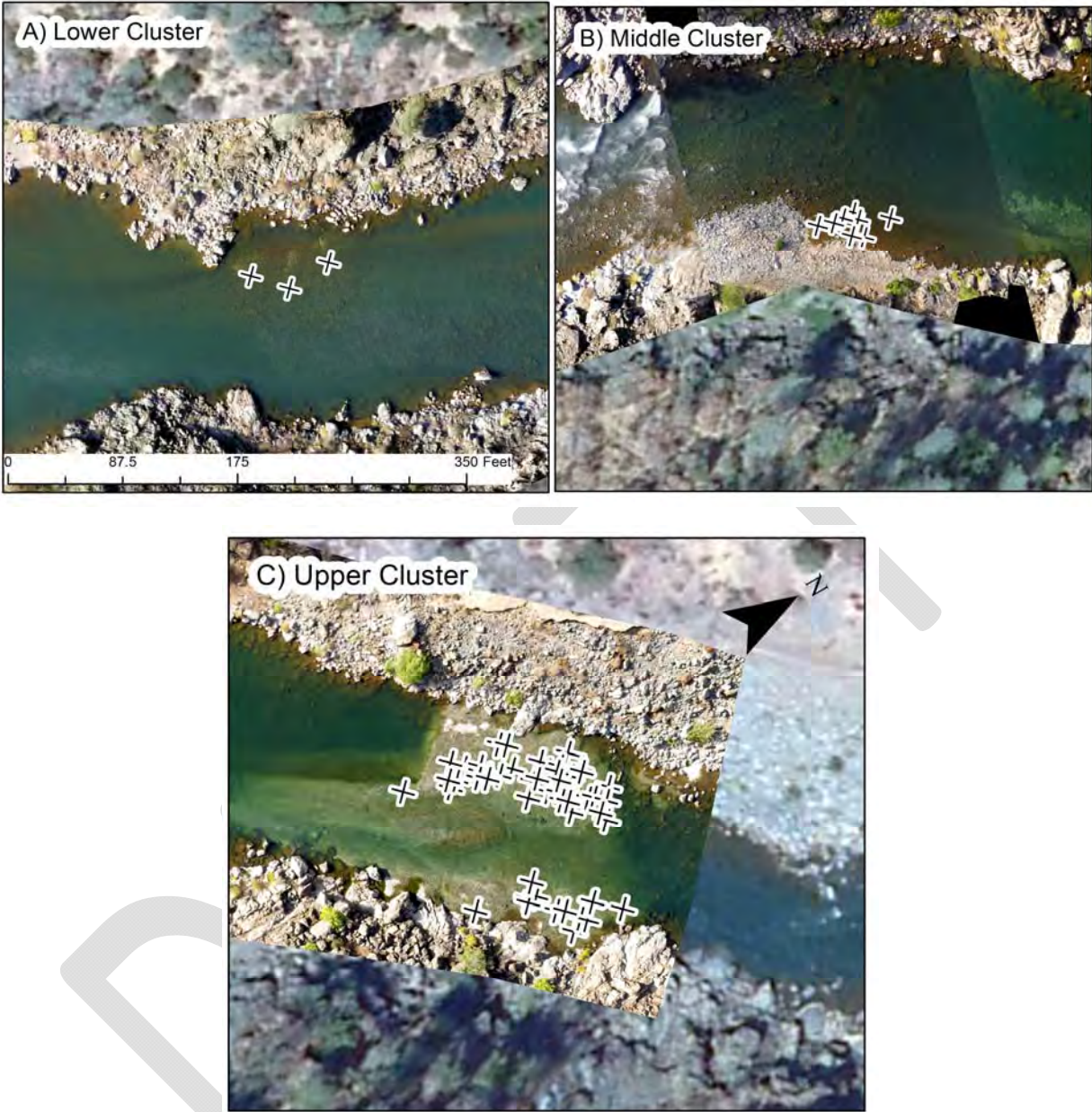


Figure 24. Zoomed in views of the three spawning clusters observed showing that they occurred on deposits from the gravel injection, though fill depth was variable.

6.5. Survey and Instrumentation Error (SIE) Functions

A new aspect of the TCD analysis in this report was the development and application of survey and instrumentation error (SIE) functions unique to each TCD epoch and extent. Previously, in Carley et al. (2012) and Brown and Pasternack (2012), existing empirical functions developed in TCD studies in the United Kingdom (Heritage et al., 2009) were used to convert observed local variance in topographic data to an SIE estimate. In this study, local SIE functions were created for the EDR using the method of Milan et al. (2011), which is a more sophisticated and more certain method.

Since there were two epochs investigated and two data sets for each epoch, then to compare each against each other meant that six total SIE functions were needed. However, the October 2012 upstream area was used for two TCD epochs, so it was not necessary to make an SIE function for that twice. As a result, only 5 unique SIE functions were developed. Moreover, as each SIE function is dependent on the standard deviation of elevation (σ_z) and the error from interpolation (Δz) plots of these two variables are provided along with the final SIE functions. These functions may be used in future reports or new functions can be developed each time.

All of the plots of local surface elevation variation versus elevation error illustrate that as the variability of surface increases so does the range of elevation error (Figs. 27 - 30), consistent with Milan et al. (2011). In fitting a trend model to the binned standard deviation of elevation error linear and polynomial functions were iteratively adjusted to determine trends that maximized R^2 values. For values outside the binned local surface elevation linear models were assumed (e.g.

Table 17 for the range 0.-25 σ_z , the SIE function is $y=0.18$). This was done because it was thought to be more conservative than reducing the SIE's to zero outside of data limits. For the downstream areas the SIE functions were best fit with polynomials (Table 16 and

Table 17) and for the upstream areas piece-wise linear models worked best (Table 18, Table 19). For all of the data the standard deviation of elevation error increased until the σ_z was 1.5-2 and in some cases decreased (Figs. 27 - 30).

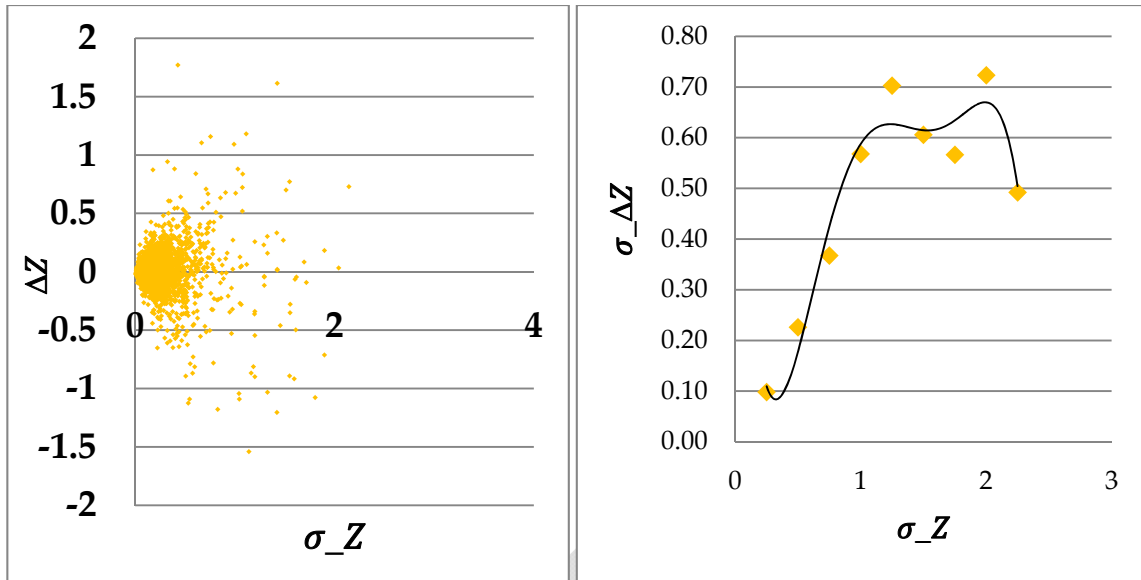


Figure 25. Plots of elevation error and local surface elevation variation (σ_Z ; LEFT) and standard deviation of elevation error ($\sigma_{\Delta Z}$) versus local surface elevation variation (σ_Z ; RIGHT) for the downstream area of the 2007 data.

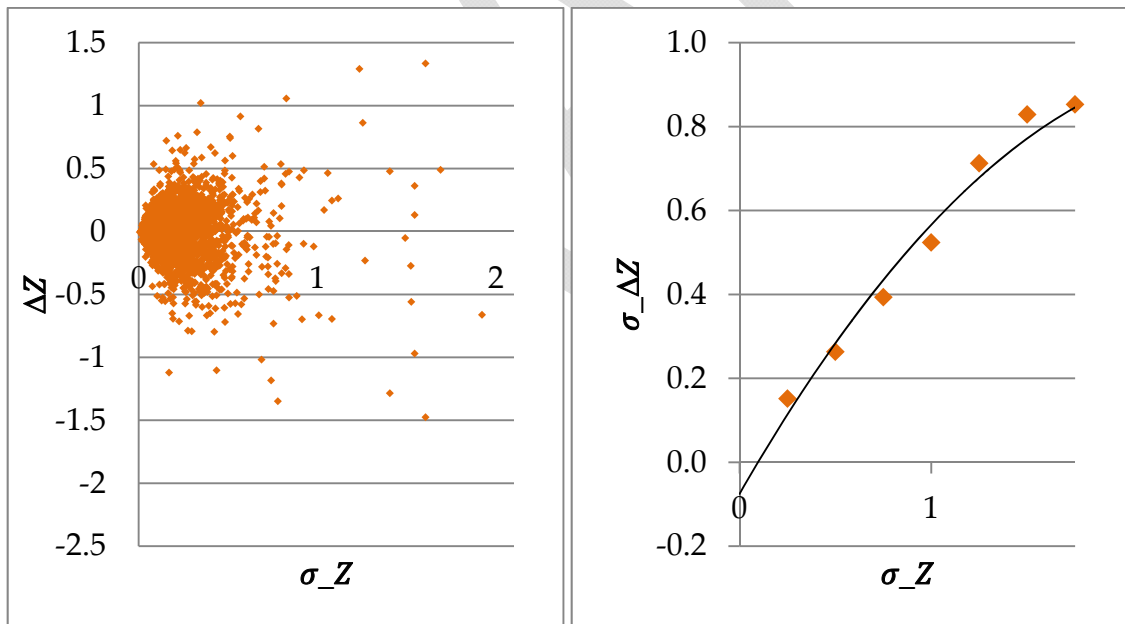


Figure 26. Plots of elevation error and local surface elevation variation (σ_Z ; LEFT) and standard deviation of elevation error ($\sigma_{\Delta Z}$) versus local surface elevation variation (σ_Z ; RIGHT) for the upstream area of the 2007 data.

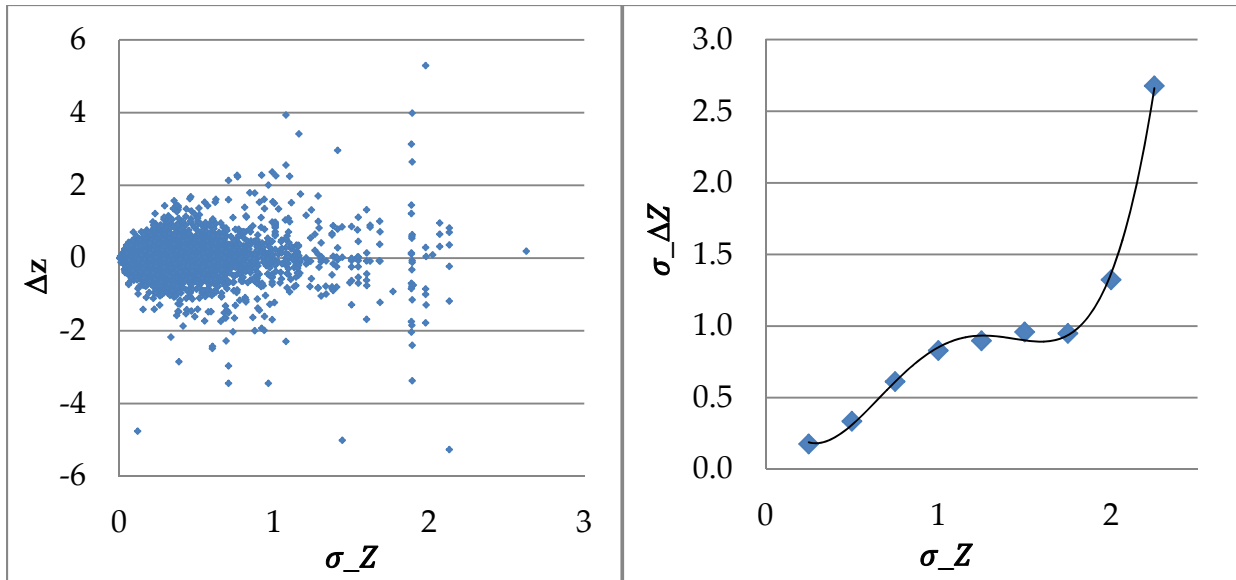


Figure 27. Plots of elevation error and local surface elevation variation (σ_Z ; LEFT) and standard deviation of elevation error ($\sigma_{\Delta Z}$) versus local surface elevation variation (σ_Z ; RIGHT) for the downstream area of the October 2012 data.

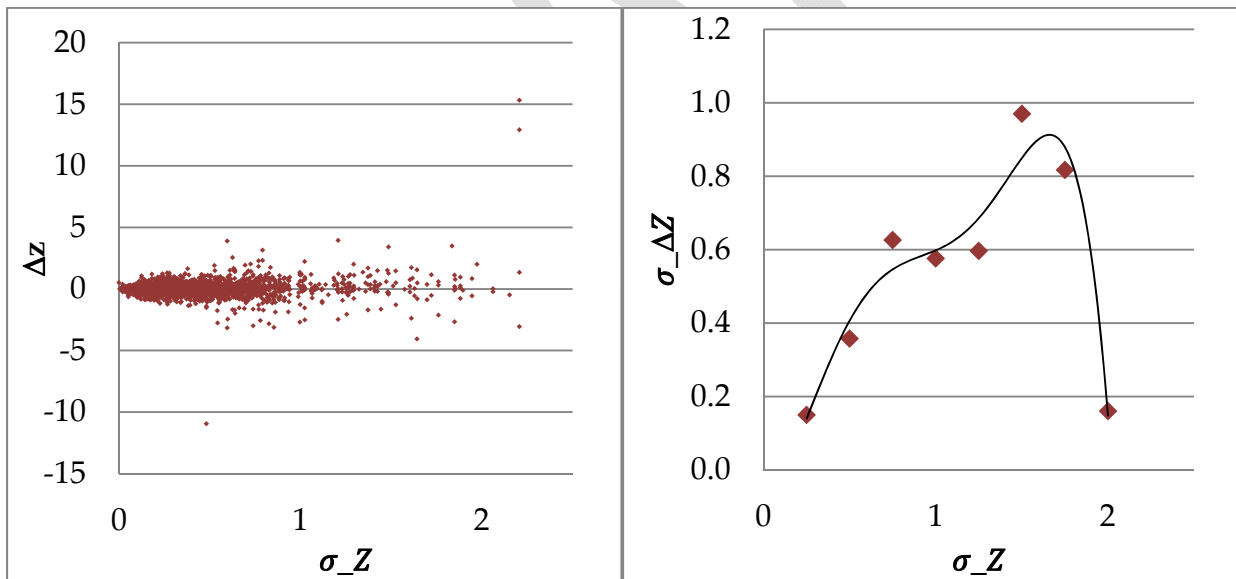


Figure 28. Plots of elevation error and local surface elevation variation (σ_Z ; LEFT) and standard deviation of elevation error ($\sigma_{\Delta Z}$) versus local surface elevation variation (σ_Z ; RIGHT) for the downstream area of the October 2011 data.

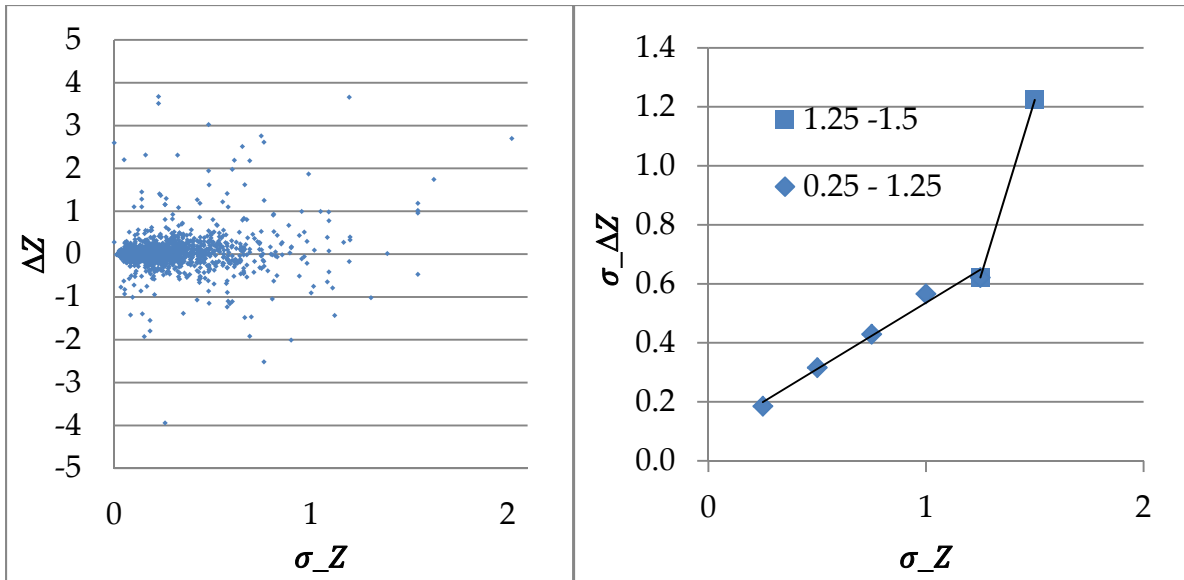


Figure 29. Plots of elevation error and local surface elevation variation (σ_Z ; LEFT) and standard deviation of elevation error ($\sigma_{\Delta Z}$) versus local surface elevation variation (σ_Z ; RIGHT) for the upstream area of the October 2011 data.

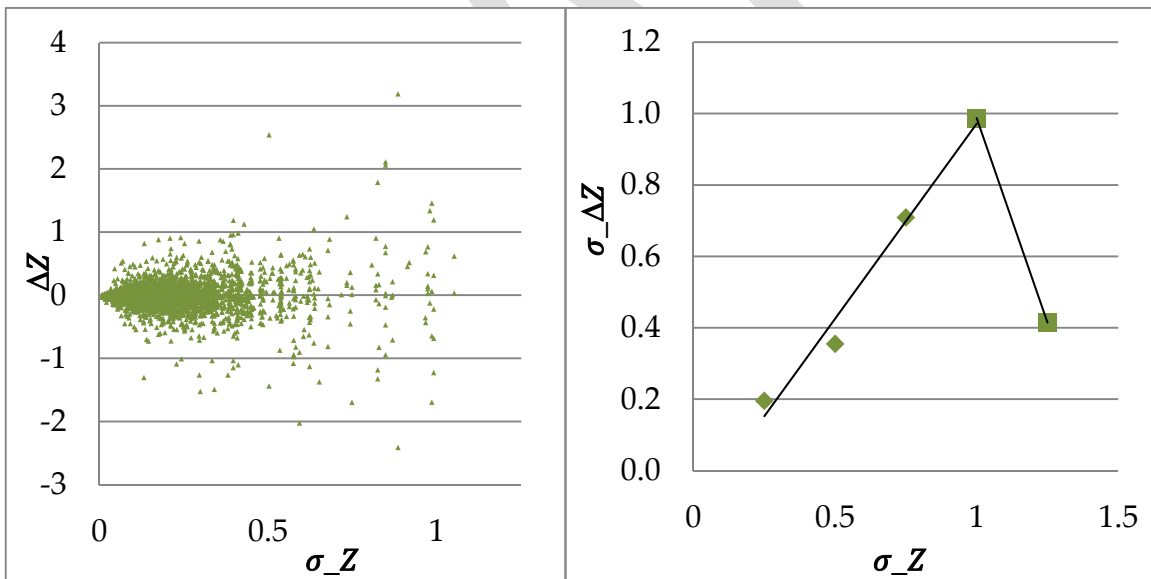


Figure 30. Plots of the elevation error and local surface elevation variation (σ_Z ; LEFT) and standard deviation of elevation error ($\sigma_{\Delta Z}$) versus the local surface elevation variation (σ_Z ; RIGHT) for for the upstream area of the October 2012 data.

Table 14. Ranges of applicability and SIE functions with R² values for the downstream area of the 2007 data.

Range	Function	R ²
0 - 0.25	y=0.10	1
x	y = -0.9041x ⁵ + 5.7449x ⁴ - 13.485x ³ + 13.953x ² - 5.5309x + 0.8095	0.9461
> 2.25	y=0.49	1

Table 15. Ranges of applicability and SIE functions with R² values for the upstream area of the 2007 data.

Range	Function	R ²
0-02	y = -0.1533x ² + 0.7945x - 0.0752	0.9802

Table 16. Ranges of applicability and SIE functions with R² values for the downstream area of the October 2012 data

Range	SIE Function	R ²
0 - 0.25	y = 0.18	1
0.25 - 2.5	y = 1.5053x ⁴ - 6.3119x ³ + 8.5432x ² - 3.5096x + 0.6244	0.9722
>2.5	y = 2.68	1

Table 17. Ranges of applicability for SIE functions with R² values for the downstream area of the October 2011 data

Range	SIE Function	R ²
0- 0.25	y=0.15	1
0.25 - 2	$y = -1.4242x^5 + 6.2326x^4 - 9.3703x^3 + 5.3x^2 - 0.0962x - 0.0438$	0.9405
> 2	y=0.16	1

Table 18. Ranges of applicability for SIE functions with R² values for the upstream area of the October 2011 data

Range	SIE Function	R ²
0 - 0.25	y = 0.19	1
0.25 - 1.25	y = 0.4489x + 0.0867	0.99
1.25 - 1.5	y = 2.4078x - 2.3884	1
>1.5	y=1.22	1

Table 19. Ranges of applicability for SIE functions with R² values for the upstream area of the October 2012 data

Range	SIE Function	R ²
0 - 0.25	y = .2	1
0.25 - 1.0	y = 1.0921x - 0.1209	0.981
1- 1.25	y = -2.2915x + 3.279	1
> 1.25	y = .41	1

6.6. TCD and Sediment Budget Analyses

Results of topographic change detection come in the form of final adjusted DoD rasters where the LoD for each pixel was subtracted out. Final DoD rasters exist for upstream and downstream areas as well as for two different epochs for both upstream and downstream. Summaries of the results were in the form of tabular amounts, spatial plots, and elevation change distributions for erosion and deposition. All results reported in this section are in units of short tons, as previously defined and explained in section 5.3.3.

6.6.1. October 2011 to October 2012 TCD

The upstream TCD analysis yielded 383 tons of erosion and 3908 tons of deposition for this epoch (Table 20). In addition, 874 tons were detected and estimated from the aerial photographs in the river and near the staging area, yielding a net of 4,399 tons of deposition. While a spatial coherence filter of 100 ft² was implemented, patterns of erosion appear patchy and associated with bank roughness elements such as large boulders on the channel edge. Erosion was also predominantly low magnitude, with 50% and 75% of all erosion cells being less than 0.13 and 0.28 ft, respectively. A modest amount of low-magnitude erosion was predicted on river left just below the gravel injection area causing the histogram to have a large peak in the -0.5 to 0 ft bin (Fig. 32). Deposition was focused primarily in the injection area, but there were also some patches of channel fill at the downstream limit of this TCD analysis. Deposition was a much greater magnitude than erosion with 50% and 75% of the deposition was less than 2 and 3.6 ft.

The TCD and supplemental aerial image analysis accounted for 86% of injected gravels, leaving 14% was not accounted for. For a sediment budget of a fractured bedrock and boulder strewn channel, this is quite good closure. The missing sediment is very likely associated with the diffusive nature of smaller gravel fractions that tend to fill void spaces between cobbles and boulders. The pattern of deposition also agreed very well with the gravel injection material identified from the mosaic. Ultimately, as long as the bed is dominated by boulders and fractured bedrock it is going to be very difficult to close a sediment budget. When enough gravel/cobble is injected to fill the bed, then this monitoring problem will end.

The TCD analysis for the downstream area predicted net deposition of 321 tons of gravel, with 401 tons of erosion and 722 tons of deposition (Table 21). Statistically significant areas of deposition and erosion were dispersed in small pockets throughout the reach, but there were areas of larger coherent changes (Fig. 33). One important zone of topographic change occurred in the vicinity of the large house-sized bedrock/boulder

just downstream of the main rapid (Fig. 34). Erosion occurred in a band immediately upstream of downstream of the boulder, while deposition occurred on the shore-side flank of the erosional areas as well as on the thalweg flank of the boulder. Based on field reconnaissance it is interpreted that some of the erosion was a result of sediment landsliding on the flanks of the longitudinal bars, causing infill on the shore-side flank. It is also likely that the top of the bar was skimmed off by flows. A larger region of significant deposition was around all of the bedrock outcrops and boulders along the river left bank opposite Sinoro Bar (Fig. 33). As the river bends to the right, high flows direct the sediment across the channel and to the left under bedrock steering of the flow forces the sediment to turn too, so the deposition is occurring in a band in that flow path. At the downstream limit, just above Narrows Gateway there was widespread deposition that spanned the width of the channel. As in previous analyses, there is a coherent region of erosion through the chute adjacent to Sinoro Bar. This chute is the second hydraulic control evident in the WSE longitudinal plot (Fig. 15). Erosion was mostly ~0.5 to 0 ft, inferred from the histogram. It appears that overall the downstream section maintained a net depositional state between epochs, which is consistent with the interpretation that injected sediment is moving from the injection zone throughout the reach, especially downstream of the rapid.

Table 20. Upstream injection area volumes of erosion and deposition for the October 2011 to October 2012 epoch.

Period	Erosion (short tons)	Deposition (short tons)	Deposition from images*	Net (short tons)
October 2011 to October 2012	-383	3,908	874	4,399

*For the October 2011 to October 2012 epoch the net tons of material accounts for 874 tons of gravel that was accounted for using images and field measurements of gravel deposits near the staging area.

Table 21. Downstream area volumes of erosion and deposition.

Period	Erosion (Short Tons)	Deposition (Short Tons)	Net (Short tons)
October 2011 to October 2012	-401	722	321

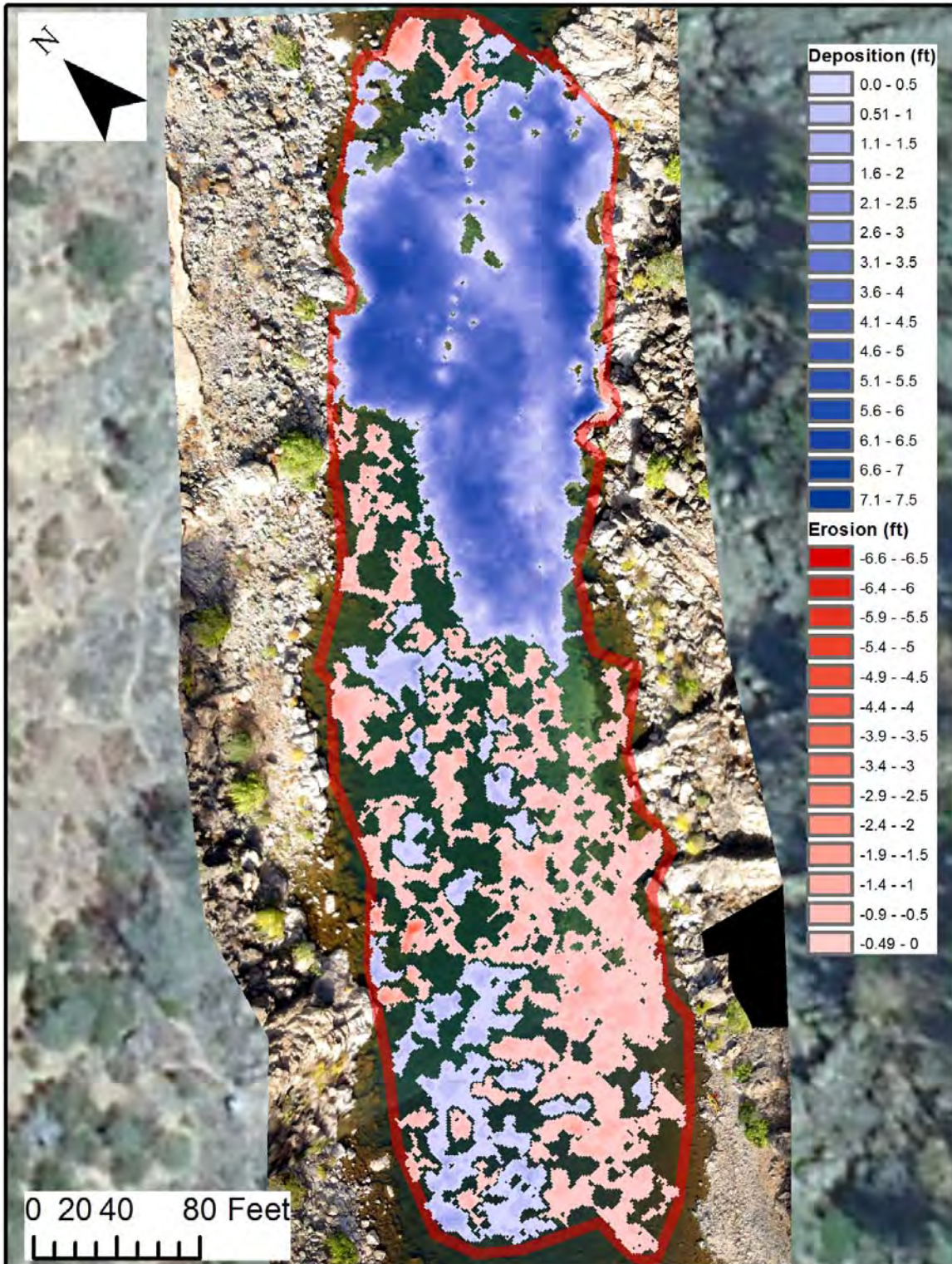


Figure 31. Upstream injection area patterns of erosion and deposition for the October 2011 to October 2012 epoch.

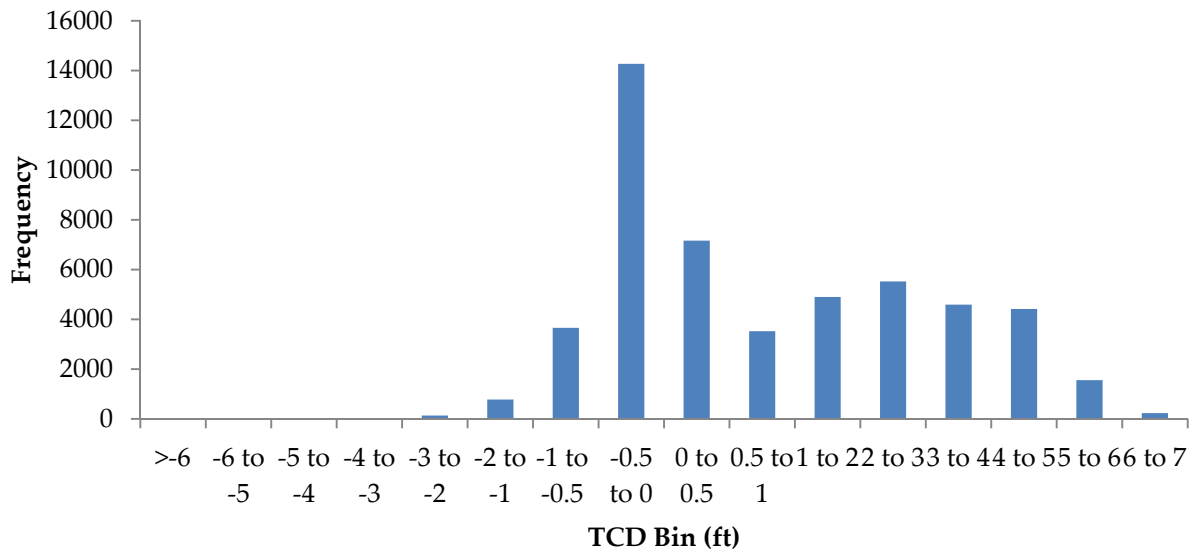


Figure 32. Elevation change histogram for the upstream area for the October 2011 to October 2012 epoch.

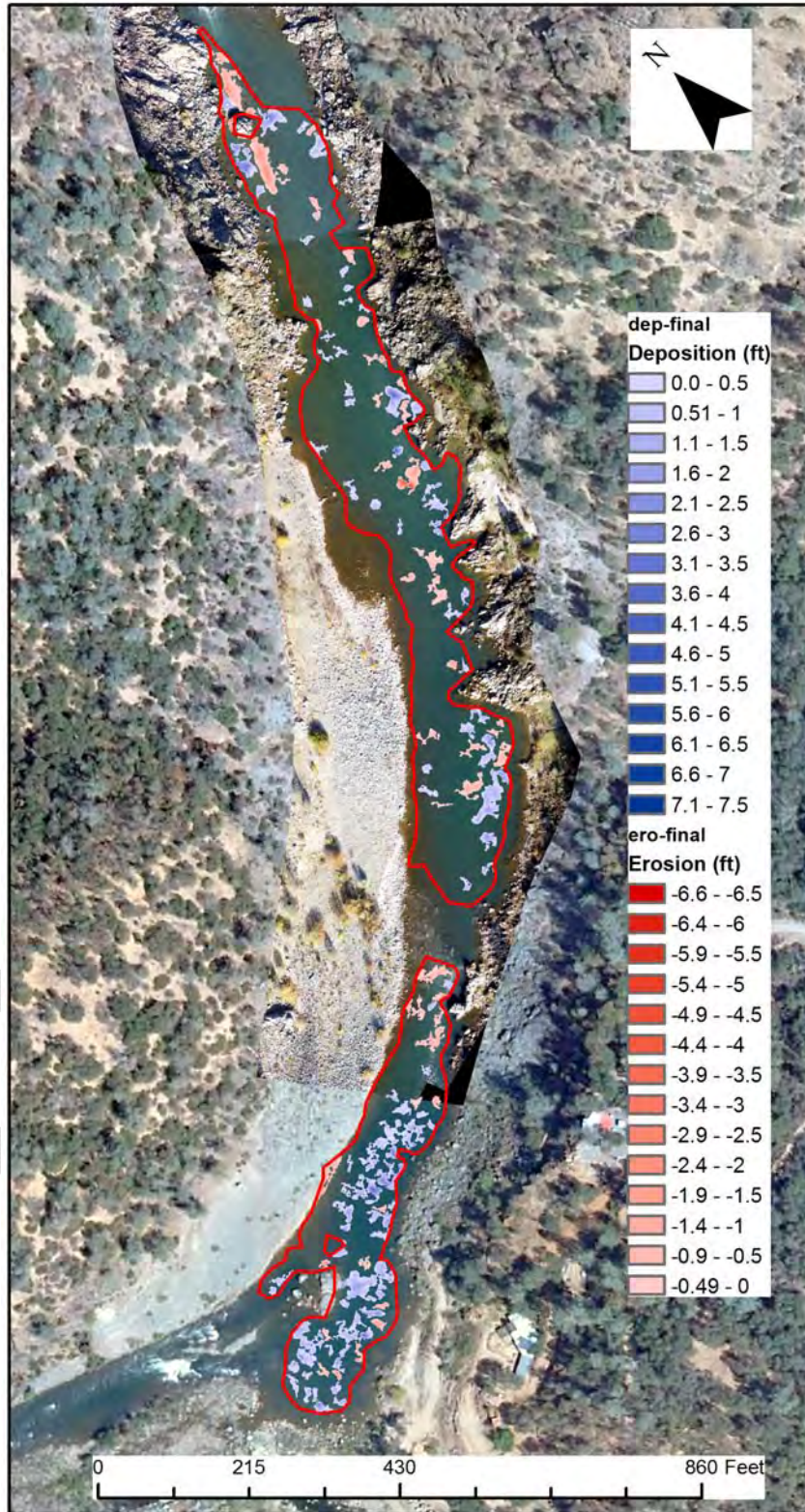


Figure 33. Spatial patterns of deposition and erosion for the downstream area for the October 2011 to October 2012 epoch.

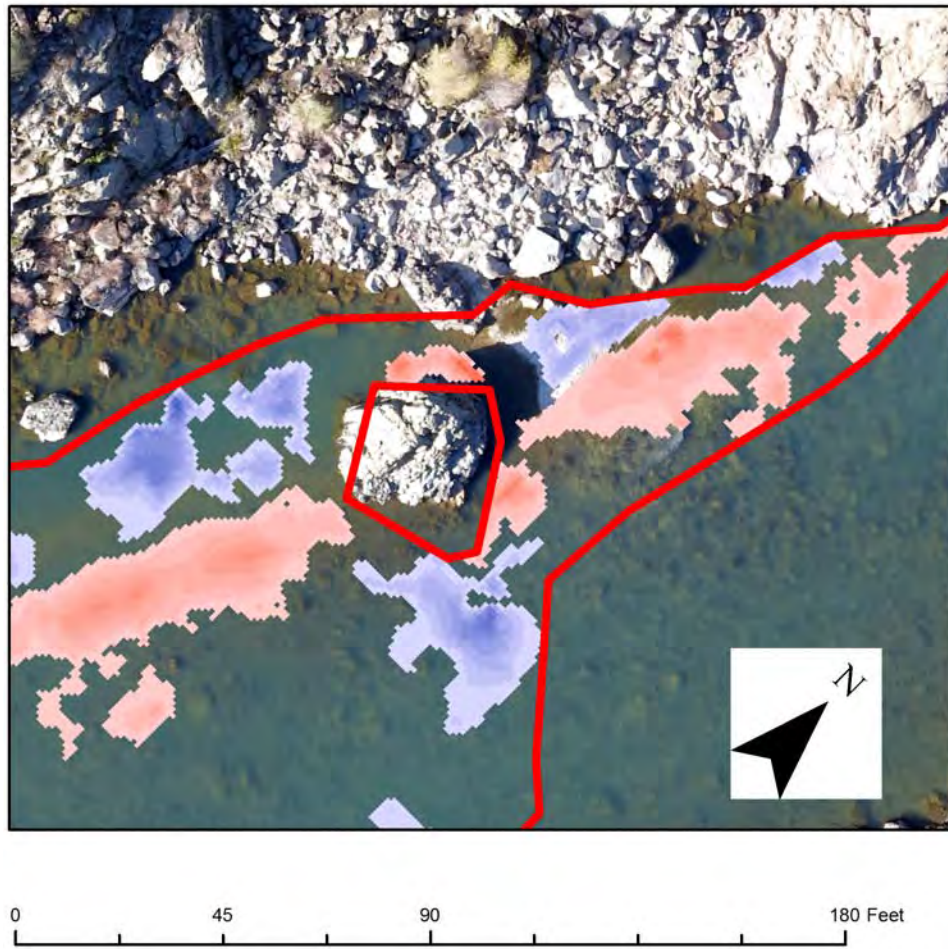


Figure 34. Close up of TCD in the vicinity of the large boulder just downstream of the main rapid. The legend is the same as in Figure 31.

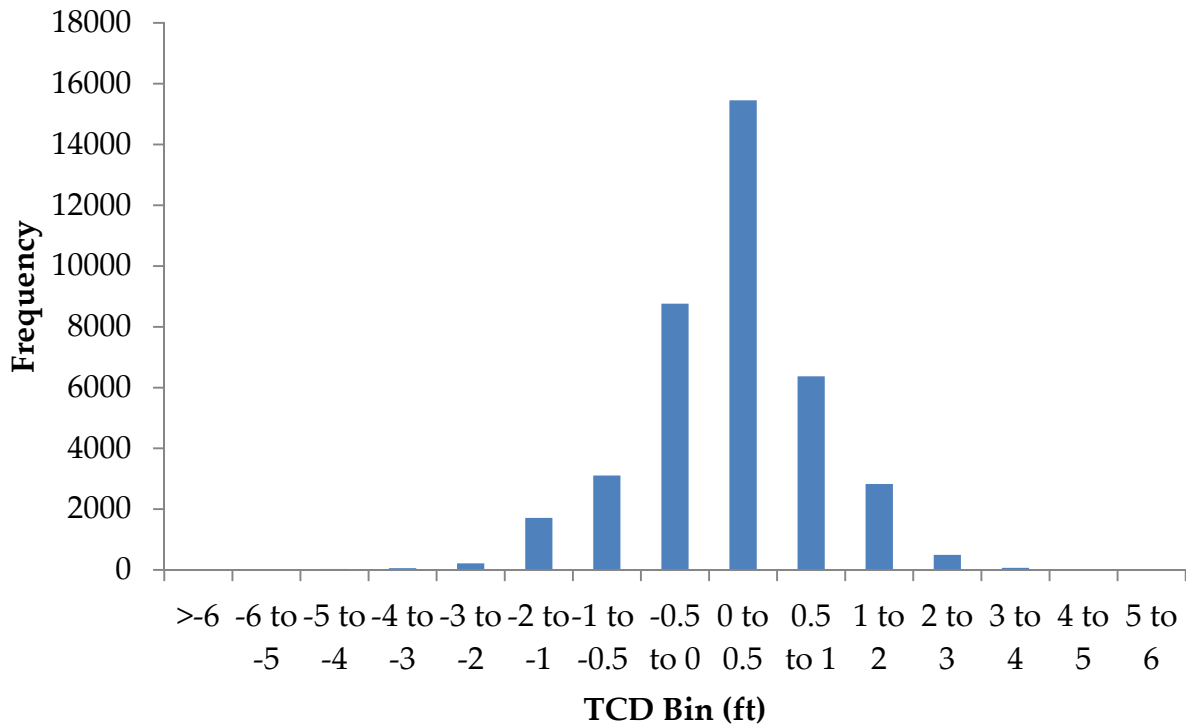


Figure 35. Elevation change histograms for the downstream area for the October 2011 to October 2012 epoch.

6.6.2. Narrows Reach Reconnaissance

In addition to the TCD analysis a visual assessment of the Narrows reach downstream of EDR was made before the 2012 injection. From this reconnaissance it is evident that a very small amount of material has entered the Narrows from the project area and deposited in at least two areas from the prior year’s spring floods (Fig. 36). Because the area past the Narrows Gateway rapid is outside of the area for this study, it cannot be assessed whether any of this material created new spawning habitat or if deposition has occurred in areas below the water line that are not visible. Thus far, no one has ever mapped the river in the Narrows.

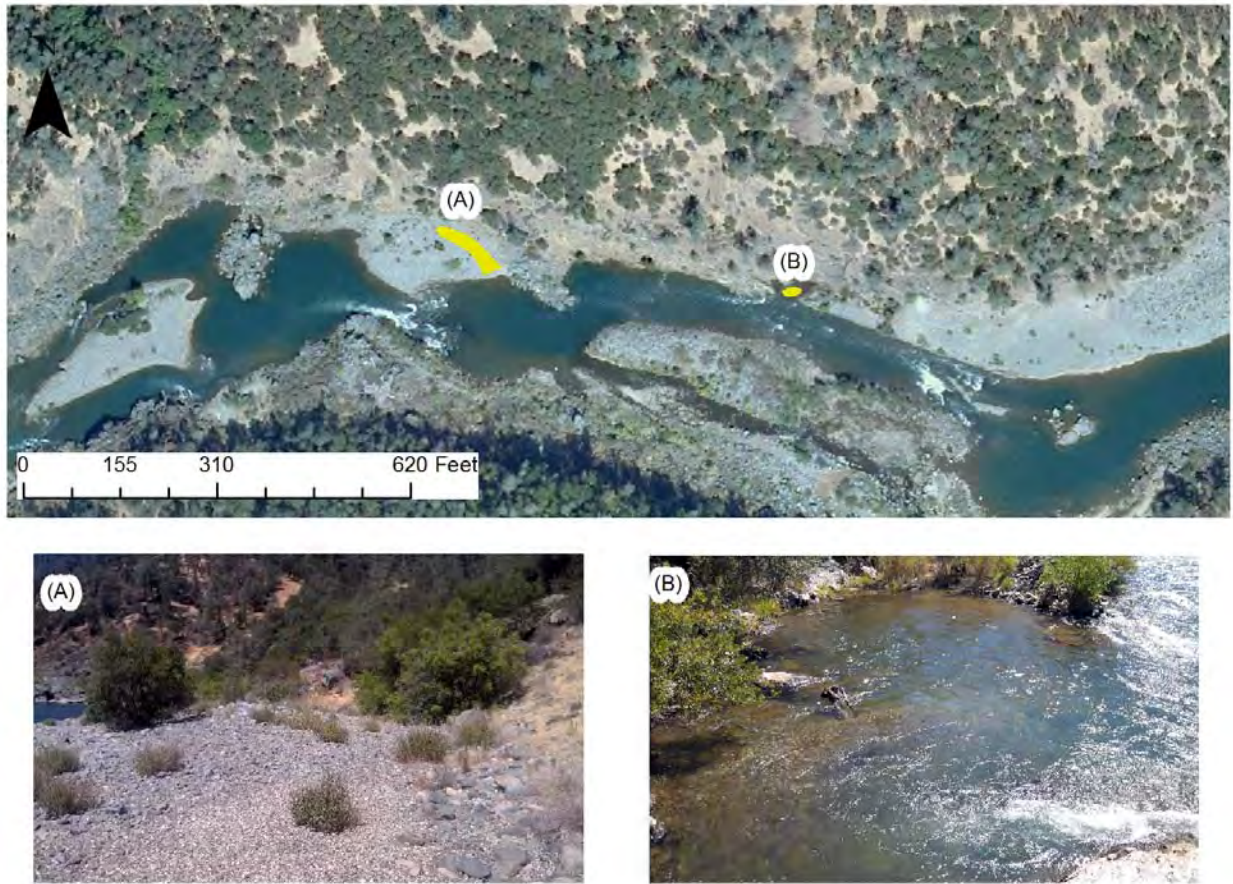


Figure 36. Evidence of injected gravel in the Narrows Reach from a reconnaissance on August 2, 2012 at two locations (A,B).

6.6.3. 2007 to October 2012 TCD

An additional TCD analysis was performed to assess the overall progress of gravel injection in EDR, considering the 2007 to October, 2012 epoch. In the upstream area, the TCD analysis yielded 72 tons of erosion and 6,130 tons of deposition. An additional 959 tons of deposition were also determined from analyzing the aerial extent of gravel that was outside of what the TCD analysis already predicted. Together, this resulted in a net of 7, 017 tons of deposition (Table 22), which implies that there is still some material in the upstream area from the 2011 injection because only 5,000 tons were injected just before the October, 2012 surveys. The dominant range of deposition was from 0 to 1 ft and then there is a broad distribution of deposition from 1 to 6 feet, most likely associated with the gravel injection riffle created in the summer of 2012 (Fig. 37).

For the downstream area TCD analysis predicted 619 tons of erosion and 4,739 tons of deposition, with an additional 260 tons detected from the aerial photographs yielding a net of 4,380 tons (Table 23). Similar to the upstream area deposition was dominant in the 0 to 0.5 ft range, with low magnitude erosion spread amongst a wide range (Fig. 38). The downstream area differs however, in that after this range the magnitude of deposition rapidly falls off. The magnitude of erosion was uniformly distributed between 0 and 2 ft. The spatial patterns of erosion and deposition show that both occur in relatively distinct zones (Fig. 40). Erosion is focused primarily in the chute approximately 400 ft from the downstream study limit. Deposition however, is broadly distributed across most of the TCD study area with the exception of the aforementioned chute.

Combining the two areas together, there was a total gain of 12,088 short tons. In 2007, 2010/2011, and 2012 there were injections of 453, 5000, and 5000 short tons, respectively, yielding a total addition of 10,453. Comparing the observed versus expected amount of sediment, there is an excess of 15.6%. A key difference from 2007 versus the later injections is that extra gravel was purchased to insure that at least 5,000 short tons did indeed go into the river, but the exact overage is not known, but is within ~25-100 tons. Note that the section of EDR between Narrows I and Narrows II powerhouses was actually mapped in 2005, while most of the rest of the reach was mapped in 2007, which is why it is called a 2007 map. However, it is very possible that during the 7 year period from 2005 to 2012, significant erosion took place in the river between the Narrows II powerhouse and the top of the GAIP injection zone, which might have contributed angular rock to the riverbed in the study area. Also, it is unknown how much angular rock slid and washed down into the river from the hillsides and canyon walls during rain storms- a process that has been observed on several occasions. Meanwhile, a total of 691 short tons of pre-existing bed material present in 2007 left the reach by 2012. The vast majority of this was due to natural erosion of sediment at the chute that currently serves as the second major hydraulic control in the reach (Fig. 40, pink/red area). Overall, the sediment budget is closed pretty well for a sediment budget in a bedrock/boulder canyon. The most impressive aspect of the TCD from 2007 to October 2012 is that deposition is fairly ubiquitous throughout the reach, which proves that the injections are working in terms of beginning the process of filling in the riverbed as desired, predicted, and expected in the GAIP.

Table 22. Volumes of erosion and deposition for upstream area for the 2007 – October, 2012 epoch.

Period	Erosion (short tons)	Deposition (short tons)	Deposition from images*	Net (short tons)
2007 to October, 2012	-72	6,130	959	7,017

*For the 2007 to October 2012 epoch the net tons of material accounts for material deposits identified from both the 2011 and 2012 aerial imagery.

Table 23. Volumes of erosion and deposition for upstream area for the 2007 – October, 2012 epoch.

Period	Erosion (short tons)	Deposition (short tons)	Deposition from images*	Net (short tons)
2007 to October, 2012	-619	4,739	260	4,380

*For the 2007 to October 2012 epoch the net tons of material accounts for material deposits identified from both the 2011 and 2012 aerial imagery.

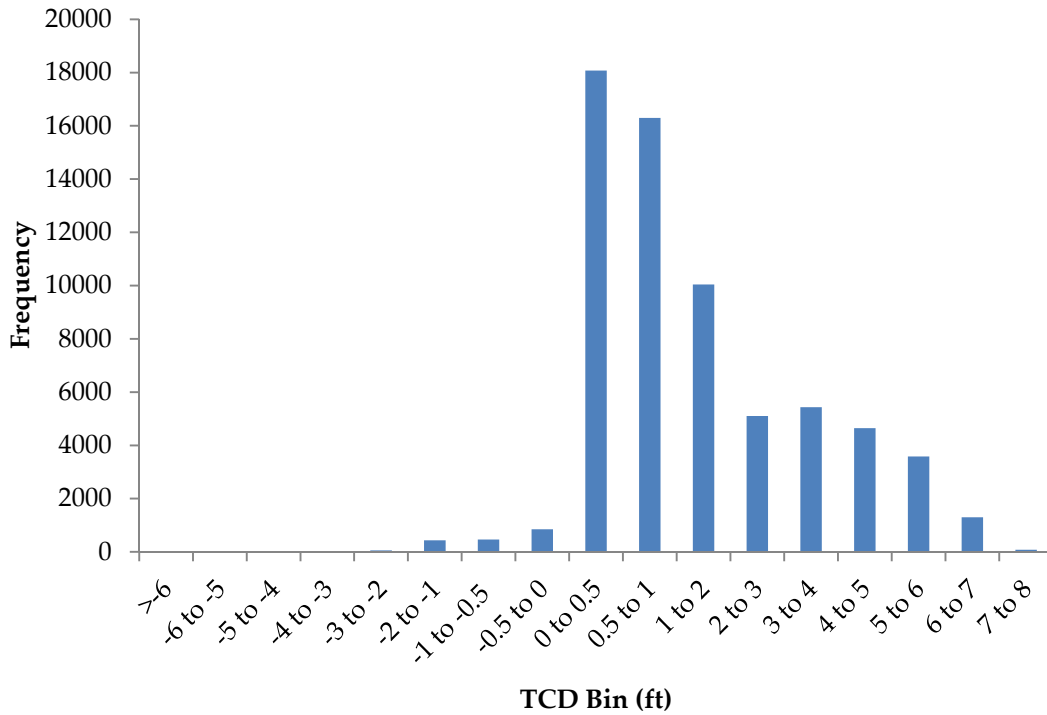


Figure 37. Elevation change histogram for the upstream area for the 2007 to October 2012 epoch.

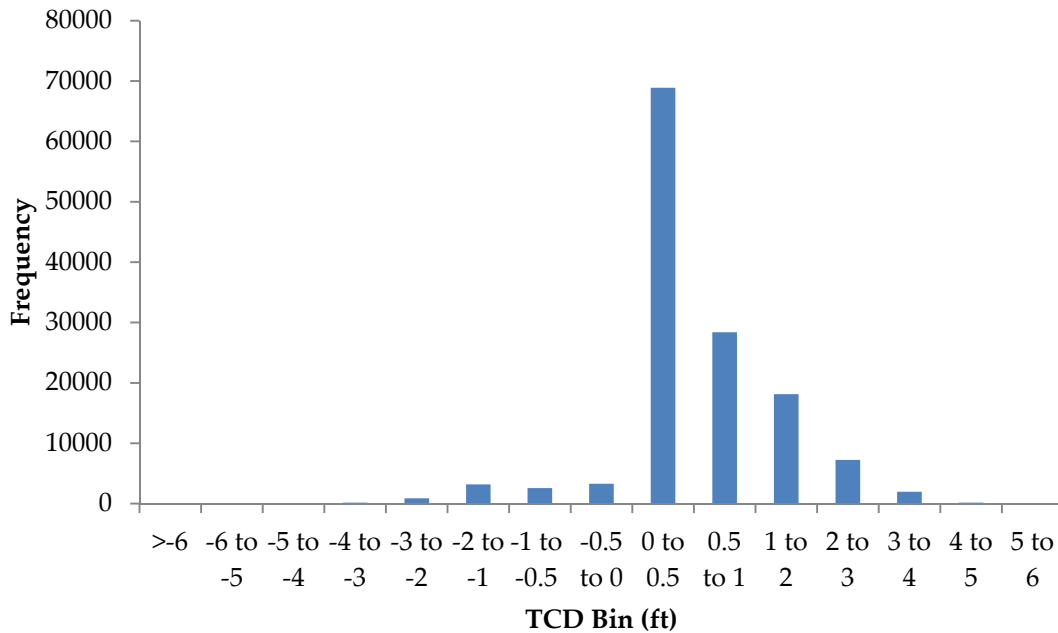


Figure 38. Elevation change histogram for the downstream area for the 2007 to October 2012 epoch.

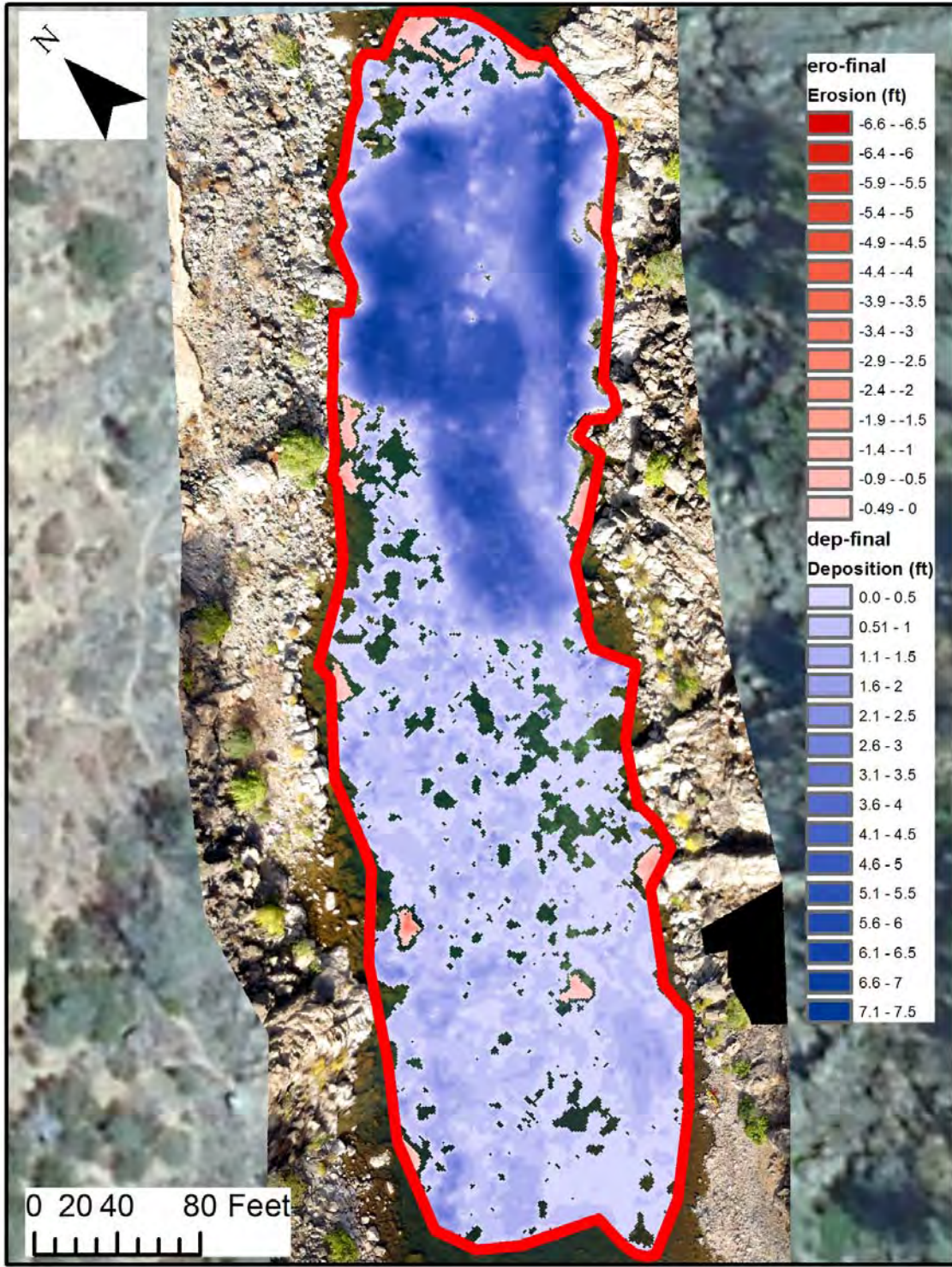


Figure 39. Spatial patterns of deposition and erosion for the upstream area for the 2007 to October 2012 epoch.

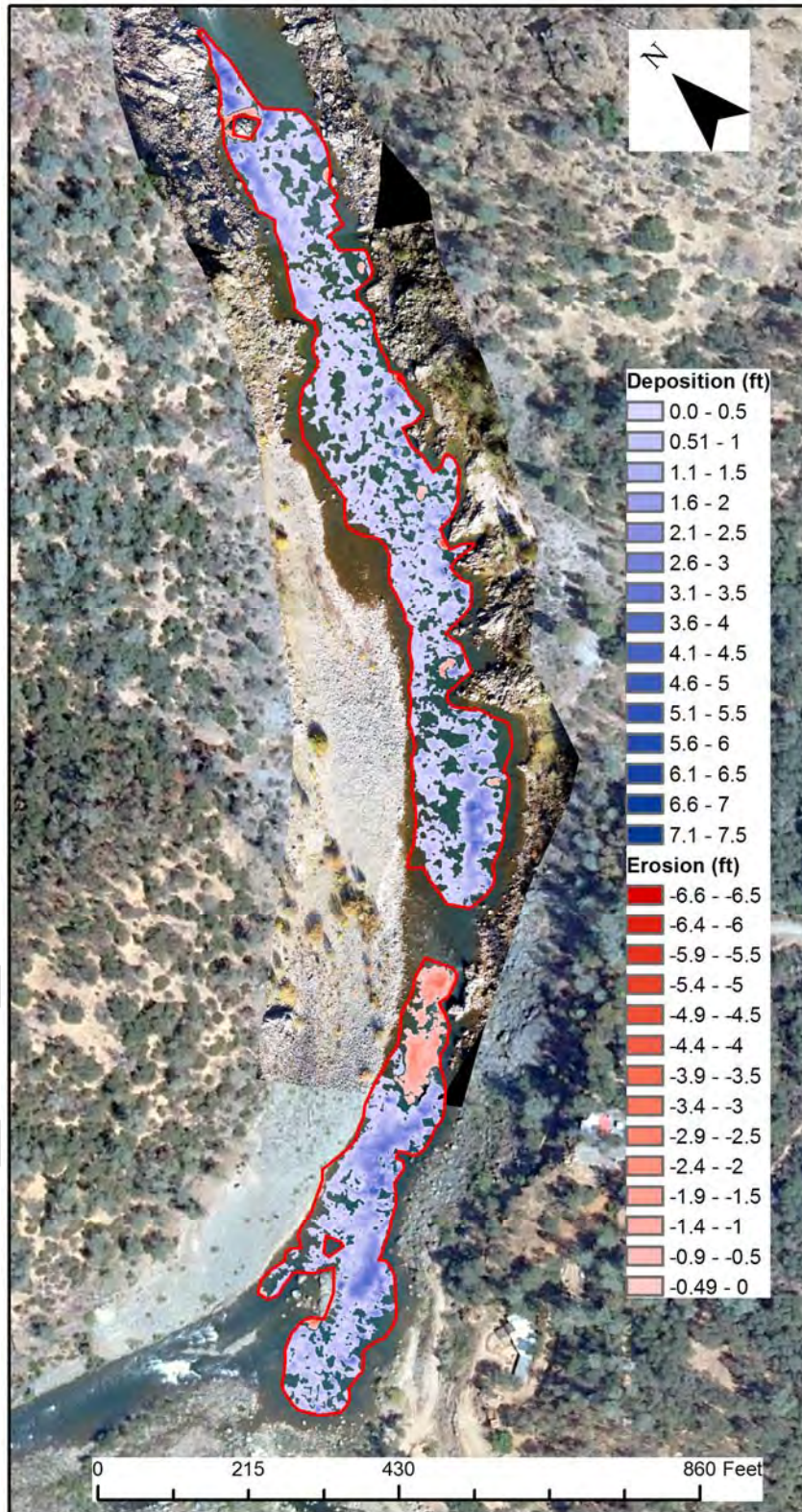


Figure 40. Spatial patterns of deposition and erosion for the downstream area for the 2007 to October 2012 epoch.

6.6.4. Gravel/Cobble Storage Mechanisms

Similar to last year, direct observation, blimp imagery, and topographic change detection of the spatial pattern of re-deposition all confirm that the mechanisms of sediment deposition proposed in section 2.1.1 occurred between October 2011 and October 2012. First, blanket filling of the bed within interstitial zones of bed roughness elements such as boulders, shot rock, and bedrock is occurring widespread in the downstream reach. Second and third, large bedrock and boulder protrusions promote deposition both upstream (i.e. “highsiding”) and downstream (i.e. “eddying out”). The former was the dominant form of deposition where Chinook salmon spawning was observed; it occurred on the cobble bar just upstream of the big rapid and just upstream of the bedrock outcrop at the top of Sinoro Bar. The latter was evident in the eddies alongside the rapid and downstream of the house-size boulder just downstream of the rapid. As flow converges through the rapid eddy shedding from the rough bedrock boundary occurs pushing sediment outward out of the main zone of flow convergence into topographic nooks. Fourth, curvature of the channel (especially at Sinoro Bar) appears to steer flow and sediment to the outer bend where the sediment gets caught up by the earlier three mechanisms within areas of bedrock variability on river left opposite Sinoro Bar. Finally, at several locations the channel expands (in width and depth), which decreases velocity and causes a general tendency for deposition. Where flow moves straight through these expansions, there are long lines or bands of deposited material.

Erosion was primarily limited to areas influenced by large bedrock protrusions that promote convective acceleration around them. The mechanisms for this were researched and explained by Thompson (2001, 2006, 2007). The largest example of this is at the second bed step (i.e. chute, second hydraulic control) in the reach, which is opposite Sinoro Bar, and this was observed last year in this location, too. As constrictions in bedrock channels are agents of pool maintenance this is an expected outcome. Interestingly, it does appear that some incision occurred in Narrows Gateway from inspection of the new rating curve information but there is also some blanket fill deposition immediately upstream of this area. It appears that selective filling nooks and crannies among boulders, shot rock, and bedrock fractures is widespread, but difficult to quantify. Another noteworthy point is that it does appear deposition occurred more so on river left before the rapid. At high flow the streamlines go to that side, pushing the sediment there as well. As a result, gravel/cobble gets pushed up against the pre-existing shot rock cobble bar there in sufficient depth to create spawning habitat. This is a positive sign that natural bar growth can occur even with modest amounts of injected gravel in some locations.

6.7. Habitat Suitability Modeling

6.7.1. GHSI Bioverification

Comparing GHSI values at the locations of 2012 observed redds to the availability of 2D model-predicted GHSI values for the whole domain, areas predicted to be high quality habitat using the Beak, Inc. hydraulic HSCs were utilized by adult Chinook spawners preferentially to build redds. Recall that an electivity index (EI) > 1.07 for a GHSI bin indicates preference, while an EI between 0.93 – 1.07 indicates tolerance and an EI < 0.93 indicates avoidance. The EI analysis found that observed redds had a very strong preference for GHSI bins ≥ 0.6 (Fig. 41). The EI value for the 0.6-0.8 GHSI bin was 2.9 and that for the 0.8-1.0 GHSI bin was 4.1 (Fig. 41). Overall, the results show that the predictive microhabitat model making use of a combination of (a) Beak hydraulic HSCs, (b) presence/absence of gravel/cobble, and (c) 2D model predicted depth and velocity is bioverified for use in EDR according to the bioverification requirements presented in section 5.4.3. Specifically, there exist both preferred and avoided GHSI bins and the bins that are preferred are the ones that conceptually represent the highest quality habitat bins, while those that are avoided are the ones that conceptually represent the lowest quality habitat bins. EI decreases with decreasing GHSI bin values, which is within the bioverification expectation that decreasing GHSI value should mean lower quality habitat and thus less utilization relative to habitat availability.

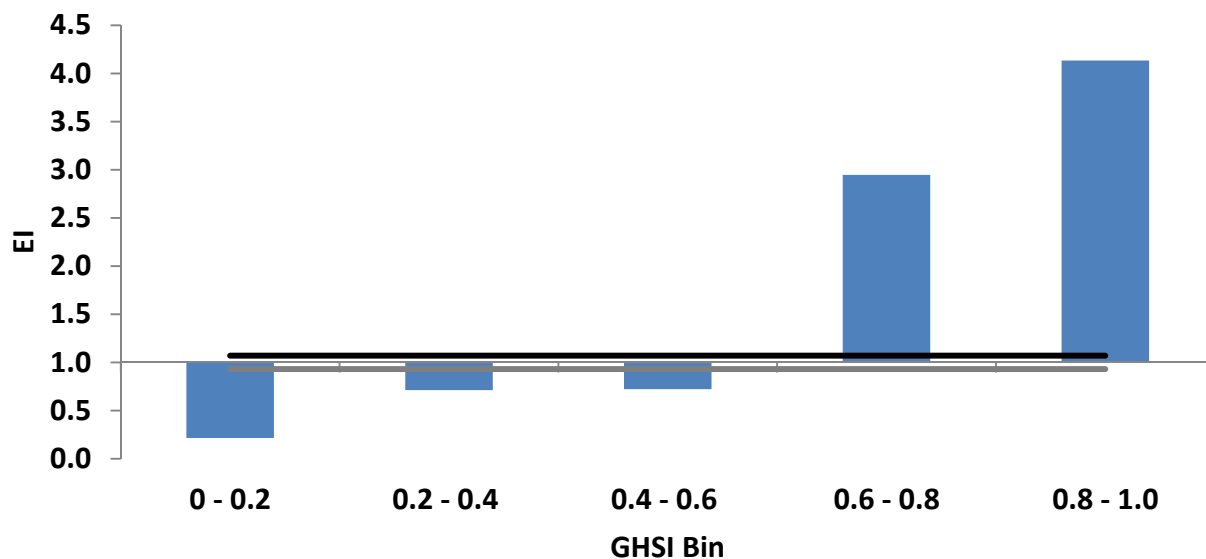


Figure 41. Electivity index (EI) for each GHSI bin. Bars above thick black line were preferred by spawners and those below the dark grey line were avoided. For the category of 0-0.2, that is excluding values of exactly 0. Therefore, the available area used in calculating EI excluded the vast area with an EI=0, because that would skew the results in exactly the way that makes the forage ratio invalid (i.e. yield such small areas for the non-zero GHSI bins that all GHSI bins would have a high EI).

6.7.2. Abundance of Preferred Habitat

Given that the majority of the EDR still lacks an alluvial, gravel/cobble bed, the 2D model coupled with the Beak, Inc. hydraulic HSCs predicted that there is still very little Chinook spawning habitat at this early stage of long-term gravel augmentation. Given Annual GAIP injections are quite modest in these early years to allow for development of logistics, strategy, and scientific understanding. Compared to the total wetted area of the EDR, the area that gained enough gravel/cobble substrate to produce shallow, moderately fast hydraulic conditions was small, simply because the sediment storage deficit for the reach is still very large- only 10-16% of the total deficit has been addressed at this point in GAIP implementation. At least 90% of the total wetted area was predicted to be non-habitat (GHSI=0) or low quality habitat for each of the six model runs for October 2012 (Fig. 42). By excluding areas with GHSI=0 (domain that for this study must be considered as not available for spawning on the basis of no appropriate alluvium), it is possible to determine the distribution of available habitat quality amongst bins with GHSI>0. From the EDR 2012 bioverification in the previous

section, preferred habitats at this time are those with GHSI ≥ 0.6 . On that basis, 17% of the available habitat has preferred conditions (Fig. 43). For the rest of the lower Yuba River Chinook salmon also prefer areas with GHSI between 0.4 to 0.6, but not for EDR at this time. Thus, even though habitat is extremely limited and there are fish-density driven effects evident in the river, Chinook salmon are actually being highly preferential in where they will choose- the vast majority would rather all cram into the small area of high quality habitat rather than spread out in to the other peripheral areas of medium quality habitat. Gravel augmentation is at an early state of creating habitat in the EDR and the evidence thus far all suggests that we can accurately predict where Chinook salmon will spawn in EDR, now and in the future as injections occur.

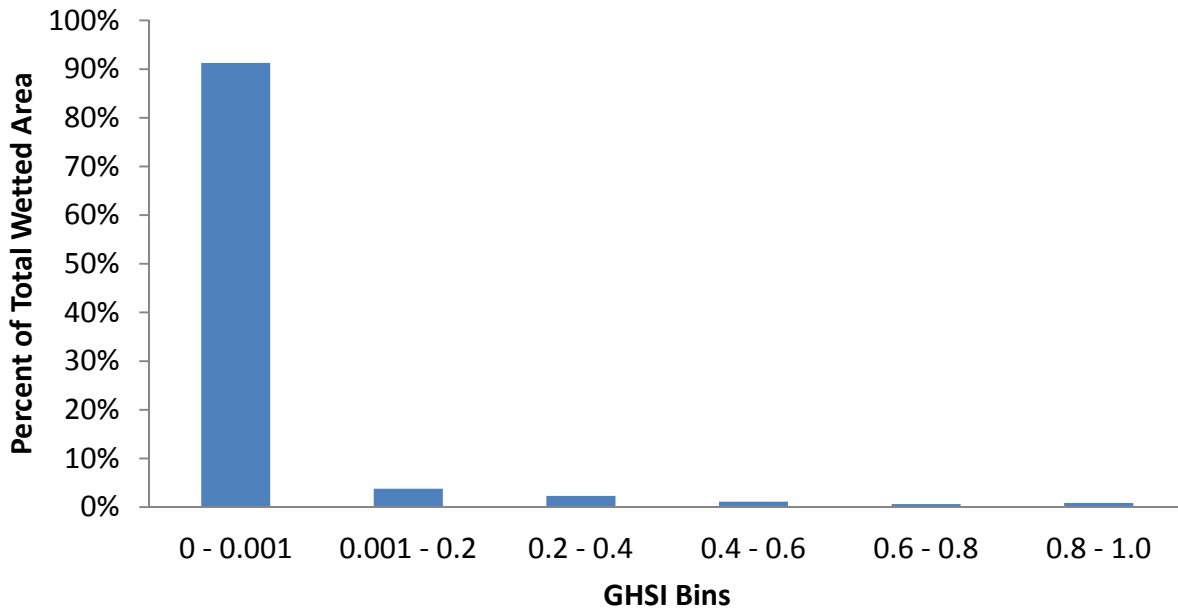


Figure 42. Model predicted fractional area for each GHSI bin at 996 cfs, including 0 values for the entire wetted area of the EDR. At this time most of the river lacks an alluvial, gravel/cobble bed.

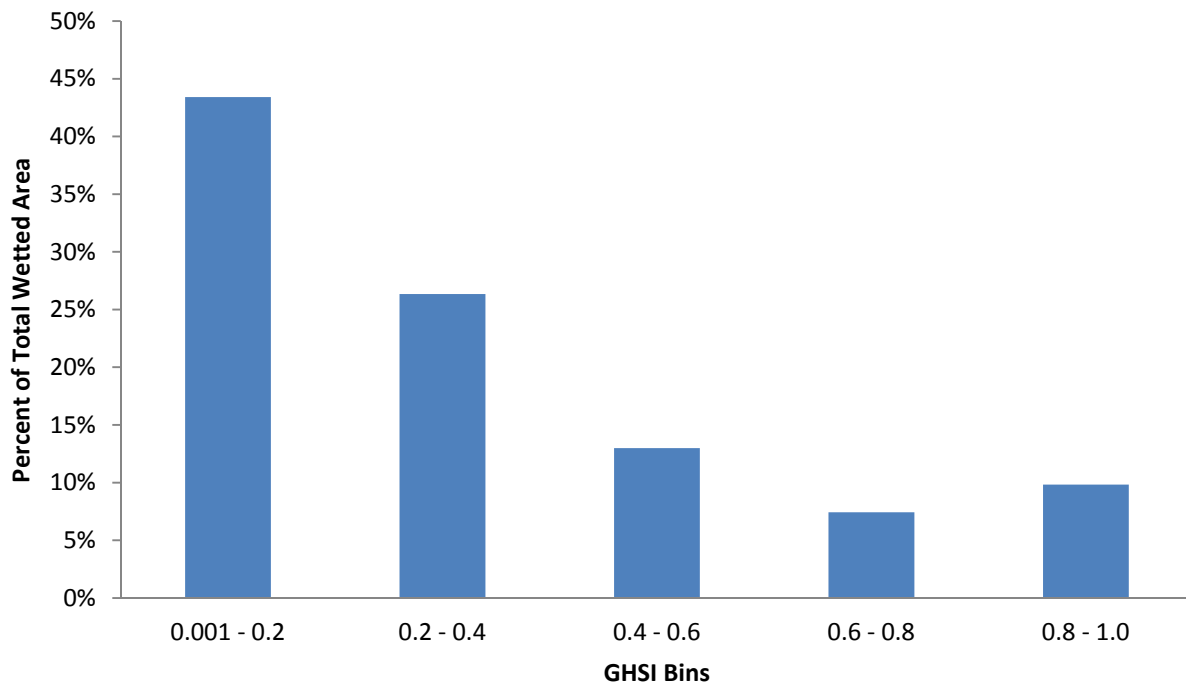


Figure 43. Model predicted fractional area at 996 cfs for each GHSI bin, excluding areas where GHSI=0 (i.e., non-habitat).

6.7.3. 2D Model Chinook Spawning Habitat Predictions

To illustrate the overall patterns of DHSI, VHSI, HHSI, and GHSI a series of plots for the 966 cfs evaluation were made (Fig. 44). The plots show that hydraulics present conflicting habitat conditions that are currently a major impediment to having good spawning habitat. Based on the DHSI raster, it is evident that excessive depth limits spawning throughout much of the reach and the only suitable habitat for depth is along the rocky flanks of the channel (Fig. 44a), which is a major reason why a lot more gravel/cobble substrate is needed to shallow up the river. Meanwhile, VHSI shows the exact opposite spatial pattern (Fig. 44b), with suitable velocity widespread down the center of the channel and an absence of preferred velocity along the flanks. The occurrence of a correlation between high velocity and high depth is representative of U-shaped channel lacking longitudinal alluvial bedforms and landforms. Brown and Pasternack (2008) explain how this geomorphic-hydraulic mechanism works with regard to spawning habitat availability. Alluvial rivers with excellent salmonid spawning habitat exhibit an inverse relationship between depth and velocity at spawning flows. In addition to this confounding hydraulic regime, it appears that suitable substrate is also a limiting factor, as the GHSI accounting for substrate and

hydraulics (Fig. 44d) has a much smaller area of preferred physical habitat than the HHSI accounting for hydraulics alone (Fig. 44b). Thus, gravel augmentation is a necessary mitigation to managing physical habitat by (1) filling in the river with alluvium to reduce depth throughout the EDR, (2) shifting the geomorphology steering the relation between depth and velocity at spawning flows and (3) providing suitable gravel/cobble substrate on the bed surface.

Analyzing close views of predicted GHSI patterns illustrates observed redds clustered on sizable, coherent patches of model predicted GHSI values > 0.8 . For example, at 966 cfs it is evident that almost all observed redds in the injection zone occurred in areas where the model predicted spawning habitat to be present and to mostly have GHSI values > 0.8 . However, in the middle cluster of redds that was on substrate from the 2010-2011 injection just upstream of the cobble bar adjacent to the main rapid, no predicted habitat occurred there... While only one discharge was modeled for 2012 due to the steadiness of the flow, the 2011 condition reported by Brown and Pasternack (2012) showed a nearly identical result for a range of spawning flows.

Two factors could contribute to why observed redds were not exactly on the highest possible predicted habitat. First, the cluster sites are so small in this initial phase of gravel augmentation that there simply is not enough high-quality habitat for all the spawners, so many either have to interfere with each other or move off to the flank of the optimal locations into marginal areas. Second, the mapping-grade Trimble GeoXT GPS units used by the Pacific States Marine Fisheries Commission for recording the geographic coordinates of redds has an accuracy of $\sim 0.5 - 2$ m (especially considering the blockage of line-of-site with satellites from being in a canyon), which is less than the precision needed for fairly testing the detailed accuracy possible with the 2D model.

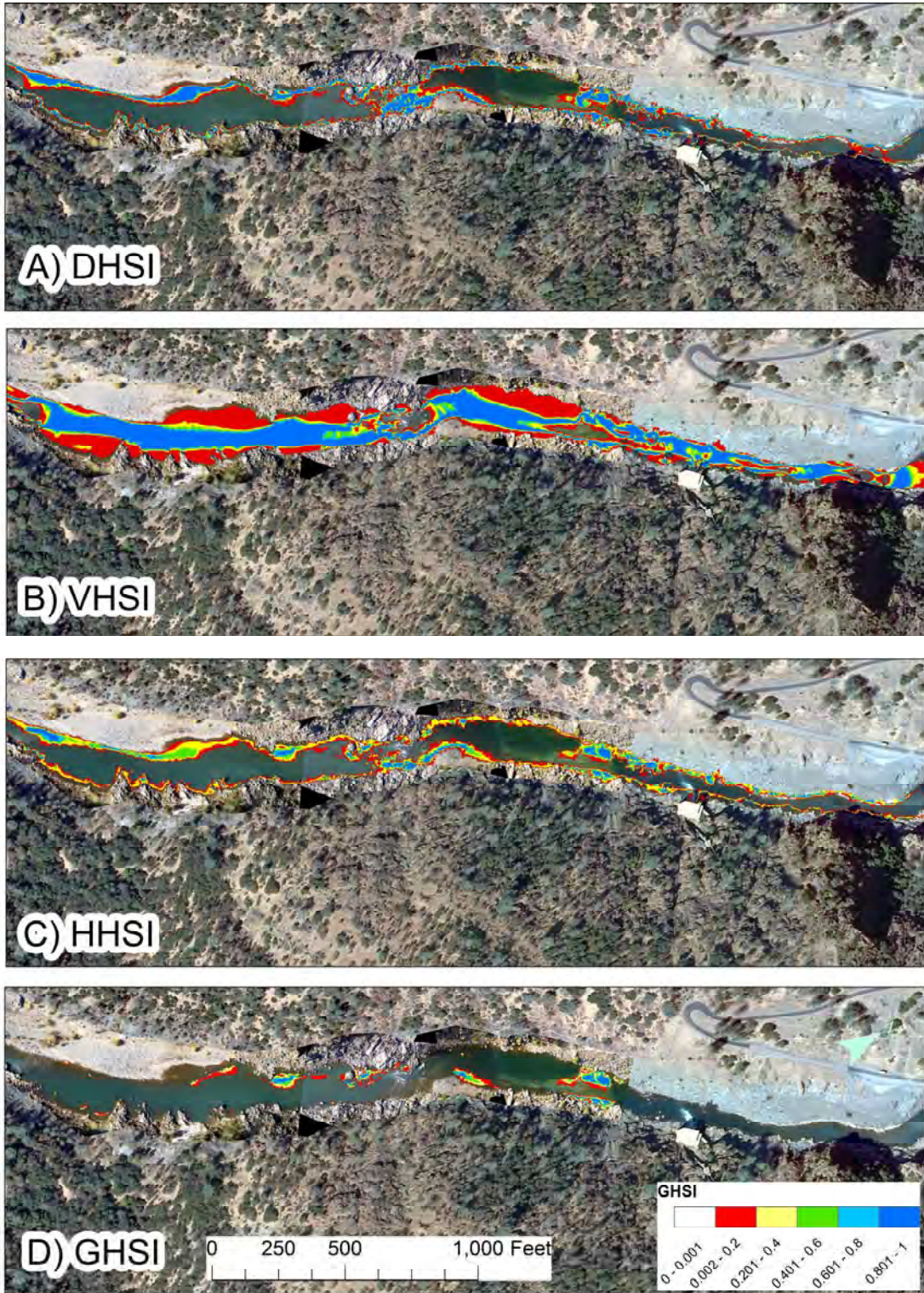


Figure 44. DHSI, VHSI, HHSI, and GHSI predicted by the 2D model for 966 cfs.

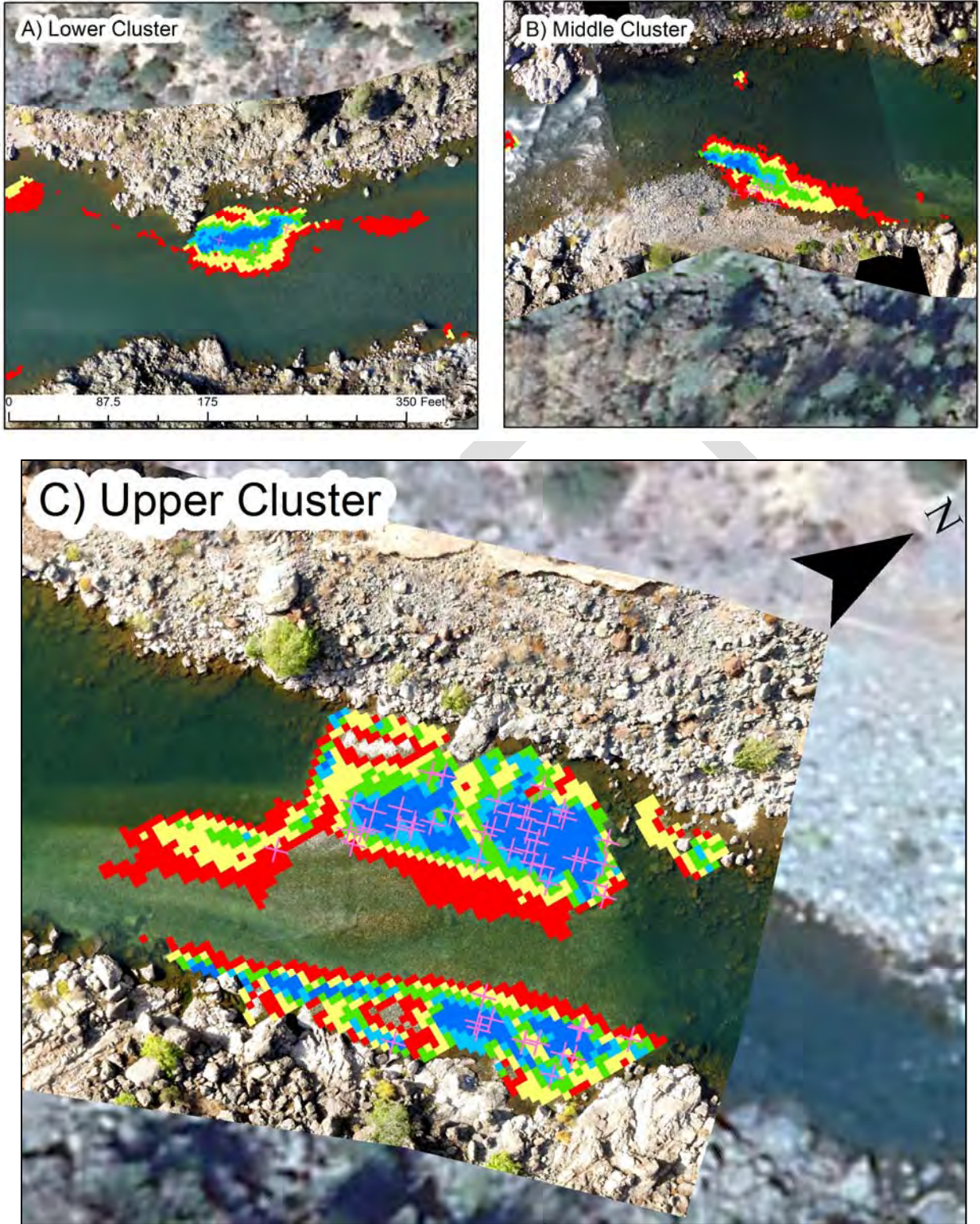


Figure 45. Close views of the GHSI raster for 966 cfs with observed redds shown as magenta colored crosses for the a) lower, b) middle, and c) upper clusters. The color legend is the same as in Figure 44.

It's worthwhile at this point to look closer at the constructed spawning riffle to examine habitat suitability associated with depth and velocity and how those two combined to create the final GHSI raster. Figure 46 show DHSI, VHSI, and GHSI overlaid on the photo mosaic. It appears most of the laterally placed material had sufficient depths for spawning, but the center chute of the channel was outside of the depth criteria for Chinook salmon. Similarly, along the channel margins there are high quality velocity zones a few feet from each bank but the center of the channel has unsuitable velocities. Combined, the two depth and velocity HSI predictions show that the chute in the center of the riffle is unsuitable for spawning. Therefore, the most suitable habitat is limited to the channel margins a few feet from each of the banks. Note that it is unavoidable to have a chute at this site, because the channel in the injection zone is narrow due to canyon constriction and there has to be a deeper thalweg to allow the volume of water released by the upstream facilities to move through. It will take much more infill of alluvium before a larger contiguous area of high quality habitat will be present either in the injection zone or just downstream of it.

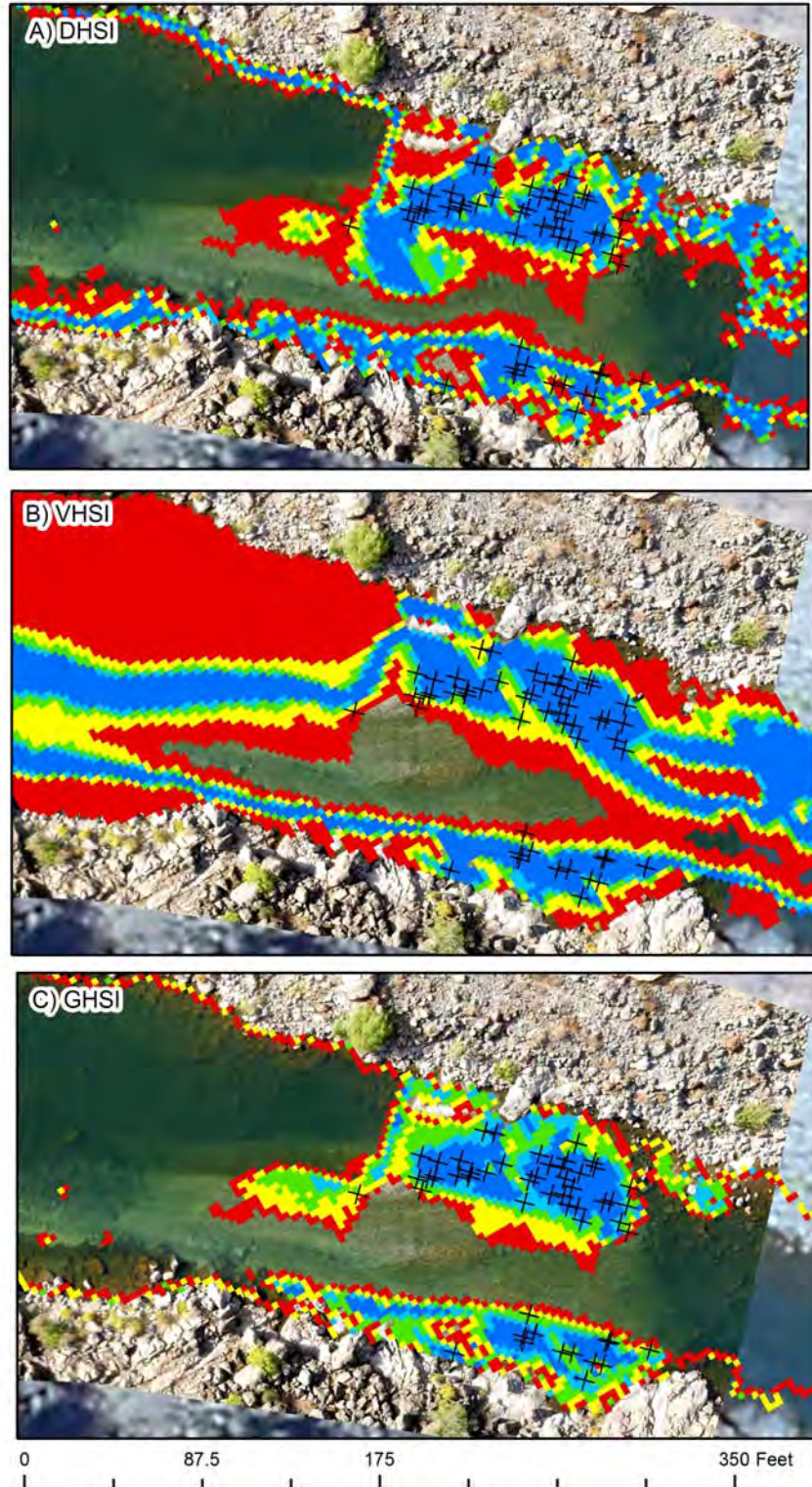


Figure 46. Close views of the a)DHSI, b)VHSI, and c)GHSI raster for 966 cfs with observed redds shown as magenta colored crosses for the constructed spawning riffle. The color legend is the same as in Figure 44.

6.7.4. Observed Spawning use and Deposition

As shown earlier all observed 2012 redds were located on areas with injected gravels, either in the injection zone or where it moved downstream since November 2010, as identified from blimp- image analysis (Fig. 23). Because the spawning that occurred in 2011 could only occur downstream of the injected zone due to flows mostly evacuating the injection area, Brown and Pasternack (2012) were able track topographic changes for everywhere downstream of that zone. There were two redds outside of the constructed spawning riffle that were associated with naturally deposited sediments, but most redds utilized the constructed feature (Fig. 48). Twelve redds were not associated with any TCD predicted deposition. Similar to last year's findings, we conjecture that the new downstream deposits are attracting spawners, but may not be as thick as needed or desired for optimal embryo survival and fry production. It is interesting that no redds were detected near the Narrows Gateway Rapid this year, but this could be related to incision in this area. Considering that this second injection has only met ~10-16% of the gravel/cobble deficit for the reach, this outcome is not surprising. *Substantially more of the deficit will have to be addressed before deep and resilient spawning sites are available at downstream locations.*



Figure 47. Observed redds and boundaries for upstream and downstream TCD analysis. Note that the upper cluster is located in the constructed riffle and the middle cluster was outside of the TCD boundary.

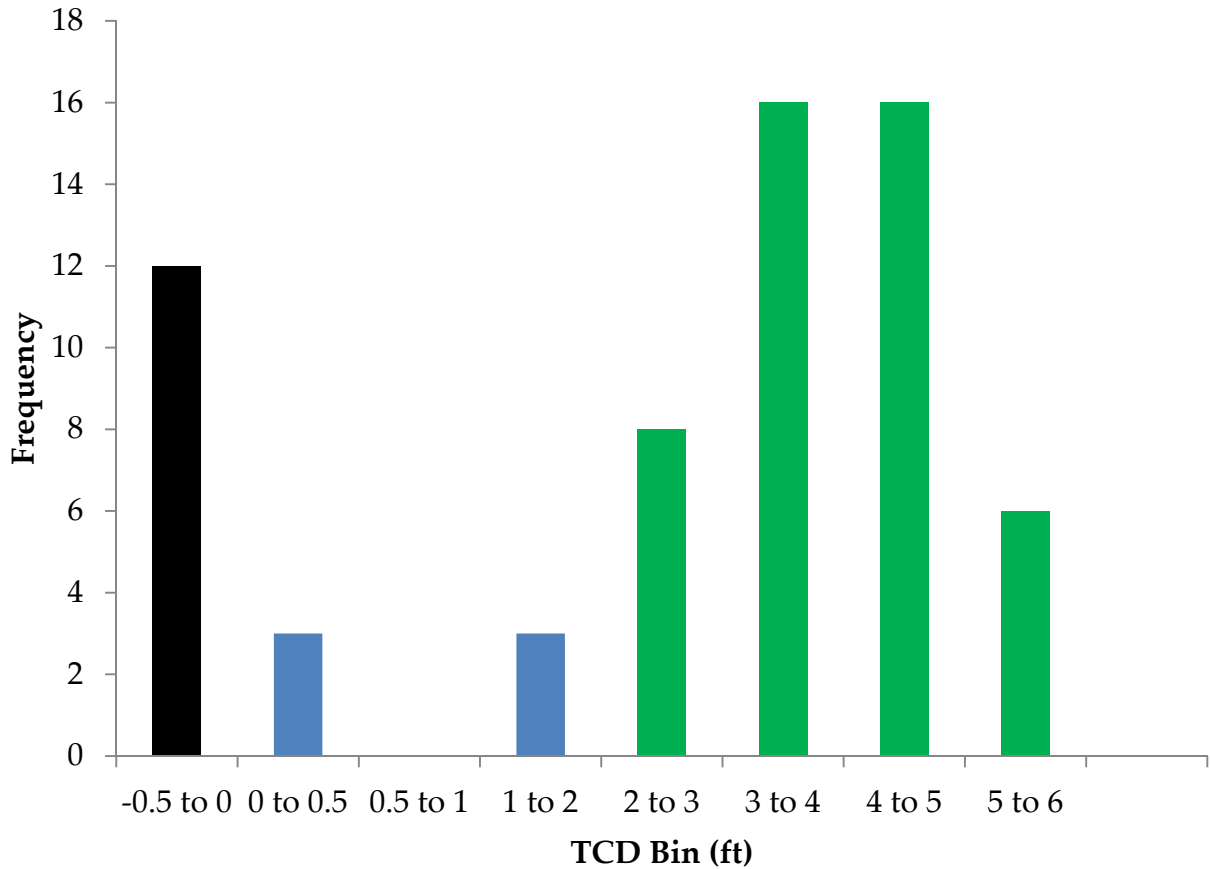


Figure 48. Histogram of TCD predicted deposition and redds showing the thickness of deposits for redds. Black represents redds that were not associated with any TCD predicted deposition, blue represents redds associated with TCD deposition outside of the constructed spawning riffle, and green are redds built on the constructed spawning riffle.

6.7.5. Redd proximity analysis

The next step was to test hypothesis 3 of the GAIP, which states that structural refugia in close proximity to spawning habitat should provide resting zones for adult spawners and protection from predation and holding areas for juveniles. As illustrated in Figure 49, pool morphologic units (from Wyrick and Pasternack, 2012) for adult holding are in proximity of all three clusters and are dominantly abundant throughout EDR. The primary resting and rearing refugia in close proximity to red clusters consisted of complex banks bedrock protrusions, boulders, and large cobble (Fig. 49). Bedrock and boulders were observed to provide local shading on the spawning riffle. Little riparian vegetation was along the banks of the baseflow channel, which is not surprising given

the predominance of bedrock and lack of fine sediment for plant establishment. None of the clusters were associated with any large streamwood, but there is abundant large streamwood in EDR further up the banks on both sides of the river that is outside the wetted width of spawning flows.

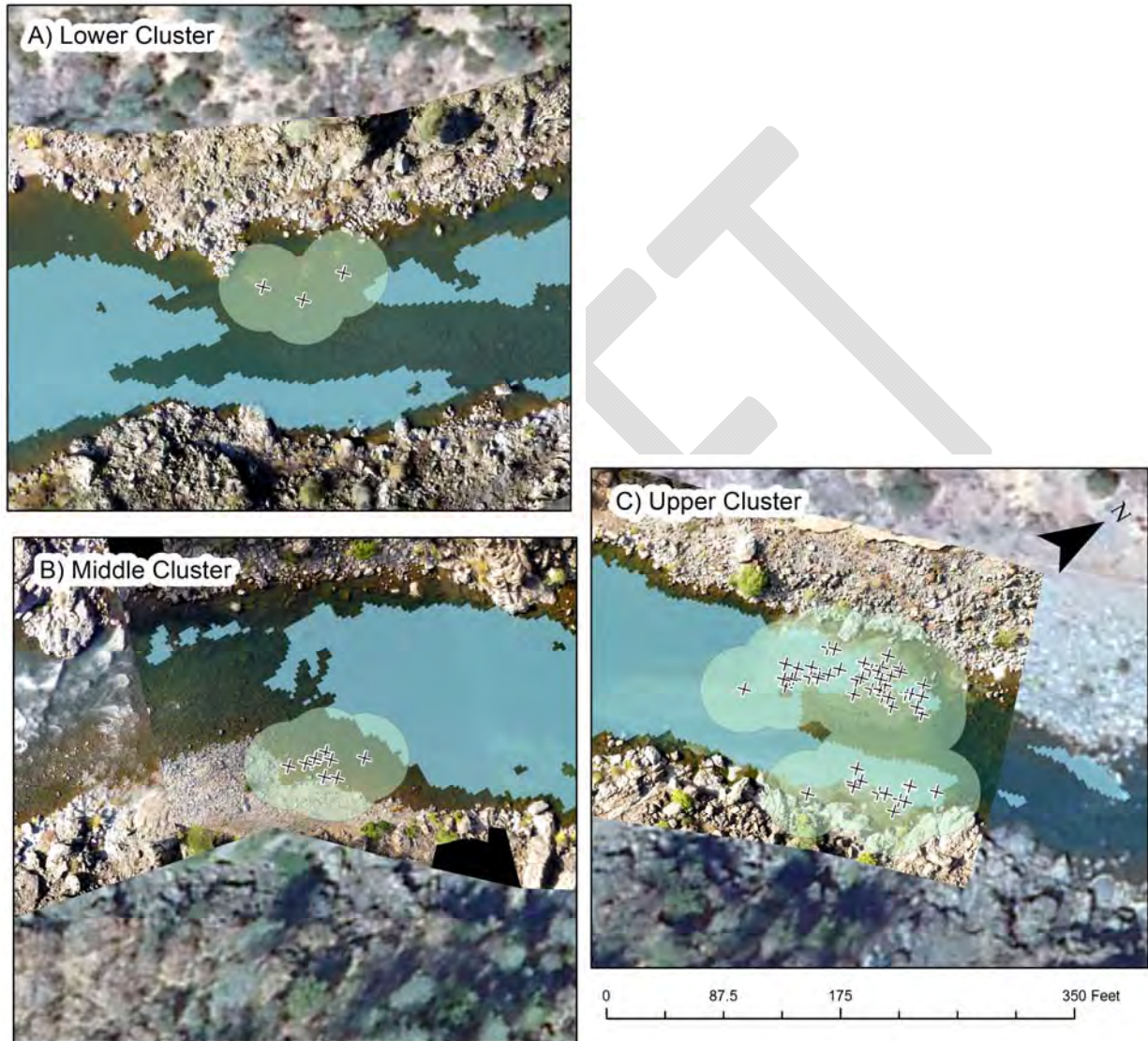


Figure 49. 10-m buffers around the redds in the three clusters. Redds are indicated with a black “X” and buffers are shown in transparent green. Also shown in light blue are pool morphologic units *as they existed in 2007* from Wyrick and Pasternack (2012).

7.0 GAIP Hypothesis Testing Evaluation

In this section succinct evaluations of the outcome of the 2012 gravel augmentation relative to the GAIP hypotheses are presented.

7.1. Hypothesis 1 - Total Sediment Storage Should Be At Least Half of the Volume at the Wetted Baseflow

After two GAIP- gravel/cobble injections, ~16% of the estimated minimum deficit has been addressed. Whereas the previous annual assessment yielded a ~10% net surplus of sediment, this one yielded a net deficit of ~14%, which is again not surprising given the roughness of the bedrock/shotrock topography. In all evaluation (2009, 2011, and now for 2012), it has been found that some amount of sediment is infiltrating into the porous and fractured bed. Because the GAIP's estimate of total volume hinges on the 2007 topographic map, which does not fully capture the available roughness-scale storage capacity of the bed, the estimate based on the half-volume at wetted baseflow should be viewed as the minimum total deficit.

Considering the period of 2007 to 2012 spanning all injections thus far, virtually all of EDR is filling in, except the highly constricted chute opposite Sinoro Bar, which is naturally eroding (Figs. 39 and 40). Furthermore, very little material is leaving the reach, even given the occurrence of several floods. Thus, the river is changing in the direction hoped for in the GAIP, but it will take more time and more injections to fill the sediment deficit.

No final conclusion about hypothesis 1 will be attainable until enough sediment has been injected to yield sizable alluvial morphological units that are not hiding behind or high-siding in front of obstructions.

7.2. Hypothesis 2

7.2.1. Hypothesis 2a - SRCS Require Deep, Loose River Rounded Sediment for Spawning

River-rounded gravel and cobble were added to the EDR bedrock/shotrock river corridor. In years prior to adding any gravel, the corridor was devoid of salmon spawning. Chinook were observed attempting to spawn on bedrock. After all three gravel injections done thus far, Chinook were attracted to the new material and used it to construct redds. In the EDR since 2007, spawning only occurs on injected gravel/cobble. This was reinforced even more this year as 80% of the spawning in the EDR occurred in the spawning riffle created during the 2012 injection. Once again,

these are strong indications in support of the hypothesis. More than 13 times more sediment needs to be added before the full benefit will be attainable.

7.2.2. Hypothesis 2b - Spawning Habitat Should Be As Close To GHSI High Quality Habitat as Possible

Similar to last year's analyses this study found that 2D model predicted patches of medium and high quality GHSI were utilized by spawners in far greater occurrence than their areal availability, indicating a strong nonrandom preference. Low quality and very poor quality areas were avoided by spawners this year as were non-habitat areas. These results further bioverify the use of 2D hydrodynamic modeling and the LYR habitat suitability curves produced by Beak Consultants, Inc (1989) for California Department of Fish and Game using the method of non-parametric tolerance limits. Every test of these HSC on the LYR has confirmed the strong predictive ability of this pairing of mechanistic 2D model and utilization-based empirical HSC.

Most importantly, the findings confirm that spawners do not merely require gravel addition, but that preferred depths and velocities are also requisite for spawning to occur. Figure 46 demonstrates this very clearly. In addition, the modifications made to the injection system allowed a spawning riffle to be created that provided high quality areas of habitat based on depth and velocity. Thus, it appears reasonable to continue to focus on using gravel addition to create habitat that is as close as possible to high quality GHSI as represented for the LYR.

7.3. Hypothesis 3 – Structural refugia in close proximity to spawning habitat should provide resting zones for adult spawners and protection from predation and holding areas for juveniles.

All observed redds were located mostly within 10 m of structural refugia such as overhanging bedrock and large boulders. Even on the large spawning riffle it was observed that fish congregated near the bedrock edges or when in the center of the channel near large boulders that were not fully buried in new gravel. The redd clusters were also within ~ 20 m of deep pools. Because structural refugia and pools are ubiquitous in EDR, obtaining this outcome is easy.

7.4. Hypothesis 4a - Designs Should Promote Habitat Heterogeneity and Provide Habitat for All Species and Life stages

Similar to last year there are presently no large alluvial deposits in EDR with homogenous hydraulics. Gravel addition is at too early of a stage to worry about

excessive homogeneity of spawning riffles. There remains ample complexity of bedrock landforms along the banks and deep pools throughout the reach.

7.5. Hypothesis 5a - There are no mechanisms of riffle-pool maintenance in the EDR and it is not feasible in this section of the river

The presence of bedrock, lack of alluvium from Englebright Dam, and history of anthropogenic activities prohibit the presence of archetypal free-formed riffle pool units such as those found in the Lower Yuba River. Despite this, evidence of forced riffle-pool scour and maintenance associated with bedrock was observed in the EDR located ~600 feet upstream of the Narrows Gateway. On the other hand, there are locations where the canyon is narrow and shallow such that scour is always focused on bedrock plateaus (Pasternack, 2008). It remains to be seen whether mechanical rehabilitation of Sinoro Bar, shot rock removal, and continual gravel augmentation makes this process more widespread within the EDR and whether this will maximize SRCS habitat and its stability.

7.6. Hypothesis 5b - Flows overtop Englebright Dam and erode placed sediments

Consistent with earlier 2D hydrodynamic modeling and site observations, high flows do have the ability to erode placed sediments and transport them through the EDR. Injected gravel continues to arrive from the quarry smaller than commonly found on the LYR, so erosion risk is higher than anticipated by the GAIP. It is very important that future injections enforce stricter adherence by the quarry to the gravel/cobble mix design. It can be difficult for quarries to produce the correct mix, but through careful and frequent monitoring, they can be given feedback and encouragement to keep to the required mix design.

8.0 Annual Volume and Placement Design

8.1. Gravel Placement Design Development

Under the current augmentation implementation approach the contouring of gravel features at the injection site is problematic and of questionable value. First, the site is relatively inaccessibility to heavy equipment without significant disturbance that was deemed unacceptable in the Environmental Assessment. Second, the sluice pipe is rigid, heavy, and difficult to position- though advances were made in positioning the outlet with the aid of a cableway and floats. As technological adaptations improve, contouring will become more feasible. Finally, even if an appropriate gravel/cobble mix

could be perfectly placed according to a design, the fact is that the canyon is too narrow at the injection site to yield sustainable spawning riffles there that can survive right there in the face of floods. That is not saying that gravel/cobble injection in EDR as a whole is unsustainable, but just that the injection site itself is a transport corridor, not a depositional zone. The primary benefit of this injection location is that it promotes downstream distribution of the sediment throughout EDR, but that is also its limitation. Downstream distribution is working very well. Every effort continues to be made to place sediment in the injection zone to obtain a temporary spawning landform for the first spawning season after injection (when injection is done in the summer), but there should not be expectations for the landform to persist- in fact, it should be expected to be completely redistributed downstream after any sizable flood. Once there is enough alluvium throughout EDR, this will be inconsequential as the injection site can serve purely as a location for gravel injection and then pre-existing spawning habitat landforms in the downstream sections of the river will be sustained by the injections.

8.2. Annual Injection Volume Assessment

Gravel/cobble injection was done faster and with fewer problems in this second in sluicing operation than occurred during the first one. The trajectory is clearly one of improvement through time as the contractor gains more experience with the site and bring forward more advanced technological adaptations. Commonly, regulators limit gravel/cobble augmentation projects for anadromous salmonids in California to a narrow period of roughly July to mid-September (sometimes less). For the EDR, when all injected sediment exports from the injection zone and moves downstream, there is no reason why gravel sluicing cannot occur any time year round. Regulatory agencies are most comfortable with the pre-specified period, but the first injection in 2010-2011 was outside that period and no one indicated any problems. Discussions have been held informally in Yuba Accord River Management Team meetings and regulatory agency representatives have indicated some flexibility for expanding the window of injection earlier in July and even into June.

Conducting gravel/cobble injections using 5,000 ton pilot projects was necessary to work out scientific and engineering constraints and to be cautious. At this point there is no further need for such caution- everything significant that can be learned from 5,000 ton injections has been learned and now there is no reason to hold back increasing the annual injections to 10,000 tons. It is time to learn lessons operating at that annual magnitude.

With a remaining deficit of at least 53,000 short tons, the minimum time to completion of erasing the reach's sediment deficit time with annual injections of 5,000 short tons is

11 years. However, the faster the sediment deficit is eliminated, the sooner ecological goals can be achieved and perhaps the more resilient the whole project would be against large floods. Given that it is feasible to inject 10,000 short tons per year, then the minimum remaining deficit could be addressed in 6 years (considering that 2013 is likely to be a 5,000 short ton addition). If efforts with 10,000 short tons are tested and found to be feasible either in the existing period or in an expanded period, then it might be appropriate to test a 15,000 short ton injection. However, that amount would very likely require an expanded period to be achievable, so that regulatory constraint would have to be addressed first. If the sequence of injection was 5,000 in 2013, 10,000 in 2014, and then 15,000 thereafter, then the minimum deficit could be addressed in 5 years.

9.0 Lessons Learned

9.1. Gravel Sluicing Operations

Prior to performing the 2010-2011 gravel/cobble injection there was substantial uncertainty about the potential effectiveness of the gravel sluicing method for a moderately sized, remote canyon. Having completed two projects now, it is certain that sluicing is an effective and appropriate strategy for use in EDR. The number of breaks in the pipeline reduce each time a project occurs, as the operators gain experience with controlling gravel and water flow through the pipe and judging when to rotate a pipe section to avoid excessive abrasion on one side of the inside of the pipe. Positioning the rock hopper at the switchback was a successful change, especially because it substantially reduced the length over which clogs could occur. Using a cableway and multiple floats on the pipe to help position the pipe outlet in the river was highly effective. The one notable enhancement anticipated for the 2013 gravel injection is an increasing in the size and power of the water pump. Using a stronger pump would even further help to reduce clogging in the pipe after the hopper.

9.2. Enhanced Yuba-specific Gravel Mix

A new gravel mix was developed for this project through consensus-based discussions among stakeholders and the gravel/cobble-sluicing contractor. The new mix design was developed to reflect Yuba-preferred spawning conditions, while still being achievable with gravel sluicing (Table 24). The size fraction of < 32mm gravels was reduced to the same 20% as observed on the river. Meanwhile, the majority of the material will be in the gravel/cobble size range of 32-90 mm.

Because the new mix design involved coarser particles, there was uncertainty about

gravel-sluice performance. Operational performance was good during the 2010-2011 injection, and numerous enhancements to sluicing for 2012 significantly increased efficiency and helped accommodate the abundance of larger particles. Unfortunately, the actual material delivered to the project from the quarry was always finer than the specified mix (Fig. 11). Part of the reason this happened was that contractually there was flexibility allowed in case problems arose. Also, pebble counts collected during the project were not carefully analyzed until after the project.

Given that so many lessons were learned during the 2012 project, it is ok that this one issue was not solved this time. However, for the 2013 gravel/cobble injection it is highly recommended that no contractual flexibility be allowed. Further, we will work closer and more frequently with all project participants to test delivered materials more frequently during the project and provide regular feedback to the quarry about how the mix is doing.

Table 24. Planned 2012 gravel/cobble mix design.

Size (mm)	class	Size (in)	class	% retained	Fractional %
90-128		3.5 to 5		30	30
32-90		1.25 to 3.5		80	50
19-32		¾ to 1.25		88	8
13-19		½ to ¾		96	8
6-13		¼ to ½		100	4

9.3. Gravel/Cobble Sourcing*

Scientific requirements and concerns for sourcing of gravel and cobble for the GAIP was never formally addressed in the GAIP. That occurred because sourcing was previously discussed by participants of the Lower Yuba River Technical Working Group in meetings in 2006 and a consensus was reached by all involved, including agency staff at USFWS, NMFS, and CDFG. However, since then staff have changed and a broader community has become concerned with a variety of geomorphic and sedimentary issues in the EDR. As a result, it is important to clarify gravel/cobble sourcing.

The lower Yuba River valley has hundreds of millions of tons of hydraulic mining alluvium, which is composed of all sizes of sediment from clay to boulder. Apart from a few remnant sedimentary high terraces that pre-date hydraulic mining and a very

small contribution from Dry Creek downstream of Virginia Ranch Dam, virtually all sediment in the LYR corridor is hydraulic mining alluvium. Therefore gravel/cobble supply for the GAIP that is going to come from within the basin is going to come from hydraulic mining alluvium.

Much land in the river corridor is owned by commercial suppliers of aggregate. Individual commercial suppliers can extract hundreds of thousands to millions of ton of alluvium per year for different commercial purposes. To gain an understanding of the suitability of the hydraulic mining alluvium as a starting source for further processing to obtain the final gravel/cobble mixture for the GAIP, it is helpful to read statements from the commercial suppliers in the LYR (without endorsing any):

“Teichert’s Hallwood Plant has actively operated in the Yuba Gold Fields since 1953 and offers examples of modern active gravel mining techniques, equipment, and award-winning active and complete mine reclamation.” (<http://reclaimingthesierra.org/teichert-materials/>)

“SRI operates year round, and mines some of the world’s finest aggregate from the Yuba Gold Fields in Yuba County. The chemical and physical characteristics of the Yuba Gold Fields resource enables us to manufacture multi-functional products. One of the most unique aspects of this reserve is the full spectrum size range (diameters) of quality aggregate, and the wide variety of reserves available from a single source... we conduct our own state-of-the-art washing, screening, drying, grading, and packaging operations” (<http://www.sri-sand.com/>)

To be perfectly clear, there is no intent to scoop up raw hydraulic mining alluvium and dump it “as is” into EDR. The raw LYR alluvium is the starting source, but then the material must be washed, screened, and graded according to common best practices for gravel augmentation and as required by water quality permitting and other regulatory requirements. It has been demonstrated in this study that Chinook spawners intensively use the injected sediment. There appears to be no aversion of spawners to utilize the injected mix.

10.0 Conclusions

The purpose of this study was to evaluate the status of the EDR as of December 1, 2012 and the efficacy of past gravel injections into the EDR with regard to making progress toward meeting the geomorphic and ecological goals stated in the GAIP. By design, ~5,000 short tons of gravel/cobble was to be added into the EDR just downstream of the Narrows 1 powerhouse, filling no more than an additional 8 % of the reach’s coarse sediment deficit. Sluicing was a successful method of gravel/cobble addition with extremely low environmental impact compared to other methods. It is recommended that gravel sluicing be continued as the preferred method to implement the GAIP, with

new enhancements to the method being tested as opportunities arise.

Whereas there were multiple floods between the time that the 2010-2011 project was done and subsequent spawning, this time the Chinook spawners entering the reach in autumn 2012 got to experience a pristine spawning riffle. When they did, they went ahead and spawned heavily on it, but still, it was just 5,000 short tons. That does not make a large area compared to the Chinook population. The outcome was that the spawners heavily used the high-quality habitat created by the project. Further, the combination of 2D hydrodynamic modeling and Beak, Inc. HSCs once again accurately predicted where the Chinook would spawn. After two years of accurate performance in EDR documented by GAIP research and two years of accurate performance for the alluvial LYR documented by the RMT (Pasternack et al., 2013), there is no doubt that this is a useful and valid tool for spawning habitat rehabilitation and enhancement for the LYR, including EDR.

Analysis of sediment distribution in a remote canyon is not easy, but this study used state-of-the-art methods of topographic change detection account for uncertainty in digital elevation models and the propagation of that uncertainty through DEM differencing. According to the resulting sediment budget, nearly all of the measurable amount of gravel/cobble injected in the EDR stayed in the EDR, despite moderate flood peaks and long flood durations. It is likely that the sediment will transport out of the reach eventually, which is why the GAIP calls for adding sediment annually to match losses after the initial sediment deficit is eradicated.

This study found that the mechanisms of sediment deposition in the EDR canyon are myriad as hypothesized in

Table 2. Local hiding spots consisting of bedrock/shotrock nooks and crannies absorbed some sediment, larger obstructions captured some sediment in their upstream stagnation zone and their downstream eddy zone, and flows of different magnitudes interacted with stage-dependent channel geometric variables to steer sediment into different depositional locations. At this time there are still ample locations in EDR for sediment to be stored, so continued implementation of the GAIP is recommended.

Chinook spawning habitat is something that occurs on top of alluvial landforms, and for the lower Yuba River the ones that are preferred more than random likelihood are riffles, riffle transitions, and runs (RMT, unpublished analysis). When gravel is injected into a reach and distributed downstream, the potential for creating such features depends on the volume added compared against the sediment deficit as well as the topographic structure of the channel. In this second injection, no more than 16 % of the gravel deficit was met, so there is no reason to expect that a large amount of habitat would be created. Landform creation and spawning habitat utilization is a highly nonlinear phenomenon in terms of the amount of utilization that occurs per unit of gravel added (Elkins et al., 2007), because a small addition on top of a degraded alluvial landform will yield dramatically more habitat than a large addition at the bottom of a deep bedrock pool that is non-habitat. Consequently, appropriate caution must be used in devising utilization metrics and extrapolating in time or space. Calculating the number of spawners served per ton of gravel added and extrapolating from that ratio is scientifically invalid.

Overall, gravel/cobble injection by gravel sluicing is working in that the sediment is getting added to the channel, it is moving downstream and creating landforms in the river, it is staying in the canyon for now (helping to reduce the sediment deficit), the hydraulics over the created landforms includes high quality habitat that is preferred for spawning more than random likelihood, and Chinook spawners are making use of that habitat. Section 7.0 draws on the data and analyses to report on the outcomes of GAIP hypothesis testing. At this time there is no need to modify the GAIP, as the results of the study support the hypotheses. Annual gravel/cobble addition should continue and the interim outcomes monitored until the sediment deficit is eradicated. At that point, the long-term plan in the GAIP should commence. No pause or delay in annual gravel injection should occur.

11.0 References

Abu-Aly, T. R. 2012. Quantifying the effects of spatially-distributed roughness parameters derived from Airborne Light Detection and Ranging (LiDAR) on a 2D

- hydrodynamic model of the Lower Yuba River, CA. M.S. Thesis. University of California, Davis.
- Barker, J.R., 2011. Rapid, abundant velocity observation to validate million-element 2D hydrodynamic models. M.S. Thesis, University of California at Davis, Davis, CA, 82 pp.
- Brown, R. A. and Pasternack, G. B. 2008. Engineered channel controls limiting spawning habitat rehabilitation success on regulated gravel-bed rivers. *Geomorphology* 97:631-654.
- Brown, R. A. and Pasternack, G. B. 2009. Comparison of Methods for Analyzing Salmon Habitat Rehabilitation Designs For Regulated Rivers. *River Research and Applications* 25:745-772.
- Campos, Casey And D Massa.2012. Redd Monitoring And Mapping In The Englebright Dam Reach Of The Lower Yuba River, Ca. Summary Report September 12, 2011 – December 19, 2011. Prepared For The U. S. Army Corps Of Engineers. February 28, 2012
- Carley, J. K., Pasternack, G. B., Wyrick, J. R., Barker, J. R., Bratovich, P. M., Massa, D. A., Reedy, G. D., Johnson, T. R. submitted. Accounting for uncertainty in topographic change detection between contour maps and point cloud models. *Geomorphology*.
- Elkins, E. E., Pasternack, G. B., and Merz, J. E. 2007. The Use of Slope Creation for Rehabilitating Incised, Regulated, Gravel-Bed Rivers. *Water Resources Research* 43, W05432, doi:10.1029/2006WR005159.
- Heritage, G.L., Milan, D. J., Large, R.G., Fuller, I.C. 2009. Influence of survey strategy and interpolation model on DEM quality. *Geomorphology* 112, 334-344.
- Ivlev, V.S. 1961. *Experimental ecology of the feeding of fishes*. Yale University press, New Haven, CT.
- Lowe, D.G. 2004. Distinctive image features from scale-invariant keypoints. *International Journal of Computer Vision* 60 (2), 91-110.
- MacWilliams, M. L., Wheaton, J. M., Pasternack, G. B., Kitanidis, P. K., Street, R. L. 2006. The Flow Convergence-Routing Hypothesis for Pool-Riffle Maintenance in Alluvial Rivers. *Water Resources Research* 42, W10427, doi:10.1029/2005WR004391.
- Pasternack, G. B. 2011. *2D Modeling and Ecohydraulic Analysis*. Createspace: Seattle, WA.
- Pasternack, G. B., Wang, C. L., and Merz, J. 2004. Application of a 2D hydrodynamic model to reach-scale spawning gravel replenishment on the lower Mokelumne

- River, California. *River Research and Applications* 20:2:205-225.
- Pasternack, G. B., Gilbert, A. T., Wheaton, J. M., Buckland, E. M. 2006. Error Propagation for Velocity and Shear Stress Prediction Using 2D Models For Environmental Management. *Journal of Hydrology* 328:227-241.
- Pasternack, G. B. 2009. Current Status of an On-going Gravel Injection Experiment on the Lower Yuba River, CA. Prepared for the U.S. Army Corps of Engineers.
- Pasternack, G. B. 2010. Gravel/Cobble Augmentation Implementation Plan (GAIP) for the Englebright Dam Reach of the Lower Yuba River, CA. Prepared for the U.S. Army Corps of Engineers.
- Pasternack, G. B. and A.E. Senter. 2011. 21st Century instream flow assessment framework for mountain streams. California Energy Commission, PIER. CEC-500-XXXX-XXX.
- Pasternack, G. B., Fulton, A. A., and Morford, S. L. 2010. Yuba River analysis aims to aid spring-run Chinook salmon habitat rehabilitation. *California Agriculture* 64:2:69- 77.
- Sawyer, A. M., Pasternack, G. B., Merz, J. E., Escobar, M., Senter, A. E. 2009. Construction constraints on geomorphic-unit rehabilitation on regulated gravel-bed rivers. *River Research and Applications* 25:416-437.
- Thompson, D.M., 2001. Random controls on semi-rhythmic spacing of pools and riffles in constriction-dominated rivers. *Earth Surface Processes and Landforms* 26, 1195–1212.
- Thompson, D.M., 2006. The role of vortex shedding in the scour of pools. *Advances in Water Resources* 29, 121–129.
- Thompson, D.M., 2007. Turbulence characteristics in a shear zone downstream of a channel constriction in a coarse-grained pool. *Geomorphology* 83, 199–214.
- Wheaton, J. M., Pasternack, G. B., and Merz, J. E. 2004. Spawning Habitat Rehabilitation - 1. Conceptual Approach & Methods. *International Journal of River Basin Management* 2:1:3-20.
- Wheaton JM, Brasington J, Darby SE and Sear D. 2010a. Accounting for Uncertainty in DEMs from Repeat Topographic Surveys: Improved Sediment Budgets. *Earth Surface Processes and Landforms*. 35 (2): 136-156. DOI: 10.1002/esp.1886
- Wheaton JM, Brasington J, Darby SE, Merz JE, Pasternack GB, Sear DA and Vericat D. 2010b. Linking Geomorphic Changes to Salmonid Habitat at a Scale Relevant to Fish. *River Research and Applications*. 26: 469-486. DOI: 10.1002/rra.1305.

Van Asselt, M. B. A., and J. Rotmans. 2002. Uncertainty in integrated assessment modeling—from positivism to pluralism. *Climatic Change* 54:75–105.

DRAFT